DOCTORAL THESIS

Development of new types of composite electrodes based on natural clays and their analytical applications

PhD student **Adela Maghear**

PhD supervisors **Prof. Dr. Robert Săndulescu**
Dr. Alain Walcarius

UNIVERSITÉ DE LORRAINE

UMF UNIVERSITATEA DE MEDICINĂ ȘI FARMACIE IULIU HAȚIEGANU CLUJ-NAPOCA

"We are what we repeatedly do. Excellence, then, is not an act, but a habit."

~Aristotle~

To my supervisors...

Acknowledgements

Now, when I've reached the end of the path I started four years ago, I look back to express a special gratitude and I realize the list of the people I have to thank is quite long…

My work is the result of a fruitful collaboration between two research groups: the Department of Analytical Chemistry which is part of the Faculty of Pharmacy, University of Medicine and Pharmacy" Iuliu Haţieganu", Cluj-Napoca, Romania, and Laboratoire de Chimie Physique et Microbiologie pour l'Environnement– Université de Lorraine, Villers-lès-Nancy, France.

I would like to express my deep and special gratitude to my thesis supervisor Prof. Robert Săndulescu for providing me the opportunity to join his research group and for making everything possible during all these four years. His optimism and dedication to science are impressive and I must thank him for his continuous and endless support and also for all the fruitful scientific and non-scientific discussions.

I am grateful to Dr. Alain Walcarius, also my PhD supervisor, for receiving me in his research group and for his key contributions to my studies. I respect his contagious dedication to science. I dedicate this thesis to my both supervisors hoping I fulfilled their ambitions and expectations.

Special thanks to Mr. and Mrs. Iuliu and Ana Marian for their endless support, encouragement, availability, understanding, and priceless lessons in science and life.

I would also like to thank Dr. Cecilia Cristea and Dr. Mathieu Etienne for their help and guidance in the research lab, for their support and encouraging ideas.

Special thanks to my colleagues Mihaela Tertiş and Luminiţa Fritea for their help, support, friendship, and hard work. I would also like to acknowledge the valuable contribution of all co-authors and collaborators from Romania and France for making this thesis possible, especially to Tamara Topală, Dr. Emil Indrea, Dr. Cosmin Farcău, Ludovic Mouton, and Pierrick Durand.

For the financial support I am grateful to the Agence Universitaire de la Francophonie and to UMF "Iuliu Haţieganu" for the research project POS-DRU 88/1.5/S/58965.

And, of course, I grace my family for their encouragement and support throughout my life.

LIST OF PUBLICATIONS

1. **Adela Maghear**, Andreea Cernat, Cecilia Cristea, Ana Marian, I. O. Marian, R. Săndulescu, New Electrochemical Sensors Based on Clay and Carbon Micro and Nanoparticles for Pharmaceutical and Environmental Analysis, Proceedings of NSTI-NanoTech Conference (18-22 June 2012, Santa Clara, California SUA), www.nsti.org, ISBN 978-1-4665-6274-5 Vol.1, 574-577;

2. **Adela Maghear**, Cecilia Cristea, Ana Marian, Iuliu O. Marian, R. Săndulescu, A novel biosensor for acetaminophen detection with Romanian clays and conductive polymeric films, Farmacia, LXI, 1 (2013) 1-11;

3. **Adela Maghear**, Cecilia Cristea, Ana Marian, I. O. Marian, R. Săndulescu, Physico-chemical and electroanalytical characterization of two Romanian clays with possible applications in pharmaceutical analysis, Farmacia, LXI, 4 (2013) 648-657;

4. **Adela Maghear**, M. Etienne, Mihaela Tertiș, R. Sandulescu, A. Walcarius, Clay–mesoporous silica composite films generated by electroassisted self-assembly, Electrochimica Acta, 112 (2013) 333-341;

5. Cecilia Cristea, Andreea Cernat, **Adela Maghear**, Robert Săndulescu, Applications of nanomaterials in biomedical and environmental analysis. In Sergey Lishevky (Editor), Dekker's Encyclopedia of Nanoscience and Nanotechnology, vol 6, Marcel Dekker, New York, 2013, *in press*;

6. **Adela Maghear**, Mihaela Tertiș, Luminţa Fritea, I. O. Marian, E. Indrea, A. Walcarius, R. Săndulescu, Tetrabutylammonium-modified clay film electrodes: characterization and application to the detection of metal ions, Talanta (2013) *submitted*.

Table of Contents

ABBREVIATIONS

ac	acetate
CEC	cation exchange capacity
CLME	clay-modifed electrodes
CNT	carbon nanotube
CO	cholesterol oxidase
CPE	carbon paste electrode
CTAB	cetyltrimethylammonium bromide
CV	cyclic voltammetry
DPASV	differential pulse anodic stripping voltammetry
FAD	flavin-adenine dinucleotide
GA	glutaraldehyde
GCE	glassy carbon electrode
GOX	glucose oxidase
Hb	hemoglobin
HRP	horseradish peroxidase
ITO	indium tin oxide
LDH	layered double hydroxide
MB	methylene blue
MPS	mesoporous silicas
Mb	myoglobin
MV	methyl viologen

PEI	polyethylene imine
pH-FET	pH sensitive field effect transistor
PPO	polyphenol oxidase
SCE	saturated calomel electrode
SWV	square wave voltammetry
TBAB	tetrabutylammonium bromide
TEOS	tetraethoxysilane

INTRODUCTION

Along with the progress in the industrial and technological fields, pollution has been one of the main concerns all over the world. Its impact on environment has lead among time to the development of different approaches to detect, prevent, or minimize its damaging effects. In this way, electrochemistry offers a wide variety of techniques that aim to control by different means the impact of pollution in the living world.

Heavy metals are among the most important soil and biological contaminants. The interest for their detection has therefore increased a lot in the recent years. Heavy metals show high toxicity, they can accumulate in human, animal, and plant tissues and they are not biodegradable, so their quantitative determination in different media is an issue of primary importance nowadays. Electrochemistry is likely to cope with this high demand by offering new types of electrodes for real-time detection of trace metal contaminants in natural waters and also in biological and biomedical samples.

Clay-modified electrodes are mostly used for this type of application. If in the past centuries clays were just used in cosmetics or to produce ceramics, in the last three decades they attracted the interest of electrochemists due to their catalytic, adsorbent, and ion exchange properties which have been exploited in the development of chemical sensors. Moreover, the adsorption of proteins and enzymes on clay mineral surfaces was intensively applied in biosensor fabrication.

This research was directed towards the modification of different types of electrodes using indigenous Romanian clays for the development of sensors applied in the detection of heavy metals from matrices of biopharmaceutical and biomedical interest and biosensors for the detection of different pharmaceuticals.

The studies presented here are mainly focused on electrochemical methods (voltammetry, differential pulse methods, anodic stripping) and ion-selective electrodes based on different types of clays, in order to improve the performances of the existent devices and also to develop other methods for the determination of heavy metals in various matrices.

The aims of this thesis are summarized as follows:

- To confirm the physico-chemical and structural characterization of the indigenous Romanian clays
- To develop new clay-modified electrodes by employing different methods to immobilize the clay at the electrode surface:
  a. the embedment of the clay in carbon paste;
  b. the incorporation of the clay in polymeric conductive films;
  c. the immobilization of clay using a semipermeable membrane;
  d. the entrapment of the clay in a sol-gel matrix.
- To study the electrochemical behavior of the new electrode configurations and to apply them in trace heavy metal detection or in pharmaceutical analysis:
  a. the analysis of acetaminophen, ascorbic acid, and riboflavin using clay-carbon paste-modified electrodes;
  b. the development of a HRP/clay/PEI/GCE biosensor for acetaminophen detection;
  c. the development of tetrabutylammonium-modified clay film electrodes covered with cellulose membranes for heavy metal detection;
  d. the development of a copper(II) sensor using clay–mesoporous silica composite films generated by electro-assisted self-assembly.

STATE OF THE ART

1 Clay-modified electrodes

A "chemical sensor is a small device that, as the result of a chemical interaction or process between analyte and the sensor device, transforms chemical or biochemical information of a quantitative or qualitative type into an analytically useful signal" [1]. A chemical sensor consists of two basic components: a chemical recognition system (receptor) and a transducer [2]. In the case of biosensors, the recognition system uses a biological mechanism instead of a chemical process. The role of the transducer is to transform the response measured at the receptor into a detectable signal. Due to their remarkable sensitivity, experimental simplicity, and low cost, electrochemical sensors are the most attractive chemical sensors reported in the literature. The signal detected by the transducer can be a current (amperometry), a voltage (potentiometry), or impedance/conductance changes (conductimetry).[2]

An important feature of the chemically modified electrodes consists in their ability to preconcentrate the analyte into a small volume on the electrode, allowing lower concentrations to be measured than possible in the absence of a preconcentrated step (adsorptive stripping voltammetry)[2]. Among the wide range of electrode modifiers, clays have attracted the interest of electrochemists, in particular for their analytical applications.[3, 4]

1.1 Clays – definition, classification, properties

The use of clay minerals as electrode modifiers is the result of electrochemists desire to achieve a high quality electrode surface with the required properties, but also the result of their three decades effort to understand and control the processes that take place at electrode surface. The clay minerals employed in this case belong to the class of phyllosilicates-layered hydrous aluminosilicates. Their layered structures comprises either one sheet of SiO_4 tetrahedra and one sheet of AlO_6 octahedra (1 : 1 phyllosilicates)or an Al-octahedral sheet is sandwiched between two Si-tetrahedral sheets (2 :1 phyllosilicates).[3, 5, 6] The role of the exchangeable cations (Na^+, K^+, NH_4^+ etc.) bound on the external surfaces for 1 :1 phyllosilicates and also in the interlayer in the case of 2 :1 phyllosilicates is to balance the positive charge deficiency of the layers. An important characteristic of the clay mineral is the basal distance which depends on the number of intercalated water and exchangeable cations within the interlayer space. Other important properties of this structure regard the relatively large specific surface,

ion-exchange properties, and ability to adsorb and intercalate organic compounds. All these features recommend phyllosilicates, especially a group of smectites, for preparation of clay-modified electrodes.[3]

There are two classes of clays: cationic clays that have negatively charged alumino silicate layers, and anionic clays, with positively charged hydroxide layers, the neutrality of these materials being ensured by ions, cations or anions, depending on the clay type in the interlayer space, that balances the charge.[2] Cationic clays are among the most common minerals on the earth's surface, being well known due to their applications in ceramic production, pharmacy, cosmetics, catalysts, adsorbents, and ion exchangers.[7, 8] Smectite clays are mostly used in the development of electrochemical sensors due to their ability to incorporate ions by an ion-exchange process and also due to their adsorption properties. Therefore, proteins adsorption is intensively used in the development of biosensors. [9]

Due to its cation exchange capacity (CEC) (tipically between 0.80 and 1.50 mmol g^{-1}) and anion exchange about four times lower, montmorillonite is the most used smectite. On the other hand, thixotropy recommends montmorillonite to be used as a stable and adhesive clay film. Besides smectites (montmorillonite, nontronite, hectorite), literature describes some other clay minerals (vermiculite, kaolinite, sepiolite) which can be exploited for electrodes modification.[3]

1.2 Clay-modified electrode preparation

The preparation method is the one that mostly influences the electrochemical behavior of CLME. Several techniques have been employed to cast the clay films, such as the slow evaporation of colloidal suspensions on electrode surfaces (i.e., platinum, glassy carbon, indium tin oxide, and screen printed electrodes), physical adsorption (the most widely used technique due to its simplicity and ease), spin coating thin clay films, and clay-carbon paste-modified electrodes.[2] A more sophisticated strategy uses silane linkages to couple clay to the underlying electrode surface.[10] Langmuir–Blodgett method was applied to prepare thin film of clays on electrode surfaces.[11-14] Another study reported a hybrid film of chiral metal complex and clay, prepared by the Langmuir–Blodgett method for the purpose of chiral sensing.[15, 16] The electro-deposition of kaolin and montmorillonite using rotating quartz crystal microbalance disk electrodes or indium tin oxide (ITO) was also realized.[17, 18]

1.3 Electrochemistry at clay-modified electrodes

Electron transfer at clay-modified electrodes (CLME) has been extensively studied in the 1990s.[19-22] Poor charge transport is an important issue when using nonconductive solids to modify electrodes, which is related to either physical diffusion in the channels and/or to charge hopping. In the case of clays, electroactive species can

be accumulated within the clay layer at different places, but only a small fraction of these species display redox activity (≈10–30%) (Figure 1).[2]

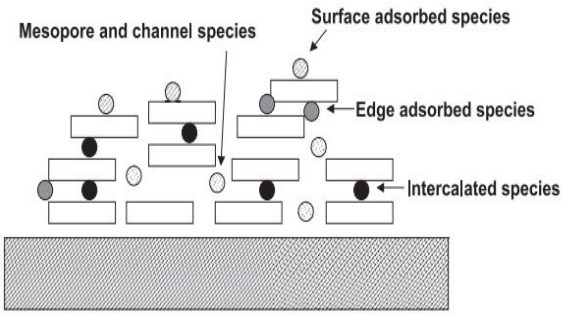

Figure 1 Different adsorption sites at clay-modified electrode [2]

Mass transport processes through cationic and anionic clays were investigated by electrochemical quartz crystal microbalance measurements.[23-25] The results showed that the charge balancing during a redox reaction was accomplished by the leaching or insertion of mobile ions at the clay solution interface. Taking in to account that this phenomenon depends on the nature and the concentration of the electrolyte, modifications in the swelling properties of the clays can occur.[2] The enhancement of charge transport within the clay film can be achieved by delamination processes that give less ordered coatings and consequently allow access to the channels.[2] Different strategies can be applied for this: the use of smaller size particles (laponite instead of montmorillonite), pillaring agents (alumina, silicate) to obtain a porous clay heterostructure, or by the intercalation of molecules (surfactants or polymers).[26, 27] Other methods describe the enhancement of electron hopping using electron relay, making use of the redox active cation sites within the crystal lattice (i.e., iron, cobalt, or copper for cationic clays and nickel, cobalt or manganese for anionic clays) to transfer electrons from intercalated ions to the conductive substrate.[28-32] Other possibilities for delivering charges consist of using a conductive polymer (polypyrrole) within the clay interlayer[33, 34] or by using a composite conducting material (V_2O_5).[35] In spite of all inconveniences regarding electron transfer at CLME, many applications have been found for these modified electrodes, such as electrocatalysts, photocatalysts, sensors, and, biosensors. The direct electrochemistry of heme proteins (i.e., cytochrome *c*, cytochrome *P*450, myoglobin (Mb), etc.) was reported at a CLME.[36-40] In most of these cases, the protein-clay films were prepared by depositing a certain concentration of protein onto the CLME, the heterogeneous electron transfer process between the protein and the electrode surface being facilitated by the clay modification on the electrode surface.[2] It is stated that the interaction of the proteins with the clay particles

didn't seriously affect the heme Fe (III)/(II) electroactive group of the incorporated proteins.[2]

1.4 Applications in environmental and biomedical analysis

1.4.1 Heavy metal detection using clay-modified electrodes

1.4.1.1 Clays implication in heavy metal detection

Heavy metals are well-known as important environmental and biological contaminants: they are not bio- or photodegradable, they accumulate in human, animal, and plant tissues and they have high toxic effects. Their density is 6.0 g/cm^3 or more (much higher than the average particle density of soils which is 2.65 g/cm^3). Even they occur naturally in rocks, their concentrations are frequently elevated as a result of contamination. Arsenic, cadmium, chromium, mercury, lead, and zinc are the most important heavy metals with regard to potential hazards and occurrence in contaminated soils.[41]

Metal mining, metal smelting, metallurgical industries, and other metal-using industries, waste disposal, corrosions of metals in use, agriculture and forestry, fossil fuel combustion, and sports and leisure activities are the main sources of heavy metal pollutants. Large areas worldwide are affected by heavy metal contamination. Heavy metal pollution is mostly present close to industrial sites, around large cities and in the vicinity of mining and smelting plants. Heavy metals can transfer into crops and subsequently into the food chain, which affects seriously the agriculture in these areas.[41]

The increasing requirement for an efficient and real-time monitoring of trace heavy metals that pollute the environment led to the development of new detection methods and new specific sensors capable to perform *in situ* measurements with minimum disturbance of natural system.

The ion exchange capacity and the ion exchange selectivity of clays recommended them to be applied to the accumulation of charged electroactive analytes.[2] Cationic exchanging clays are essentially used for sensor devices. The electroactivity of the adsorbed ions depends on the soaking time of the CLME in the analyte solution (accumulation time), on the nature and concentration of analyte, on the mode of preparation of the CLME, on the electrolyte nature, etc. Smectite clays are frequently employed at CLME because they can serve as matrices for electroactive ions as they are able to incorporate ions by an ion-exchange process, like polymeric ionomers.[2] Due to its cation exchange capacity typically between 0.80-1.50 mM g^{-1}, while anion exchange is about four times lower, montmorillonite is the most often used smectite. [2]

Carbon paste electrodes (CPEs) were generally used for cationic heavy metals preconcentration at CLME. The detection limits depend on the nature of the metal cations or on the clay species and are lower than the European norms required for drinking water.[2]

1.4.1.2 Inorganic clay heavy metal detection sensors

Determination of inorganic analytes (metal ions in the most cases) can be achieved due to the ion exchange reactions on the clay modifier.[3] Thus, the procedure consists of an accumulation step under open circuit conditions with subsequent voltammetric determination after medium exchange (Figure 2). The fact that the accumulation process is separated from the measurement step and optimum conditions can be found and applied for each other, represents a great advantage of this procedure.[3] Preconcentration conditions must be optimized due to the ion exchange and sorption reactions of clays and zeolites. After removing the electrode from the preconcentration medium is careful washed with redistilled water before it is transferred into the measurement cell containing the background electrolyte.[3]

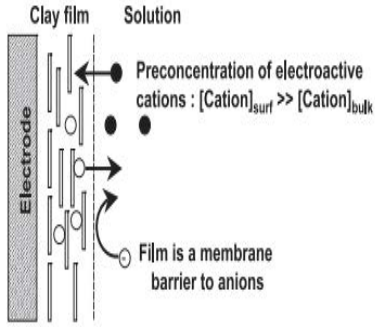

Figure 2 Preconcentration step at clay-modified electrode[2]

The composition and concentration of the background electrolyte has a great influence on the current response of clay electrode.[3] There is competition between electrolyte cations and analyte for ion-exchange sites, while electrolyte anions can influence the ion-pairing mechanism. Also, electrolyte concentration can affect the structure of the clay modifier. These aspects should be therefore taken into account during optimization of the analytical method.[3]

The ion exchange capability of clays was firstly proved using clay CPEs. The preconcentration of free Fe(III) cations into montmorillonite[42] takes places due to the replacement of the exchangeable cation in the interlayer of clay. A preconcentration model of Ag^{+} and Cu^{2+} on vermiculite modified paste electrode under open circuit conditions[43] was investigated based on the conception of the simplified ion exchange process, involving the negatively charged groups of clay minerals.[3] The values obtained

for electrochemically determined concentration equilibrium constant for the ion exchange of Ag^+ corresponded with those evaluated by atomic absorption spectroscopy. The model is therefore supposed to be applied to other systems. The exchange of metal cations onto montmorillonite, vermiculite and kaolinite was studied by repetitive CV on the clay CPEs.[44] The metal sorption is represented by the current's dependence on time or on the potential cycling and thus, one can distinguish individual clay minerals and metal cations, even only at the first approximation.[3] Copper(II) could be determined under the open circuit conditions due to its preconcentration by means of the cation exchange.[45] The exchange of other cations present in the electrolyte can be competitive with cation exchange[42, 46, 47], a formation of metal complexes must be considered, too, in this case (e.g., the exchange of the cationic complexes $[Cu(ac)]^+$ occurred on montmorillonite and vermiculite[47]).

A vermiculite CPE was employed as a model for a soil-like phase and the binding interactions of Cu(II) ions with the mineral were studied.[48] When investigating the influence of selected pesticides on the Cu(II) uptake from the solution to vermiculite, it was shown that Cu(II) uptake significantly depended on binding affinity of pesticides to vermiculite, so on their ability to form coordination compounds with Cu(II) ions. The different effects some substances of environmental importance have on the metal ion uptake to clay mineral were also described. Then research was extended, when employing different soils in their native form as electrode modifiers in order to study soil-heavy metal ions interactions by means of CPE for the first time.[49] The binding capabilities of the soils were examined in a model solution of Cu(II) ions, together with the correlation between the copper ions accumulation and the standard soil parameters (ion exchange capacity, soil pH, organic matter and clay content.[3] The nature of soil samples should be considered when developing an environmental sensor based on soil modified CPE suitable for on-site testing of soils.[37] For example, the soil used as a modifier should be fully characterized due to the fact that the soil modified electrodes strongly depend on the type of soil.[49]

In order to obtain a reproducible measurement the renewal of the CPE surface is important. Carbon paste surface can be easily removed by polishing and a new surface can be prepared. It was shown that standard deviation is 5% if a measurement is always performed on the mechanically renewed surface.[45] Regeneration by washing the electrode with water and measurement on one surface during one day was also described.[42] In the case of Cu(II) determination on a vermiculite modified electrode[50], a short-term regeneration step (0.05 M KCN for 2 min and 0.1 M $HClO_4$ for 1 min) was applied after each voltammetric measurement, while a long-term preconditioning step (0.1 M $HClO_4$ for 24 hours, 0.05 M KCN for 2 min and 0.1 M $HClO_4$ for 1 min) was applied after mechanical renewal of the surface. The regenerated surface was applicable for one week without mechanical renewing the paste).[3] Another study

described the renewal of surface by exposing the electrode to 0.2 M KCN in 2 M NH_3 for 2 min.[43]

During the preconcentration step, the ion exchange reaction takes place by replacing the cations initially present in the clay, like in the case of Fe(III).[42] The peak in the reduction current is the result of the reduction of the surface bound iron, while the enrichment of iron in the carbon paste is indicated by the increase of the peak height at longer preconcentration times. The renewal of the electrode surface is needed as a smoothed electrode surface should be reused. A 0.1 M CH_3COONa or 0.1 M Na_2CO_3 was employed for 1 min electrode bathing to achieve a 100% removal of iron from montmorillonite, although the regeneration step can represent a limit point of the procedure because the stated time could be insufficient for higher concentration of Fe(III).[3] The method did not show interferences with the coexisting metal ions, besides that Mg(II) and Al(III) in a 2-fold excess caused 32%, and 100% decrease of the current response, respectively. That can be explained due to ability of high valence cations to replace exchangeable cations in clays.[3]

Historically, it can be noted that greater attention was given to copper(II) determination by means of the clay CPEs. The first works reported the voltammetric response of the zeolite modified CPEs for Cu(II).[51, 52] But, the related detection limits (about 10^{-4} mol L^{-1}) were not low enough for practical use. In addition, the regeneration of the electrode surfaces was not an easy step. Cu(II) determination methods by means of the clay modified CPEs achieved better results as to the limit of detection with time.[3] Both vermiculite CPE[50] and montmorillonite modified CPE[45] used the anodic current response of the accumulated Cu(II). In the first method, clay CPE preparation was achieved by using the dry clay modifier, so in this case the activation of the electrode surface complicated the measurement.[50] The electrode was exposed to 0.1 M $HClO_4$ for 24 h which can damage the electrode surface, even authors don't state that. The electrode was treated with 0.05 M KCN for 2 min and with 0.1 M $HClO_4$ for 1 min before use. The short term (3 min) regeneration step in 0.05 KCN and 0.1 M $HClO_4$ was needed to remove copper residue in vermiculite taking into consideration the fact that the electrode surface was used for at least one week without mechanic renewing of the paste.[3] This step can also be an inconvenient in the Cu(II) determination. However, the method was promising, with relative error of 2% for ppm Cu(II) concentrations. When using the wetted modifier, no activation of the electrode surface was necessary in the case of the montmorillonite modified CPE. No regeneration step was required in this method due to the regular mechanical removing of the paste and a newly smoothed surface was used for each measurement.[45] The limit of detection achieved by this method was ten times higher in comparison with the vermiculite CPE, although the area of the montmorillonite CPE was 20 times smaller than that of the vermiculite electrode.

Some interferences were present for both methods: bivalent metal cations in a 100-fold excess (Pb, Hg, Cd, Zn)[45, 50], cations Fe(II, III), Co(II), Ni(II), Mn(II), and Bi(III) in a 200-fold excess[50], while surfactants as Triton-X100, butylammonium bromide, and methylammonium bromide did not perturb the copper signal even in a 1000-fold excess.[50] On the contrary, Cu(II) current response decreased with 50% in a 4-fold excess of humic ligands.[45] So when employing vermiculite and montmorillonite CPEs for Cu(II) determination, the methods are sensitive enough, while their selectivity remains questionable. However, the Cu(II) and Zn(II) different selectivity towards nontronite is supposed to eliminate the interference of Cu(II) in the determination of Zn(II) in their mixture.[3] The nafion/nontronite modified mercury film electrode was proved to be suitable for this purpose[53] as it exhibited square-wave stripping peak currents linear over the ranges 0 - 5 and 6 - 12 μM Zn(II) in the presence of 10 μM Cu(II).

Monovalent silver and divalent mercury could be determined using a vermiculite modified CPE.[46] Preconditioning in this case was achieved by exposition of the modified electrode in 0.1 M $HClO_4$ for 24 h. Electrode regeneration was performed in 0.1 M KCN for 2 min, followed by the activation with 0.1 M $HClO_4$ for 2 min before each measurement. The limits of detection were around 10^{-8} mol/L for both silver and mercury. The anionic complexes $HgCl_4^{2-}$ and $HgCl_3^-$ could be determined by means of montmorillonite modified CPE on the same concentration level.[54] The chlorocomplexes were also applied to determine gold on the montmorillonite modified CPE[55, 56], the determination of gold in pharmaceuticals being also possible with this method. [100]

A sodium modified montmorillonite was applied to cadmium sorption from nitrate solutions in order to simulate a cadmium polluted clay mineral. The cadmium concentration adsorbed by the clay was analyzed at equilibrium by means of differential pulse polarography showing a Freundlich sorption profile. After cadmium sorption procedure, the clay mineral was included in a carbon paste in order to investigate the cadmium content by voltammetric determination. A linear response of the CPE was observed in the 5.0×10^{-5}-1.8×10^{-4} mol g^{-1} range with good reproducibility.[57]

A selective analysis of copper (II) was also obtained at carbon microelectrode coated with monolayers of laponite clay and polythiophene by an originally developed double-step voltcoulometry.[58] Langmuir–Blodgett technique was used for the surface modification of electrodes and a detection limit of 5 mg L^{-1} was reached. Authors discuss the characteristic features of the ‘‘memory effect’’ of the laponite coating.[58]

When testing the effect of montmorillonite on the preparation of a calcium ion electrode by combining and immobilization of ionophore and montmorillonite into a polymer membrane, it was shown that the montmorillonite-modified electrode exhibited higher performance than that without montmorillonite.[59]

Good accumulation ability for the $[Cu(NH_3)_4]^{2-}$ complex ion via the ion-exchange ability of nontronite was obtained when testing a nontronite/cellulose acetate-coated GCE for the preconcentration and electroanalysis of Cu^{2+} in ammoniacal medium by square wave voltammetry (SWV). The cellulose acetate permselective membrane was applied to strengthen the mechanical stability of the nontronite coating on GCE and to prevent the interference from surface-active compounds. The obtained detection limit was 1.73 ppb in pH 10 ammonia solution. The practical application of the developed sensor was illustrated by the measurement of Cu^{2+} in tap water, groundwater, and pond water.[60]

Electrodeposition method was uses to develop a CPE modified with montmorillonite and covered with a mercury film. In this case, both electrodeposition in situ and a preliminary electrodeposition were applied to deposit the mercury film. Anodic stripping of metals deposited on the Hg film electrodes is said to be a complicated process limited by factors as time and potential of the metal electrodeposition, while accumulation and stripping of metals depends on metal nature. By using an open-circuit sorption of Cd, Pb, and Cu with subsequent anodic stripping voltammetry, higher current responses were obtained. Besides an enhanced sensitivity, superior separation of the current responses during a simultaneous stripping of metals was achieved..[61]

Ag(I) could be detected using two natural clays (kaolinite and montmorillonite) deposited onto a platinum electrode surface, by two deposition techniques and under different experimental variables. For both clays, a complete surface coverage for the electrode surface was achieved using the spin-coating technique. The detection limit of Ag(I) ions was as small as 10^{-10} M.[62]

Recently, the simultaneous determination of trace amounts of Pb^{2+} and Cd^{2+} with montmorillonite-bismuth-carbon electrodes was developed. The method was applied for determining Pb^{2+} and Cd^{2+} contents in real water samples by square wave anodic stripping voltammetry. The detection limits were 0.2 μg L^{-1} for Pb^{2+} and 0.35 μg L^{-1} for Cd^{2+}.[63]

A different approach for heavy metal detection was proposed by investigating the feasibility of amperometric sucrose and mercury biosensors based on the immobilization of invertase, glucose oxidase, and mutarotase entrapped in a clay matrix (laponite). Platinum electrodes were used to deposit the enzyme clay gel cross-linked with GA. The inhibition of the invertase activity enabled the measurement of mercury concentration. It was proved that the use of clay matrix, a cationic exchanger, for the invertase immobilization allows the accumulation of metal cations in the vicinity of the enzyme causing the enhancement of the inhibition effect, associated to a decrease of the biosensor recovery. The biosensor inhibition by inorganic and organic mercury was evaluated and a good selectivity towards mercury when studying

interferences with other metal ions. Under optimized conditions, Hg(II) was determined in the concentration range of 10^{-8} to 10^{-6} M.[64]

1.4.1.3 Organo-clay heavy metal detection sensors

Organo-clays found their applications in the treatment of wastewaters contaminated with several inorganic cations.[4] 'Organo-clays' represent, in fact, clay materials with enhanced sorption capacity obtained by introducing suitable organic molecules.[4] An important feature here is the fact that, depending on the nature of the organic molecule introduced, the surface of clay become more hydrophobic or hydrophilic.[65] The incorporation of organic molecule relates closely to the specific purpose of the modification. Therefore, the organic functionalities contain selective functional groups with high affinity towards the target species. In this perspective, organosilanes intercalated to the clays for the Hg^{2+} detection[66] demonstrated that besides the enhanced uptake of these cation at the surface charge sites of clays, the intercalated functional groups were also involved in the binding of this metal ion, which caused of the enhanced uptake.[4] In a similar way, the enhanced removal of Hg(II) from aqueous solutions using the grafted clay materials with 1,3,4-thiadiazole-2,5-dithiol[67] or 3-mercaptopropyl[68] was also described.

A CPE modified by a natural 2:1 phyllosilicate clay functionalized with either amine or thiol groups as a sensor for Hg(II) was also evaluated. Its functionalization was achieved by grafting the pristine clay via its reaction with 3-aminopropyl-triethoxysilane or 3-mercaptopropyl-trimethoxysilane. The electroanalytical procedure followed two steps: the chemical accumulation of the analyte under open-circuit conditions and the electrochemical detection of the preconcentrated species using differential pulse anodic stripping voltammetry (DPASV). The detection limits were $8.7 \cdot 10^{-8}$ and $6.8 \cdot 10^{-8}$ M, respectively, for the amine- and thiol-functionalized clays. Authors sustain that the sensor can be useful as an alerting device in environmental monitoring or for a rapid screening of areas polluted with mercury species.[69]

Na montmorillonite was transformed organophilicly by exchanging the inorganic interlayer cations for hexadecyltrimethylammonium ions (HDTA). Based on the high affinities of an organo-clay for non-ionic organic molecules, 1,3,4-thiadiazole-2,5-dithiol was loaded on the HDTA-montmorillonite surface, resulting in the 1,3,4-thiadiazole-2,5-dithiol-HDTA-montmorillonite complex, which has been shown to be an effective solid phase selective sorbent for Hg(II), that can also be applied in the preparation of a chemically modified CPE. The detection limit was estimated as 0.15 μg L^{-1}. [67]

A lower detection limit for Hg(II) was obtained by A.J. Tchinda et al. ($5 \cdot 10^{-10}$ M) using thiol-functionalized porous clay heterostructures, which have been prepared by intragallery assembly of mesoporous organosilica in natural smectite clay. The

electrode assembly consisted of a surfactant-directed co-condensation of tetraethoxysilane (TEOS) and 3-mercaptopropyltrimethoxysilane (MPTMS), at various MPTMS/TEOS ratios, in the interlayer region of the clay deposited as thin films onto the surface of GCEs and applied to the voltammetric detection of Hg(II) subsequent to open-circuit accumulation. They displayed attractive features, like fast diffusion rates, and thus great sensitivity and good mechanical stability, due to the layered morphology .[68]

The use of clays and humic acids in order to simulate soil clay-organo complex (clay humate) represents another approach to understand the soil processes related to transport and accumulation of heavy metals.[3] The clay-humate modified CPE was employed to study the clay humate system and its reaction with copper in comparison with the clays alone[45] and it was concluded that the Cu(II) sorption was significantly decreased in the case of montmorillonite-humate.

Some organic molecules with different functional groups (-NH_2, -COOH, -SH, or $-CS_2$) have been introduced within the interlayer space of montmorillonite using organic compounds, such as hexamethylenediamine, 2-(dimethylamino)ethenethiol, 5-aminovaleric acid, and hexamethylenediamine-dithiocarbamate.[70] These organo intercalated montmorillonite samples showed an increased uptake capacity for cations (i.e., Cd^{2+}, Pb^{2+} and Zn^{2+}). The suggested mechanism was that the increase in the interlayer space (between 0.3-0.4 nm) occurred due the intercalation of the organic compound, which allowed an easier access for the M^{2+} and $M(OH)^{+}$ species to the intercalated organic compound. Meanwhile, the strong binding of the $M(OH)^{+}$ species to the organic compounds contributed additionally to the metal uptake, as proved by the obtained binding constants.[4]

A voltammetric sensor based on chemically modified bentonite–porphyrin CPE has been introduced for the determination of trace amount of Mn(II) in wheat flour, wheat rice, and vegetables. The method showed good Mn(II) responses at a pH range of 3.5–7.5 and a detection limit of $1.07 \cdot 10^{-7}$ mol L^{-1} Mn(II). Authors proved that a 1000-fold excess of additive ions did not interfere on the determination of Mn(II).[71]

By combining the ion exchange capability of Na montmorillonite with the electronic conductor function of an anthraquinone, a sensitive electrochemical technique for the simultaneous determination of trace levels of Pb^{2+} and Cd^{2+} by DPASV was developed. This method used a non-electrolytic preconcentration, via ion exchange model, followed by an accumulation period, via the complex formation in the reduction stage at −1.2 V, followed by an anodic stripping proces s. The detection limit was 1 and 3 nM for Pb^{2+} and Cd^{2+}, respectively. This method found its application in the detection of trace levels of Pb^{2+} and Cd^{2+}in milk powder and lake water samples.[72]

A low-cost electrochemical sensor for lead detection developed using an organo-clay obtained by the intercalation of 1, 10-phenanthroline within montmorillonite. The results showed that the amount of accumulated Pb(II) increased with an increase of the accumulation time and remained constant after saturation. The limit of detection for lead was in the sub-nanomolar range ($4 \cdot 10^{-10}$ M), and there was no interference with copper at concentrations 0.1×[Pb(II)].[73]

1.4.2 Amperometric biosensors based on clays applied in pharmaceutical and biomedical analysis

Enzyme modified electrodes are considered the most popular and reliable kind of biosensors. A crucial feature on the commercial development of biosensor is the stable immobilization of an enzyme on an electrode surface, with complete retention of its biological activity and good diffusional properties for substrates.[2] The various enzyme immobilization methods reported in the literature include cross-linking of proteins by bifunctional reagent, covalent binding, and entrapment in a suitable matrix. Due to their hydrophilic, swelling, and porosity properties clays occupy a privileged place among all the inorganic and organic matrices described. Therefore, they were used as host matrices for enzymes (first generation biosensors), as concentration means for different redox mediators (second generation biosensors), then as mediators themselves (clay and LDH for electrons transfer), and finally, for direct enzyme regeneration (third generation biosensors).

1.4.2.1 Oxygen based biosensors (first generation)

In the first generation of biosensors, during glucose oxidation process, flavin-adenine dinucleotide (FAD) component of GOX is converted into $FADH_2$. After glucose oxidation, $FADH_2$ is reconverted to FAD in the presence of oxygen (Figure 3A).

Besombes et al.[74, 75] have shown that the analytical performance of amperometric biosensors based on (polyphenol oxidase) PO and (cholesterol oxidase) CO can be very much improved by the incorporation of laponite particles within an electrogenerated polypyrrole matrix. A similar study described that laponite matrix improved the analytical characteristics and the long-term stability of biosensors compared to the corresponding biosensors simply obtained by the chemical cross-linking of glucose oxidase (GOX) or polyphenol oxidase (PPO) on the electrode surface.[76, 77]

An inexpensive, fast, and easy method for the elaboration of enzymes electrodes is the entrapment of biomolecules in clay matrix, which consists of the adsorption of an enzyme/clay aqueous colloid mixture onto the electrode surface.[2] However, slow release of enzymes into solution can considerably reduce the biosensor lifetime. This problem was overcome by using enzyme cross linking agents, such as glutaraldehyde

(GA) [78], polymethyl methacrylate , or poly(o-phenylenediamine) [79] which have been added in the enzyme/clay coating film.[2]

GOX[80] was immobilized by clay sandwich method. A polycationic organosilasesquioxane laponite clay matrix was adopted by Coche-Guérente et al. [81-83] for biosensor development. The group proposed an enzymatic kinetic model for the PPO amplification process. Amperometric detection of glucose was intensively studied, mainly due to the physiological importance of this analyte, the stability of glucose oxidase, and the diversity of sensing methods applied. The oxidizing agent used by GOX electrode is molecular oxygen, while the amperometric detection of glucose can be carried out via the electrooxidation of the enzymatically generated H_2O_2 at a Pt electrode:[2]

$$\text{Glucose} + O_2 \xrightarrow{\text{GOX}} \text{gluconic acid} + H_2O_2$$

$$H_2O_2 \rightarrow 2H^+ + O_2 + 2e^-$$

Interferents like ascorbic acid and uric acid, which are commonly present in biological fluids, can also be oxidized due to the high polarizing voltage applied ($E_{app} \approx$ 0.6–0.8 V) leading to nonspecific signals [2]. To overcome this problem, Poyard et al. [84, 85] used clay-semipermeable polymer composite electrodes to decrease the permeability to organic interfering compounds. Due to the fact that hydrogen peroxide can be reduced by redox mediators immobilized within CLME, another possibility consists in using redox mediators to decrease the electrode potential.[2] Based on this concept, cationic methylviologen (MV^{2+})[80], ruthenium complexes[79, 86] associated to structural iron cations, or TiO_2 underlying films[76] were employed in the development of CLME based glucose biosensors.

A particular example of amperometric biosensor for glucose detection is GOX/luminol/clay electrode which works by means of electrochemiluminescence.[87]

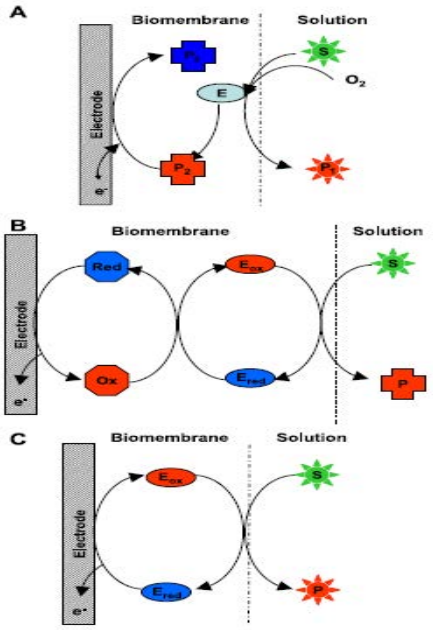

Figure 3 Amperometric biosensors: (A) first generation, (B) second generation, (C) third generation.[2]

A biosensor for phosphate detection has been fabricated by the co-immobilization of three enzymes (GOX, maltose phosphorilase and mutarotase) with complementary activities.[88] The amperometric detection in this case corresponded to H_2O_2 oxidation.[2]

Taking into account that a large percentage of environmental pollutants are known to act as enzyme inhibitors, the development of a series of sensors is based on the measurement of this property.[2] In this way, a novel hypoxanthine sensor based on xanthine oxidase immobilized within a polyaniline film was developed by Hu et al. [89] The detection in this case is based on oxygen consumed due to the enzymatic reaction measured at a montmorillonite-MV^{2+} carbon paste-modified electrode.[2]

1.4.2.2 Mediator based biosensors (second generation)

In the second generation of biosensors, O_2 was replaced by redox mediators (i.e., tetrathio fulvalene or dopamine) as oxidizing agents.[90-92] The amperometric measure of glucose concentration (Figure 3B) represents therefore the current flowing through the reoxidation of electron transfer agents at the electrode surface.[2] In a similar way, bienzymatic configurations, consisting of GOX, horseradish peroxidase (HRP), and redox mediators coated on CLME could be applied to the detection of glucose at 0.0 V with good sensitivities and with no interferences and preventing any possible oxidation of ascorbate and ureate.[93, 94]

Laponite was particularly used as immobilization matrix for several other oxidase enzymes immobilized on CLME, and the resulting biosensors have been used to detect NADH, lactate, ethanol, and also a wide variety of water pollutants, such as cyanide. [2, 76, 77, 94-100] The biosensors achieved by Cosnier's group were based on laponite-electrogenerated polymer composites.[76, 93, 95-97]

Hydrogenase[101] was immobilized by clay sandwich method and bovine serum albumin + GA[90] were used as enzyme cross linking agents.

The redox mediators methylene green, poly 3,4 dihydroxybenzaldehyde, and 2,2'-azinobis-3-ethylbenzothiazoline-6-sulfonate were co-immobilized within the clay matrix as electron shuttles between the redox center of HRP and the electrode. [93, 94, 102]

A biosensor configuration based on the entrapment of diaphorase or dehydrogenase within laponite gel containing methylene blue (MB) as electropolymerized mediator for NADH oxidation was described.[95, 96] The presence of PolyMB in the biolayer allowed an electron transfer communication between enzymes and the electrode surface and Poly MB/dehydrogenase/laponite-modified electrode was successfully applied for electroenzymatic detection of lactate and ethanol via the mediated oxidation of NADH at 0 V.[2]

A comparative study described the properties of two different biosensors based on the immobilization of PPO within the two different kinds of clay matrices: one cationic (laponite) and the other anionic (layered double hydroxides, LDHs).[99] Due to the high permeability and the structure and charge of the particles of the LDH-based biosensors, the PPO/[Zn–Al–Cl] LDHs biosensor showed remarkable properties such as high sensitivity and good storage stability.[2]

1.4.2.3 Directly coupled enzyme electrodes (third generation)

The enzymatic detection of hydrogen peroxide has been reported either at mediated HRP-CLME or by direct enzyme regeneration at CLME (3rd generation, Figure 3C).[2]

The synthesis of carbon nanotubes (CNTs) on clay mineral layers and the preparation of H_2O_2 sensor based on CNT/Nafion/Na-montmorillonite composite film for the detection of H_2O_2 were achieved and the developed sensor showed high sensitivity and applicability.[103]

Step-by-step self-assembly was employed to incorporate HRP into a laponite/chitosan-modified glassy carbon electrode (GCE). The self-assembled enzyme maintained its biological activity and showed an excellent electrocatalytic performance for the reduction of H_2O_2 with fast amperometric response (10 s), broad linear range, good sensitivity, and low detection limit.[104]

The direct electron transfer of heme proteins (HRP, myoglobin, hemoglobin, cytochrome *c*) found its applications in sensors for the determination of H_2O_2, as well nitrite, NO, and trichloroacetic acid.[105-109] The direct electron transfer of Mb was realized by immobilizing Mb onto an ionic liquid–clay composite film modified GCE. The composite was biocompatible and promoted the direct electron transfer between Mb and electrode. The reduction of hydrogen peroxide demonstrated the biocatalytic activity of Mb in the composite film. [40]

Nanocomposite matrix based on chitosan/laponite was employed to construct an amperometric glucose biosensor. It is stated that GOX immobilized in the material maintained its activity well as the usage of GA was avoided.[110]

Taking into consideration that the majority of the amperometric glucose biosensors need stabilization membranes to prevent enzyme release and to improve selectivity, a comparative study between some of the most common membranes and two more innovative systems based on Ti and Pd hexacyanoferrate hydrogels was carried out on electrodes modified by a Ni/Al hydrotalcite (HT) electrochemically deposited on Pt surfaces, together with the GOX enzyme. The results showed that the Pd hexacyanoferrate hydrogel was the best system in terms of sensitivity, selectivity and allowed to determine glucose levels in bovine serum samples which were perfectly in agreement with the one declared by the analysis certificate.[111]

The direct electron transfer between GOX and the underlying GCE could be achieved via colloidal laponite nanoparticles as immobilization matrix. Due to the decrease of oxygen electrocatalytic signal, the laponite/GOX/GCE was successfully applied in the reagentless glucose sensing at −0.45 V. The electrode exhibited fast amperometric response (8 s), low detection limit ($1.0 \cdot 10^{-5}$ M), and very good sensitivity and selectivity.[112]

An amperometric biosensor for phenol determination was fabricated based on chitosan/laponite nanocomposite matrix. The composite film enabled the PPO immobilization on the surface of GCE. The role of chitosan was to improve the analytical performance of the pure clay-modified bioelectrode. The biosensor had good affinity to its substrate, high sensitivity catechol, and remarkable long-term stability in storage (it retained 88% of the original activity after 60 days).[113]

The comparison between four amperometric biosensors for phenol, prepared by means of immobilization of tyrosinase in organic and inorganic matrices, is also reported. In this case, the enzyme was entrapped within two organic matrices (polyacrylamide microgels and polyvinylimidazole). On the other hand, enzyme was absorbed on two inorganic matrices (laponite clay and calcium phosphate cement, called brushite) and subsequently was cross-linked by GA. Phenolic compounds were detected in aqueous and organic media by direct electrochemical reduction of the

enzymatic product, o-quinone, at −0.1 V versus saturated calomel electrode (SCE). Authors attributed the large differences found in biosensors performance to the environment surrounding the enzyme, or the biomaterial layers used in the fabrication of the biosensor. The best results in detection of monophenols and catechol in aqueous solution was achieved with the sensors based on inorganic matrices.[114]

The immobilization of lactate oxidase on a GCE modified with laponite/chitosan hydrogels for the quantification of L-lactate in alcoholic beverages and dairy products was also described. The study used ferrocene–methanol as artificial mediator and aimed to determine the best hydrogel composition from the analytical point of view. [115]

2 Mesoporous silica materials and their applications in electrochemistry

Silica-based mesoporous materials have had a great impact on electrochemistry research in the past two decades, especially due the tremendous development in the field of mesoporous materials.[116]

Ordered mesoporous silicas (MPS) present attractive intrinsic features which enabled their application in electrochemical science.

Being the first reported class of mesoporous materials, ordered MPS were usually obtained by inorganic polymerization in the presence of a liquid-crystal-forming template (ionic or non-ionic molecular surfactant or block copolymer). These materials are in fact amorphous solids with cylindrical mesopores ranging from 20 to more than 100 Å in diameter, spatially organized into periodic arrays that often mimic the liquid crystalline phases exhibited by templates.[117-120] The removal of the hybrid mesophases can be achieved by calcination or extraction. This process gives rise to stable mesoporous materials with extremely high surface area (up to 1400 $m^2 g^{-1}$), mesopore volume greater than 0.7 ml g^{-1} and narrow pore size distribution.[121]

In the large field of chemically modified electrodes, researchers have recently included sol-gel materials[121-125] as inorganic modifiers (along with clays,[3, 126] or zeolites[127, 128]) as a result of their need to couple the intrinsic properties of a suitable modifier to a particular redox process. More recently, due to the development in nanoscience and nanotechnology, nanomaterials have found their applications in electrochemistry, in particular to build nanostructered electrodes with improved performances.[129-132] The most important features that recommend nanomaterials for applications in electrochemistry are: (i) large surface areas (high number of surface-active sites, ideal support for the immobilization of suitable reagents); (ii) widely open and interconnected porous structure (fast mass transport); (iii) good conductivity and intrinsic electrocatalytic properties (for noble metals and carbons); and (iv) high mechanical stability owing to their multidimensional structure.[116] The two approaches to generate nanoarchitectures on electrode surfaces are: (i) the assembly of one dimensional nanostructures (nanoparticles, nanowires or nanorods) into functional 2D or 3D architectures[133] or nanoparticulate films,[134] and (ii) the preparation of single-

phase continuous ordered and porous mesostructures from supramolecular template assemblies and their integration into electrochemical devices.[116]

2.1 The sol-gel process

Silica-based materials represent robust inorganic solids displaying a high specific surface area and a three-dimensional structure made of highly open spaces interconnected to each other via SiO_4 tetrahedra, generating highly porous structures.[116] Generally, the sol-gel process involves the following steps:

- **Hydrolysis**

The preparation of a silica glass begins with an appropriate alkoxide, such as $Si(OR)_4$ (R = CH_3, C_2H_5, or C_3H_7), which is mixed with water and a mutual solvent to form a solution. Hydrolysis leads to the formation of silanol groups (SiOH). The presence of H_3O^+ in the solution increases the rate of the hydrolysis reaction.[121]

- **Condensation**

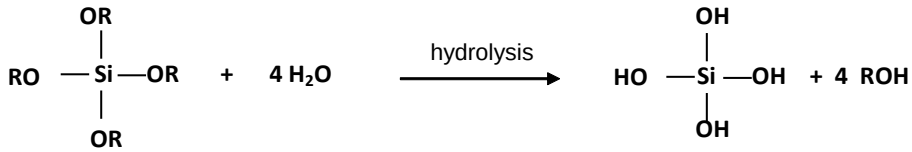

Alkoxysilane

In a condensation reaction, two partially hydrolyzed molecules can link together through forming siloxane bonds (Si-O-Si). This type of reaction can continue to build larger and larger silicon-containing molecules (linkage of additional Si-OH) and eventually results in a SiO_2 network. The H_2O (or alcohol) expelled from the reaction remains in the pores of the network. When sufficient interconnected Si-O-Si bonds are formed in a region, they respond cooperatively as colloidal (submicrometer) particles or a sol.[121]

The gel morphology is influenced by temperature, the concentrations of each species (attention focuses on R ratio, R = $[H_2O]/[Si(OR)_4]$), and especially acidity:

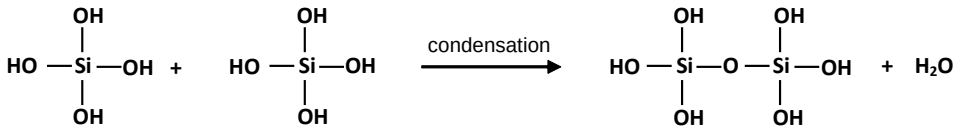

- **Acid catalysis** generally produces weakly-cross-linked gels which easily compact under drying conditions, yielding low-porosity microporous (smaller than 2 nm) xerogel structures;
- Conditions of **neutral to basic pH** result in relatively mesoporous xerogels after drying, as rigid clusters a few nanometers across pack to form mesopores. The clusters themselves may be microporous.
- **Under some conditions**, base-catalyzed and two-step acid-base catalyzed gels (initial polymerization under acidic conditions and further gelation under basic conditions exhibit hierarchical structure and complex network topology.[121]

- **Aging**

Gel aging is an extension of the gelation step in which the gel network is reinforced through further polymerization, possibly at different temperature and solvent conditions. During aging, polycondensation continues along with localized solution and reprecipitation of the gel network, which increases the thickness of interparticle necks and decreases the porosity. The strength of the gel thereby increases with aging. An aged gel must develop sufficient strength to resist cracking during drying.[116]

- **Drying**

The gel drying process consists in removal of water from the interconnected pore network, with simultaneous collapse of the gel structure, under conditions of constant temperature, pressure, and humidity. Large capillary stresses can develop during drying when the pores are small ($<$20 nm). These stresses will cause the gels to crack catastrophically, unless the drying process is controlled by decreasing the liquid surface energy by addition of surfactants or elimination of very small pores, by hypercritical evaporation, which avoids the solid-liquid interface, or by obtaining monodisperse pore sizes by controlling the rates of hydrolysis and condensation.[121]

- **Electrochemically-assisted generation of silica films**

Electrochemistry was recently proven to be attractive for synthesizing ordered mesoporous (and macroporous) deposits on electrode surfaces. The principle is based on the electrochemical manipulation of pH on the electrode surface affecting thereby the kinetics associated to the sol-gel process. The electrode is immersed in a stable silica sol (mild acidic medium: pH 3-4) where a negative potential is applied to increase the pH locally at the electrode/solution interface, inducing therefore the polycondensation of the silica precursors only on the electrode surface, which makes the process applicable to deposit thin films on non-planar surfaces (Figure 4).[121]

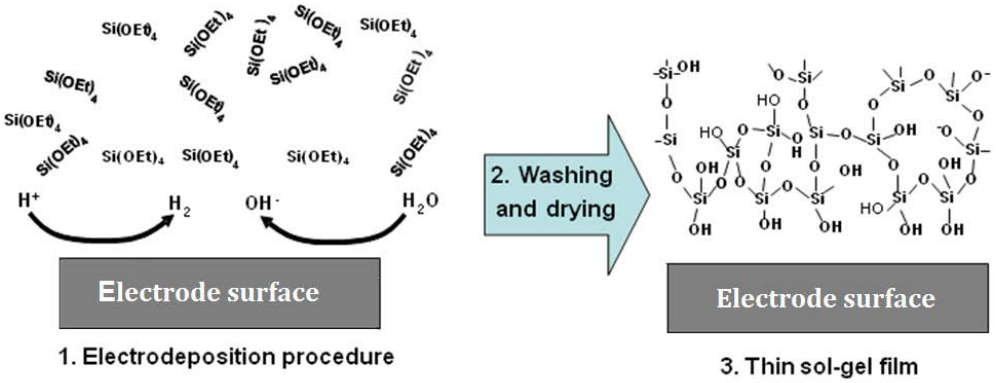

Figure 4 Electrochemically-assisted generation of silica films

2.2 Silica and silica-based organic–inorganic hybrids

Well-ordered MPS have monodispered pore sizes (typically between 2 and 10 nm) and various ionic or non-ionic surfactants can be employed for these materials preparation.[135-137] It is well known that the morphology of mesoporous silica materials depends on the synthesis conditions. ''Evaporation-Induced Self-Assembly'' (EISA) is the most common method employed to obtain mesoporous silica thin films with controlled mesostructure and pore size.[138, 139] EISA process implies a diluted sol and the formation of the film at the electrode surface is due to the evaporation of the solvent upon the extraction of the solid template from the sol (e.g., by dip-coating, spin-coating, or dropping techniques).[116] The sol solution consists of inorganic precursors alone or in mixture with organically-modified metal oxides and a surfactant usually dissolved in a water–ethanol mixture. The evaporation of volatile components takes place at the air/film interface and the concomitant self-assembly polycondensation of the surfactant and the precursors gives rise to a homogeneous mesostructured deposit (with typical thicknesses in the range of 50 nm–700 nm).[116] If in the past decades the generation of ordered porous films on solid electrode surfaces led to poorly permeable deposits (probably due to the unfavourable pore orientation) and suffered from cracks formation arising from surfactant extraction[140], the ability to precisely control the structural arrangement of silica films on the mesoscale has recently led to more accurately engineered mesoporous film electrodes with continuous structural order over wide areas and variable permeation properties depending on the film structure.[141] Mesostructure with different symmetry (cubic, hexagonal, double gyroid, rhombohedral, etc.) could be obtained by controlling the sol composition, the nature of the template, and the post-treatment temperature and humidity level.[139] The use of hard templates (nano- or microbeads) enabled the

generation of ordered macroporous thin films[142] together with the achievement multimodal hierarchical porosity.[143] Due to their defined multiscale porous networks with adjustable pore size and connectivity, high surface area and accessibility, these rigid three-dimensional matrices can be applied on solid supports (like electrode surfaces), being very promising for effective transport reactions at electrode/solution interfaces.[116]

Organically-functionalized silica-based materials are of interest in electrochemistry firstly due to their highly porous and regularly ordered 3D structure which ensures good accessibility and fast mass transport to the active centres.[116] This can be useful to improve sensitivity in preconcentration electroanalysis (voltammetric detection subsequent to open-circuit accumulation) and to enable the immobilization of a great variety of organo-functional groups improving in the meantime the selectivity of the recognition event. Secondly, due to their redox-active moieties, these materials should be able to induce intra-silica electron transfer chains, or they can be applied in electrocatalysis as electron shuttles or mediators.[116] Third, these materials can also find their applications in the field of electrochemical biosensors taking into consideration the possibility for nanobioencapsulation (e.g., enzyme immobilization[144-147]), which can lead to the development of integrated systems combining molecular recognition, catalysis and signal transduction.[116]

2.2.1 Ordered and oriented mesoporous sol-gel films

It was recently described that by electrochemistry is likely to prepare ordered and oriented mesoporous silica thin films, by the so-called electro-assisted self-assembly (EASA) method.[148, 149] In this method the formation of surfactant assemblies under potential control with concomitant growing of a templated inorganic film also takes place, but, unlike in EISA, the electrogenerated species (e.g., OH^-) do not serve in to precipitate a metal hydroxide, but they act as catalysts to gelify a sol onto the electrode surface.[116] The mechanism of EASA implies a suitable cathodic potential applied to an electrode immersed in a hydrolyzed sol solution, in order to locally generate OH^- species at the electrode/solution interface, which then induces the polycondensation of the silane precursors and the growth of silica or organically-modified silica films onto the electrode surface.[150-153] When a cationic surfactant (i.e., cetyltrimethylammonium bromide, CTAB) is present in the sol, the obtained configuration is that of hexagonally-packed mesopore channels growing perpendicularly to the electrode surface, which is the result of the electrochemically-driven cooperative self-assembly of surfactant micelles with simultaneous silica formation.[154] The main advantages of EASA are the possibility to obtain homogeneous deposits over wide areas (cm^2), even on nonflat surfaces (with thicknesses typically in the 50–200 nm range), and vertically-aligned mesoporous silica films on various electrode materials such as glassy carbon, platinum, gold, copper, or ITO. This type of

orientation with accessible pores from the surface is expected to enhance mass transport rates through the film and hence improve sensitivity of voltammetric analysis.[116] A short deposition time is required in order to avoid the formation of aggregates.[149] Insulating supports can also be employed to prepare these films using higher electric fields.[155]

2.3 Mass transport in mesoporous (organo)silica particles

The regular 3D structure consisting in mesochannels of monodisperse dimensions favors a fast mass transport, contrary to the diffusion in the non-ordered silica gel homologues.[116] This could be demonstrated through electrochemical methods by means of which the kinetics associated to mass transfer reactions between a solution and solid particles in suspension can be monitored in situ and in real time.[156] Therefore, by potentiometric pH monitoring of aqueous suspensions of mesoporous silica particles grafted with aminopropyl groups the kinetics associated to the protonation of the amine groups located in the material could be determined.[156, 157] This approach aimed to study the variation of the apparent diffusion coefficients (D_{app}) as a function of the reaction progress by assuming the diffusion of protons (and associated counter anion) inside the functionalized particles as a rate-determining step, and fitting the ''proton consumption versus time'' plot to a spherical diffusion model (silica particles have been considered as spherical in a first approximation.[157] This study was achieved on two amine-functionalized mesoporous silica samples and one non-ordered silica gel grafted with the same aminopropyl groups and it was concluded that mass transfer was faster in well-ordered mesoporous samples than in the non-ordered homologues, but only at low protonation levels, and D_{app} values decreased dramatically in mesostructured materials due to major electrostatic shielding effects when generating charged moieties onto the internal surface of regular mesochannels.[157]

2.4 Selected applications of mesoporous silica materials in electrochemistry

2.4.1 Electroanalysis, sensors and biosensors

Applications in this field include mesoporous silica and organically-modified silicates in electroanalysis,[128] mesoporous silica-based materials for sensing[158] or biosensing,[159] and templated porous film electrodes in electrochemical analysis.[160, 161]

2.4.1.1 Direct detection - electrocatalysis

Mesoporous silica is a non-conductive metal oxide which can be used as such or functionalized with appropriate catalysts.[116]

In this way, mesoporous silica-based materials were employed to host mediators. Therefore, they were dispersed in carbon paste electrodes for electrocatalytic purposes.[116]

The immobilization of polyoxometalates or Prussian Blue derivatives have been achieved in (protonated) amine-functionalized mesoporous silica due to favorable electrostatic interactions.[162-164] The amperometric detection of NO_2^- [164] and ClO_3^-/BrO_3^-[163] was therefore achieved. A redox polymer based on the poly(4-vinylpyridine) complex of $[Os(bpy)_2Cl]^+$ quaternized with methyl iodide was immobilized onto a mesoporous silica for the electrocatalytic reduction of nitrite ions.[165] A more sophisticated approach described, is that of zinc phthalocyanine adsorbed on Ag/Au noble metal nanoparticles (NPs) anchored onto thiol-functionalized MCM-41(MCM = Mobil Composition of Matter), which exhibited synergistic effects for the electrocatalytic reduction of molecular oxygen.[166]

2.4.1.2 Preconcentration electroanalysis

Due to their sorption properties, ordered mesoporous silica were employed for the preconcentration electroanalysis of metal cations,[167] nitroaromatic compounds,[168] bisphenol A,[169] ascorbic and uric acids and xanthine,[170] nitro- and aminophenol derivatives,[171, 172] and some drugs.[173, 174] Chlorophenol was also successfully accumulated onto mesoporous titania prior to sensitive detection.[175]

Heavy metal species can accumulate on mesoporous silica by adsorption (e.g., Hg(II))[176]. Even so, the adsorbent properties of this material can be significantly improved by functionalization with suitable organic groups. Mesoporous organosilica have thus found many applications as nanoengineered adsorbents for pollutant removal,[177] but also as electrode modifiers for preconcentration electroanalysis.[128] Their main advantages are, firstly, the possibility of tuning the selectivity of the recognition event (and therefore the selectivity of the detection) by an appropriate selection of the organo-functional group and secondly, the well-ordered and rigid mesostructure ensuring fast transport of reactants (and thus high preconcentration efficiency and good sensitivity for the sensor).[116] The sensitivity has been significantly enhanced when using an electrode modified with a mesostructured adsorbent instead of the non-ordered homologue, when comparing Hg(II) detection subsequent to open-circuit accumulation at thiol-functionalized silica materials (Figure 5). This proved also the fastest mass transport processes in the mesostructures silica.[178] Many primary works were focused on simple functions such as thiol[179-181]or amine groups.[182] Several other organo-functional groups have been afterwards used when trying to improve the selectivity of the accumulation step, such as quaternary ammonium,[183] sulfonate,[184] glycinylurea,[185] salicylamide,[186] carnosine,[187] acetamide phosphonic acid,[188] benzothiazolethiol,[189] acetylacetone,[190] cyclam derivatives,[191, 192] β-cyclodextrin,[193] 5-

mercapto-1-methyltetrazole,[194, 195] or ionic liquids.[196] These materials are likely to accumulate analytes via complexation and ion exchange.[116]

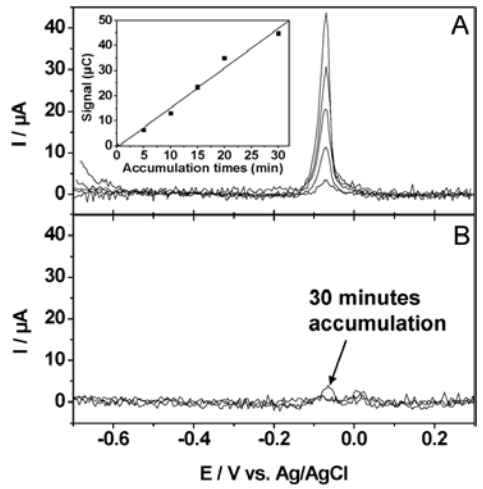

Figure 5 Influence of the preconcentration time on the voltammetric response of carbon paste electrodes modified with (A) a mercaptopropyl-functionalized mesoporous silica prepared from a TEOS/MPTMS 80 : 20 and (B) an amorphous silica gel grafted with the mercaptopropyl group; accumulation medium: $5 \cdot 10^{-7}$ M $Hg(NO_3)_2$ in 0.1 M HNO_3; detection medium: 3 M HCl; other conditions of the detection process: 1 min electrolysis at -0.7 V, followed by anodic stripping differential pulse voltammetric detection. Inset: variation of the stripping peak area with the accumulation time.[116]

Electrodes modified with mesoporous organic–inorganic hybrid silica have been employed to detect several analytes, such as Ag(I),[197] Cu(II),[192] Cd(II),[188] Hg(II),[180, 189] Pb(II),[179, 194] Eu(III),[186] U(VI).[198] The procedure generally involves first the preconcentration of the analyte in the mesostructured hybrid material, usually followed by its desorption in the detection medium, and subsequent quantitative electrochemical detection.[116] It was recently resorted to the detection of cations in a mixture (e.g., {Cd(II) + Pb(II) + Cu(II)}[181, 190] or {Hg(II) + Cd(II) + Pb(II) + Cu(II)}[196]) which were accumulated together before being selectively detected via voltammetric signals located at distinct potential values. Selectivity was sometimes achieved by the preferential recognition of the organo-functional group for the target metal in the presence of potentially-interfering species, which can be tuned by molecular engineering of the immobilized ligands.[116] Good selectivity for Cu(II)[191] was thus obtained by using mesoporous silica bearing cyclam groups, while the addition of acetamide arms on the cyclam centres resulted in shifting the selectivity towards Pb(II).[192] Both film and bulk composite electrode configurations were tested for preconcentration/voltammetric detection and it resulted that the response time of film

electrodes is often slower, especially at low analyte concentration, due to the fact that the accumulation starts on the upper part of the film contacting the solution, and thus there are very low amounts of accumulated species when operating in dilute solutions, some of them being lost after desorption in the detection medium and therefore not detectable on the electrode surface.[195] But when very thin films with mesopore channels oriented normal to the underlying electrode are employed, this effect will be minimized and the recognition even will be accelerated.[116] It should be noted that unlike the non-ordered silica gels, ordered mesoporous adsorbents can give rise to more sensitive detection in preconcentration electroanalysis, but this is applicable only when the rate determining step is the diffusion of the analyte in the material, not in the case of kinetics dominated by the complexation reaction itself.[199] Organic species like bisphenol A[200] or dihydroxybenzene isomers[201] after accumulation at aminopropyl-grafted SBA-15 (SBA = Santa Barbara Amorphous) could also be determined using functionalized mesoporous silica. A possibility to improve selectivity by rejecting interferences is by using organically-modified mesoporous silica films as permselective barriers. This was demonstrated for aminopropyl-functionalized films exhibiting ion-permselective pH-switchable behavior.[202-204]

2.4.1.3 Electrochemical biosensors and related devices

An electrochemical biosensor requires an effective and durable immobilization of huge amounts of biomolecules in an active form, and a favorable environment for efficient electron transfer reactions. Due to their attractive properties (large surface areas for immobilization of reactants and biocomponents, interconnected pore systems to ensure fast accessibility to active centres, intrinsic electrocatalytic properties or support for electrocatalysts, possibility of functionalization) silica-based mesoporous materials have been intensively applied in this field.[116]

- *Immobilization of heme proteins, direct electrochemistry and electrocatalysis*

Direct electrochemistry could be registered for heme proteins, such as cytochrome *c*,[205, 206] haemoglobin,[207, 208] or myoglobin,[209, 210] when immobilized in non-conductive mesoporous silica particles or continuous mesoporous silica layers deposited as thin films on electrode surfaces. The well-defined voltammetric responses obtained in these cases indicate that the proteins retain their biological activity once immobilized within the mesoporous material. The amounts of immobilized proteins are influenced by the pore structure and size of the host material (e.g., hemoglobin almost excluded from MCM-41 while fitting well inside SBA-15[211]) and, at similar loadings, the interconnected 3D or bimodal mesostructures resulted in higher current responses.[211, 212] Additives were used in some cases to improve the electron transfer reactions (e.g., ionic liquids[213]), or to prevent leakage of the protein out of the material

(e.g., chitosan[212]). As a result of their peroxidase activity, the immobilized heme proteins were sensitive to the presence of hydrogen peroxide, showing an electrocatalytic response towards hydrogen peroxide.[205, 207, 209, 210, 212, 213] Electrode configuration set the sensitivity of the device, while the addition of gold nanoparticles or CdTe quantum dots were reported to enhance the biosensor response.[214, 215]

- *Enzyme immobilization and electrochemical biosensors*

Mesoporous silica-based materials are suitable immobilization matrices for enzymes, as they keep their biological activity,[144-147] and for biosensor construction.[159] The first generation biosensors implied the enzyme immobilization on the material and the electrode was used to detect the enzymatically-generated products (e.g., GOX or HRP entrapped in mesoporous silica particles deposited as thin films on GCE[216-218]). Larger pore sizes were necessary for the nonconductive silica matrices, to ensure fast mass transport processes.[116] In order to overcome this problem, it was resorted to the increase the conductivity by incorporating gold nanoparticles,[219] via the use of conducting polymers,[220] or via the formation of silica–carbon composite nanostructures.[216] A hydrogen peroxide biosensor was also constructed using a purely organic ordered mesoporous polyaniline film, fabricated by electrodeposition from a lyotropic liquid crystalline phase, as an immobilization matrix for HRP.[221] The development of bienzymatic systems based on the co-immobilization of two enzymes (e.g., tyrosinase and HRP[222] or 2-hydroxybiphenyl 3-monooxygenase and GOX[223]) suggested that the confined environment of the mesoporous silica host preserves the necessary interactions.

- *Electrochemical immunosensors and aptasensors*

Due to their hosting properties, MPS were employed in fabricating ultrasensitive electrochemical immunosensors. There are two different approaches to be distinguished between for the electrochemical detection of the antigen–antibody recognition event. The first one refers to the use of mesoporous silica nanoparticles (in which the enzyme, e.g., HRP, a mediator and a first antibody have been immobilized) as nanolabels.[224] They are expected to bind to an electrode surface (bearing a second antibody) in the presence of the analyte (the antigen, in a sandwich configuration between the two complementary antibodies), and the resulting current response is directly proportional to the amount of nanolabels onto the electrode surface, and thus to the analyte concentration.[224] By improving the electronic conductivity of the nanolabel and the electrode surface, better performance of the device could be achieved.[225-227] The second approach deals with an antibody still immobilized on the mesoporous material, but coated this time on the electrode surface, while the mediator is in the solution; when the immunoconjugates are formed, the electrode becomes progressively blocked, while the signal of the electrochemical response decreases proportionally to the target analyte concentration.[228-230] More recently, some new

kinds of label-free aptasensors were described, based on graphene-mesoporous silica–gold NP hybrids as an enhanced element of the sensing platform[231-233] for the detection of ATP[231] or DNA.[232]

2.4.1.4 Other electrochemical sensors

Due to their sorption properties, mesoporous silica could be exploited in the development of electrochemiluminescence sensors.[234] Some examples dealing with electrochemical detection methods (i.e., conductivity changes, surface photovoltage measurements) include mesoporous silica for sensing alcohol vapours[235] or detection of humidity changes,[236] and tin-doped silica for NO_2 sensing.[237]

2.4.2 Energy conversion and storage

Nanoscaled engineering materials have become an important mean in designing various devices for energy conversion and storage.[116] Taking into consideration the increasing need for improved systems like batteries, supercapacitors, fuel cells, or dye-sensitized solar cells, finding innovative electrode materials with architecturally tailored nanostructures is an important focus in the research field.[116] Therefore, proton-conducting organic-inorganic hybrids, like mesoporous silica containing sulfonic acids, phosphonic acid or carboxylic acid, can be used as membranes for fuel cells, because they are likely to exhibit good thermostability and efficient proton conductivity at high temperature and low humidity.[238]

PERSONAL CONTRIBUTION

1 Clays – physico-chemical and structural characterization

1.1 Introduction

"Clay" is a collective term for a large group of sedimentary rocks with clay minerals as main components. They are generally fine-grained crystalline hydrated aluminum silicates and they exhibit plasticity when mixed with water in certain proportions.

Bentonites are clay materials and represent secondary rocks formed from the devitrification, hydration and hydrolysis of other underlying rocks (e.g. volcanic tuffs, pegmatite etc.). An important feature of all bentonites is their important content of montmorillonite with its cryptocrystalline aggregate structure, at which low fractions of quartz, feldspar, volcanic glass, amphibole, pyroxene, chlorite, limonite, halloysit, etc. are added.[239]

The name "montmorillonite" was assigned to the clay mineral with the theoretical formula $Al_2(Si_4O_{10})(OH)_2$, which has a relatively high content of water molecules adsorbed between its layers.

The most commonly accepted structure for montmorillonite minerals is similar to that of pyrophyllite, from which it differs only in the distribution of constitutive ions and in the overlapping of multiple sheets. Therefore, montmorillonite consists of two tetrahedral silica plans and a central octahedral aluminum plan.

An invariable feature of montmorillonite structure is that water and other polar organic molecules can enter the interlayer space, resulting in a shift towards the (c) axis. The dimensions of (c) axis in montmorillonite are not fixed, but vary from 9.6 Å, when there are no polar molecules in the interlayer space, up to 15 Å, in the presence of polar molecules (Figure 6). The thickness of the water layer between the structural units depends on the nature of the adsorbed cation and on the pressure of water vapors of the working environment.[240]

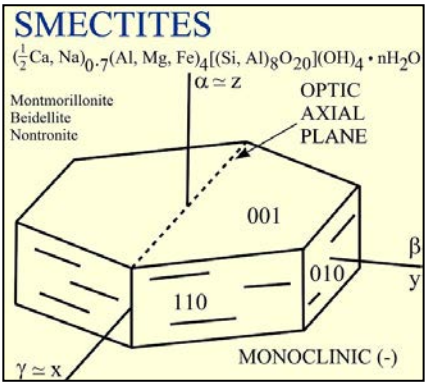

Figure 6 Smectites structure[241]

Romanian clays are cationic clays, with negatively charged alumino-silicate layers. The clays presented in this thesis are bentonites obtained from Răzoare and Valea Chioarului deposits in operation (Maramureş County, Romania). In order to compare their electrochemical behavior with their internal structure and properties, the structural characterization of the above measured clays was achieved.

1.2 Materials and methods

Physico-chemical composition studies, as well as X-ray diffraction (XRD) and transmission electron microscopy (TEM) established the properties of the two clays.

For the structural characterization of Răzoare and Valea Chioarului bentonites, it was resorted to their impurities removal, in order to obtain a higher content of montmorillonite in the resulting samples. The refinement was achieved by washing and decantation obtaining a more homogeneous product, rich in montmorillonite, the main component of their structure. All of the following characterization procedures and analytical experiments are based on these refined clay samples.

Separation was performed on different clay granulometric particle sizes by sedimentation, decantation, centrifugation, and ultracentrifugation after the procedures reported in the literature[242], according to Stockes' law. Several fractions, below 50 μm, 20 μm, 8 μm, 5 μm, 2 μm, 1μm, and below 0.2 μm were separated and characterized.

The chemical composition, the ion exchange capacity, the surface area, and the structural characteristics, *e.g.* particle size and shape, of each separated fraction were determined by XRD and TEM.

Chemical composition was achieved by gravimetry (Si), complexonometry (Fe, Al, Ca, Mg), colorimetry (Ti at 436 nm), and flame photometry (Na at 589 nm, K at 768 nm). Ion exchange capacity was obtained by treating the clay sample with an ammonium chloride solution, followed by the filtration and determination of Ca and Mg (by complexonometry), Na and K (by flame photometry).

For TEM studies, an aqueous suspension of clay was deposited on a thin layer of collodium, followed by evaporation. Examination of the samples was achieved using a JEOL JEM 1010 microscope.

Diffractometry was achieved on fine powder material using a Shimadzu X-ray diffractometer XRD 6000 N, equipped with a monochromator and a position-sensitive detector. The X-ray source was a Cu anode (40kV, 30 mA).The diffractogram were recorded in the 0-90º 2θ range, with a 0.02 step size and a collection of 0.2 s per point.

Surface area analyses were recorded with a Thermo analyzer Q Finnigam type SURF 9600 by single point method, on Răzoare clay fraction bellow 20 μm and on Valea Chioarului clay sample bellow 50 μm, respectively, without any previous thermal treatment.[239]

Thermal behavior was also studied using differential thermal analysis performed with a MOM derivatograph, type 1500D, at 10 ^{o}C/minute temperature rate, in the range of 20 ^{o}C and 1000 ^{o}C.[243, 244]

IR analyses were recorded with a Brucker FTIR spectrometer, on Răzoare clay fraction bellow 20 μm and Valea Chioarului clay fraction bellow 0.2 μm in KBr matrix, from 4000 to 400 cm^{-1}.[243]

1.3 Results and discussions

Elemental analyses confirmed clays chemical composition and revealed the differences between the two clays (Table 1). Bentonites have a high content of SiO_2 and Al_2O_3 and also significant water content. The components present in small quantities and in varying proportions are: MgO, CaO, K_2O, Na_2O, Fe_2O_3 and TiO_2. Elements such as Mg^{2+} and Fe^{3+} act as substitutes of Al^{3+} in the octahedral configuration. Alkaline metals and Ca^{2+} can fix by adsorption means in the spaces between the structural packages of the clay. The structural formulas of the clay minerals are: Răzoare $(Ca_{0.03}\ Na_{0.30}\ K_{0.06})_{\Sigma=0.39}\ (Al_{1.54}\ Mg_{0.37}\ Fe_{0.10})_{\Sigma=2.01}\ (Si_{3.84}\ Al_{0.16})_{\Sigma=4.00}\ O_{10}(OH)_2 \cdot nH_2O$, and Valea Chioarului $(Ca_{0.06}\ Na_{0.27}\ K_{0.02})_{\Sigma=0.35}\ (Al_{1.43}\ Mg_{0.47}\ Fe_{0.10})_{\Sigma=2.00}\ (Si_{3.90}\ Al_{0.10})_{\Sigma=4.00}\ O_{10}(OH)_2 \cdot nH_2O$.

Table 1 Chemical composition of Răzoare and Valea Chioarului bentonites [239]

Sample	SiO_2	TiO_2	Al_2O_3	Fe_2O_3	CaO	MgO	Na_2O	K_2O	L.C.*
Răzoare	68.60	0.22	13.89	1.36	0.30	3.38	1.50	0.45	11.30
Valea Chioarului	59.82	0.25	16.14	1.67	0.70	3.92	1.75	0.25	15.50

* Loss on calcination process at 1000°C

The higher SiO_2 quantity in the composition of Răzoare bentonite indicates the presence of an increased quantity of impurities (e.g., cristobalite).

TEM images of Răzoare (Figure 7A) and Valea Chioarului clays (Figure 7C) at higher magnification showed a diffusive, irregular, and opalescent surface. The very fine dispersed montmorillonite (bellow 0.2 nm) formed extremely thin lamellar layers with nanometer dimensions (Figure 7B).

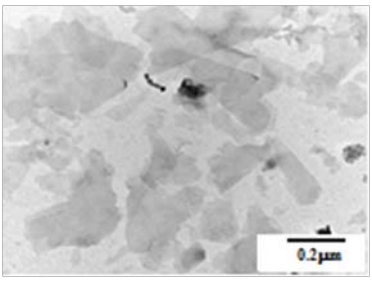

(A)

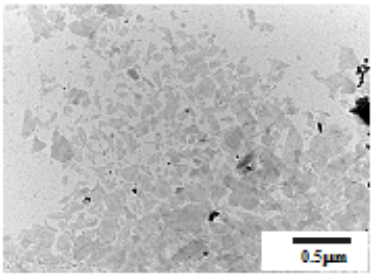

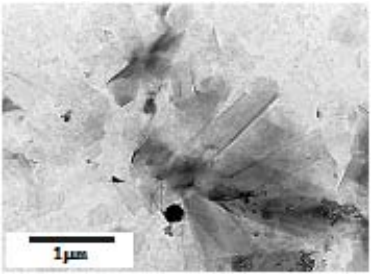

(B) (C)

Figure 7 TEM characterization Răzoare (A, B) and Valea Chioarului (C) clays

The XRD diffractogram of Razoare clay, fraction bellow 20 µm (Figure 8A) displayed the characteristic diffraction peaks of montmorillonite at 2θ (7.12°; 19.68°; 21.57°; 28.14°; 36.04°; 61.66°) and also the presence in smaller quantities of other minerals, such as cristobalite at 2θ (20.68°; 26.50°; 36.36°; 42.10°; 54.70°; 59.67°), feldspar at 2θ (23.22°; 24.10°; 27.74°; 35.08°), etc.[239, 245]

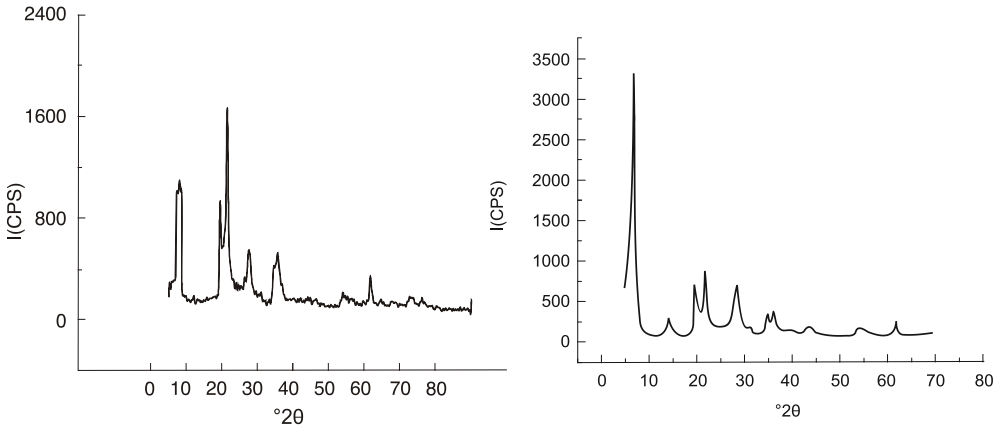

Figure 8 XRD diffractograms of Răzoare (A) and Valea Chioarului clays (B)

The XRD diffractogram obtained for Valea Chioarului clay using a sample with particle size below 0.2 μm (Figure 8B) showed a high content of montmorillonite (with its characteristic peaks at 2θ: 6.94°; 19.96°; 21.82°; 28.63°; 36.14°; 62.01°), which confirmed the position of the diffraction peaks, in agreement with literature data[245], and also the almost negligible presence of other minerals.

The presence of montmorillonite was also proved by comparing the XRD data of the below 0.2 μm sample before and after treatment with ethyleneglycol. After adsorption of ethylenglycol, it was noticed an increase in the reticular distance in c axis direction from 12.72 Å to 17.18 Å, corresponding to 6.9434° and to 5.137° peaks, respectively, characteristic for montmorillonite.

XRD diffraction patterns (see Figure 8A and 8B) illustrate the fact that the two investigated samples are multiple phase bentonite materials containing mainly montmorillonite hexagonal ($Na_{0.3}Al_2Si_4O_{16}H_{10}$) and cristobalite ($SiO_2$) crystalline phases.

Table 2 Quantitative crystalline phase analysis and the effective crystallite mean size, D_{eff} (nm), the root mean square (rms) of the microstrains , $<\varepsilon^2>^{1/2}_m$ and profile (Rp) discrepancy indices calculated by Rietveld refinement for the montmorillonite crystalline phases (X1=Valea Chioarului clay; R1=Răzoare clay)

Samples	montmorillonite [% vol.]	cristoballite [% vol.]	amorphous [% vol.]	D_{eff} [nm]	$<\varepsilon^2>^{1/2}_m \times 10^3$	R_p
X1	74.7	14.5	10.8	15.2	0.413	12.2
R1	19.6	43.0	17.4	10.4	2.846	14.3

Table 3 The unit cell parameters and profile (Rp) discrepancy indices calculated by Rietveld refinement analysis for the montmorillonite and cristoballite crystalline phases (X1=Valea Chioarului clay; R1=Răzoare clay)

Samples	a [Å]	b [Å]	c [Å]	R_p
X1 montmorillonite	5.17	5.17	12.624	17.2
X1-cristobalite	6.46	6.46	6.46	22.3
R1 montmorillonite	5.06	5.06	12.544	19.6
R1 -cristobalite	6.64	6.64	6.64	26.8

The fact that the intense peak that appears in the XRD pattern at 2θ = 7.9° (d = 1.23 nm) for montmorillonite compounds in the X1 sample is moved at 2θ = 8.2° (d = 1.21 nm) for the R1 sample (where it appears less intense) seems to indicate that the layered type of montmorillonite structure in Răzoare bentonite is largely deformed by different impurities.

The value of the specific surface of the sample bellow 20 μm of Răzoare clay was 50 m^2/g. Due to the aggregation effect which occurred during the drying process of the fine granulation prepared clay, the specific surface of the Valea Chioarului clay was determined on the sample below 50 μm. The obtained value was 190.86 m^2/g.

The ion exchange capacity of the analyzed clays was determined by replacing the compensatory ions with NH_4^+ ions, followed by their quantitative determination. Therefore, the ionic exchange capacity of Răzoare clay was 68.32 mE/100g and for Valea Chioarului clay it was estimated at 78.03 mE/100g.[239]

In order to complete the structural characterization of the Romanian clays several experiments were performed. The FTIR studies and the thermodifferential analysis showed the presence of a high percentage of montmorillonite.

Thus, the FTIR spectrum of Răzoare clay (Figure 9A) revealed the characteristic groups of montmorillonite. The broad band at 3447 cm^{-1}, with its specific peak at 3620 cm^{-1}, was attributed to the stretching vibration of the hydroxyl group. The bands at 1000-1200 cm^{-1} and 466 cm^{-1} were produced by the Si-O stretching vibration. The bands at 793 cm^{-1} and 519 cm^{-1} were assigned to the Si-O-Al group.[243, 246]

The FTIR spectrum of Valea Chioarului clay (Figure 9B) presented a broad band at 3446 cm^{-1} with the specific peak at 3625 cm^{-1} attributed to the stretching vibration of the hydroxyl group.[244] The broad band at 1000-1200 cm^{-1} was assigned to the Si-O stretching vibration and the band at 520 cm^{-1} to the Si-O-Al group, all attributed to the characteristic groups of montmorillonite. In both cases the band at 1637 cm^{-1} was assigned to the bending vibration of H-O-H group.[243, 246]

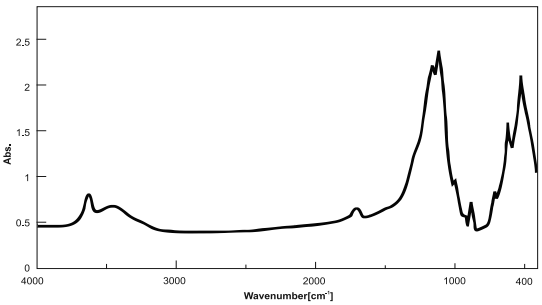

(A)

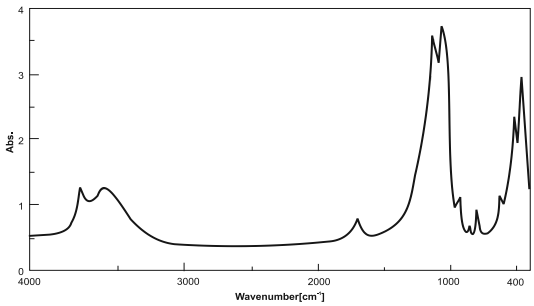

(B)

Figure 9 FTIR spectra of Răzoare (A) and Valea Chioarului clays (B)

Regarding the thermodifferential analysis (Figure 10) of Răzoare and Valea Chioarului clays, a good superposition of the thermodifferential characteristic curves of montmorillonite was noticed, confirming that montmorillonite is the main constituent of both Romanian clays.

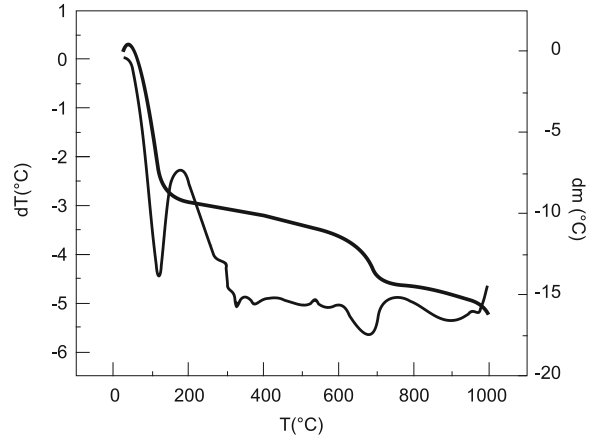

(A)

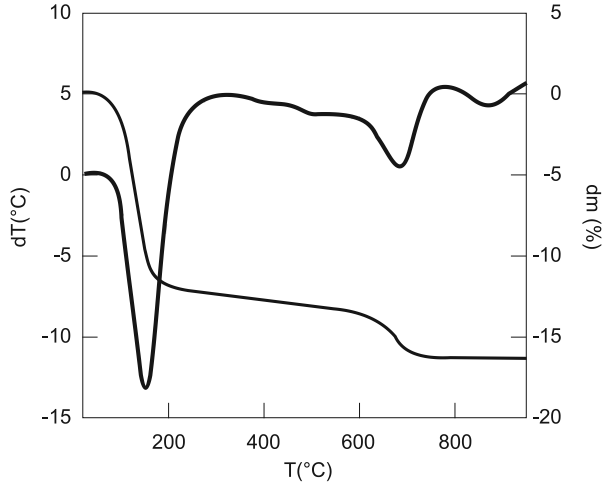

(B)

Figure 10 Thermodifferential analysis of Răzoare (A) and Valea Chioarului clay (B)

The thermogravimetric (TGA) and thermodifferential (TDA) analysis of Răzoare clay (Figure 10 A) showed the loss of the adsorbed water between 60° C and 200° C, accompanied by a strong endothermic effect at 115° C. The elimination of hydroxyl groups from the mineral network with an endothermic effect and decrease of mass occurs between 600° C and 750° C. The last endothermic effect, at 900° C, immediately followed by an exothermic one, showed a modification of the crystal structure to an inferior energetic state.

The first pronounced endothermic effect in the TDA curve (Figure 10 B) appeared between 60° C and 250° C due to the water loss. A substantial decrease in the clay mass occurred in the meantime according to the TG curve. Dehydration was a reversible process, at 250° C the clay being able to readsorb the water molecules, which could be then eliminated due to a new temperature exposure[243, 247, 248]

The second endothermic effect appeared between 600° C and 750° C, followed by a loss in the clay mass due to the elimination of hydroxyl groups. A third endothermic effect occurred at 880° C, immediately followed by an exothermic effect at 900° C due to the crystal structure modifications.[243, 247, 248]

1.4 Conclusions

Two Romanian clays from Răzoare and Valea Chioarului deposits (Maramureş County) were refined and characterized by X-ray diffraction, transmission electron microscopy, FTIR, and thermogravimetric and thermodifferential analysis. The ion exchange capacity of purified clays was determined by replacing the compensatory ions with NH_4^+ ions.[239, 243]

The clay chemical composition was confirmed by elemental analyses and the characteristic formulas for the two clays could be calculated. The diffusive, irregular, and opalescent surface of Răzoare and Valea Chioarului clays was evidenced by TEM images and the extremely thin lamellar layers of montmorillonite with nanometer dimensions were also described. The XRD diffractograms of both clays showed the characteristic diffraction peaks of montmorillonite. The presence of other minerals like quartz and feldspar was also evidenced. The specific surface for Răzoare clay was 50 m^2/g, while the value obtained for Valea Chioarului clay was 190.86 m^2/g.

The ionic exchange capacity of Răzoare clay was 68.32 mE/100g and for Valea Chioarului clay it was estimated at 78.03 mE/100g.

FTIR spectra of both clays revealed the characteristic peaks of montmorillonite and the good superposition of the thermodifferential characteristic curves confirmed its presence in both analyzed clays.

As a conclusion, all characterization methods employed revealed montmorillonite as the main component of Răzoare and Valea Chioarului clays structure. Due to its higher CEC value and larger specific surface, together with a negligible quantity of impurities, Valea Chioarului clay is highly recommended for further electroanalytical applications.

2 Electroanalytical characterization of two Romanian clays with possible applications in pharmaceutical analysis

2.1 Introduction

The high demand for simple, fast, accurate, and sensitive detection methods in pharmaceutical analysis has driven to the development of novel electrochemical sensors. CLME are likely to be used for this application.

Therefore, it is well known that montmorillonite has been used for centuries to produce ceramics. Furthermore, its applications in pharmacy, adsorbents, and ion exchangers are also reported in the literature.[7, 8] These last applications are particularly useful for the development of electrochemical sensors.[2, 239]

Clay modified electrodes have attracted considerable attention attempting to control the path and scale of electrode reactions.[3, 20, 21, 249-251] The composition of the CPE modified with clay was defined as a complex heterogeneous system consisting of conductive solids, semiconductors, and insulators, including a clay-induced aqueous phase. Phenomena of charge and mass transfer in such mixtures are extremely complicated and require a thorough characterization, moreover because the clays included in the electrode material are natural compounds whose composition and structure are subject to their place of origin. In spite of the wide range of electrode modifiers, clays have attracted the interest of electrochemists, in particular for their analytical applications.[3, 239, 252-254]

Electrochemical methods are well known as very sensitive, but they lack selectivity. Electrode modification is therefore the main issue in improving selectivity. This is why the different ways of modifying the electrode surface in order to obtain improved electrochemical signals represents a concern for researchers all over the world.

Electrode modifications concern either the improvement of sensor selectivity by increasing the affinity for a specific analyte and rejecting, in the same time, other interfering chemical species, or the improvement of the electroanalytical performances (higher accuracy and reproducibility, lower detection and quantification limits, the

possibility to determine several electroactive species without any separation process, at different oxidation or reduction potentials).

Generally, chemical sensors contain two basic functional units: a *receptor part* which transforms the chemical information into a measurable form of energy, and a *transducer part* capable to convey the energy carrying the chemical information about the sample into a useful analytical signal.

Biological sensors can be defined either as devices able to detect the presence, the movement, and the number of organisms in a given environment, or as sensors which contain in their structure a biological component (bacteria, algae, tissues, cells) as receptor, this type of devices being known as biosensors.[255] In the living world, there are a lot of examples of sensors consisting in biological receptors (proteins, nucleic acids, signaling molecules) located on the cell membrane, in all the tissues, organs, or even in circulating blood stream. Enzymes were used for decades in the sensors development and this led to the urge for a niche field in research: biosensors. More specific biosensors could be defined as sensitive and selective analytical devices which associate a biocomponent to a transducer.[256] Biosensors are applied with success in several fields (environment, food security, biomedical and pharmaceutical analysis), especially because of the stable source of the biomaterial (enzymes produced by bacteria, plants, or animal as by-products), and due to their catalytic properties and the possibility of modifying the surface of transducers in various ways.

A key step in the development and optimization of the biosensors is related to the entrapment of the enzymes at the surface of electrode, another challenge being to preserve the microenvironment of the enzyme and hence the lifetime of the biosensor. Besides the methods used before, like adsorption, cross linking, covalent binding, biological membranes, magnetic microparticles, entrapment in sol–gel, etc., the immobilization into an electrochemical polymer or polymerizable matrices was successfully used in the development of the amperometric biosensors.[256] In this case, the procedure was effective and simple and the enzyme was less affected than during other methods of entrapment.

Adsorption of proteins on clay mineral surfaces represents an important application in fields related to the agricultural and environmental sciences, but also in the pharmaceutical and biomedical analysis.[9, 243]

Organic molecules, macromolecules, and biomolecules can be easily intercalated in solids with a 2D structural arrangement that have an open structure. Therefore, clay minerals are likely to be exploited to improve the analytical characteristics of biosensors. This type of biosensors is based on three smectite clays (laponite, montmorillonite, and nontronite) and on layered double hydroxides.[2, 243]

Due to their low price and accessibility, clays offer a new immobilization method for biomolecules like enzymes. Hydrated clays represent a good environment for enzyme functioning and can improve the lifetime of the biosensor. On the other hand, a lot of electrochemical processes are controlled by diffusion and clays, due to their adsorbent properties, can improve or accelerate the diffusion of different molecules (pharmaceuticals in our case) at the electrode surface. In this way, electrochemical parameters can also be improved, allowing the recording of higher currents at lower potentials, and developing thus new electroanalytical methods with enhanced performances.

Clays show also some disadvantages, the clay deposition and the thickness of the clay film on the electrode surface being factors that can decrease the electric conductivity. In this case, the use of conductive polymers, like PEI or polypyrrole, for the clay film immobilization at the electrode surface represents a good alternative. In spite of the water and alcohol solubility of PEI, this polymer does not involve any further polymerization process (such as the use of heat, the polymerization initiators or the potential scanning) which can damage the enzyme structure and functioning.

The development of composite electrodes for biosensors construction based on HRP and clay films for acetaminophen (*N*-acetyl-*p*-aminophenol) detection is described. Acetaminophen is widely used as analgesic antipyretic drug having actions similar to aspirin. It is a suitable alternative for the patients who are sensitive to aspirin and safe in therapeutic doses. HRP has been a powerful tool in biomedical and pharmaceutical analysis. Many biosensors based on HRP applied in biomedical and pharmaceutical analysis are mentioned in the literature.[256, 257] The enzyme immobilization was performed by retention in a PEI and clay porous gel film, technique that offers a good entrapping and, in the meantime, a "protective" environment for the biocomponent.[243]

In this study, the refined bentonites obtained from Răzoare and Valea Chioarului deposits were used to modify CPEs. The electrochemical behavior of acetaminophen, ascorbic acid, and riboflavin phosphate was tested by cyclic voltammetry on the clay-modified CPEs with different clay particle sizes. The resulting CPEs revealed either better electroanalytical signals or oxidation at lower potential. The exploitation of Romanian clays in developing a biosensor for acetaminophen detection with good sensitivity and reproducibility was also achieved. The development of new clay-modified sensors using such composite materials based on micro and nanoparticles could be applied in pharmaceutical analysis.[239] The studies presented in this chapter are preliminary studies. By employing the three standard pharmaceutical substances, these studies didn't aim at the development of new analytical methods with improved sensitivity and selectivity (even they showed this could be achieved further on), but to emphasize the adsorbent and ion exchange properties of the Romanian clays. Based on

these principles, the tested molecules chosen were neutral (acetaminophen), anionic (ascorbic acid), and cationic (riboflavin).

2.2 Materials and methods

Clay water suspensions of 50 mg/mL were prepared for the fractions bellow 20 μm and 0.2 μm for Valea Chioarului clay and below 20 μm for Răzoare clay. Standard solutions of acetaminophen, riboflavin, and ascorbic acid were prepared to provide a final concentration of 10^{-3} M.

For biosensor development, standard solutions of acetaminophen and hydrogen peroxide were prepared to provide a final concentration of 10^{-4} M for acetaminophen and 0.1mM for hydrogen peroxide. The stock solutions of acetaminophen were dissolved in phosphate buffer and kept in the refrigerator. All the experiments were performed in PBS (phosphate buffer saline) (pH 7.4; 0.1M) at room temperature (25 ºC).

CPEs were modified by mixing different Răzoare clay concentrations (1%, 2.5%, 5%, and 10%) with "homemade" carbon paste prepared with solid paraffin.[239, 258]

Electrochemical studies, like cyclic voltammetry (CV) and chronoamperometry, were performed in a conventional three-electrode system: new modified carbon based electrodes (working electrodes), platinum (auxiliary electrode), Ag/AgCl 3M KCl (reference electrode), under stirring conditions. All the CV experiments were recorded at 100 mVs^{-1}. During chronoamperometry experiments the biosensor potential was kept at 0 V vs. Ag/AgCl under continuous stirring conditions. The working potential was imposed and the background current was allowed to arrive at a steady state value. Different amounts of acetaminophen standard solution were added, every 100 seconds, into the stirred electrochemical cell and the current was recorded as a function of time.

The obtained configuration was used to study the biocatalytic oxidation of acetaminophen in the presence of the hydrogen peroxide.[243]

The experiments were achieved with AUTOLAB PGSTAT 30 (EcoChemie, Netherlands) equipped with GPES and FRA2 software. The pH of the solution was measured using a ChemCadet pH-meter.

All solutions were prepared by using high-purity water obtained from a Millipore Milli-Q water purification system.

Paraffin (Ph Eur, BP, NF), graphite powder, acetaminophen (minimum 99.0 %), L-ascorbic acid (99.0 %), and riboflavin (Ph Eur) were provided by Merck and

KCl (analytical grade) from Chimopar Bucureşti. All reagents were of analytical grade, used as received, without further purification.

HRP (Peroxidase type II from Horseradish, EC 232-668-6), acetaminophen, hydrogen peroxide, monosodium phosphate, and disodium phosphate were provided by Sigma Aldrich; PEI (50 % in water, Mr 600000 – 1000000, density 1.08 g/cm^3 (20 ^{o}C)) was purchased from Fluka.

All reagents were of analytical grade, used as received.

Composite film electrodes (PEI/clay/GCE) were prepared as follows: PEI (5 mg) was stirred for 15 minutes in absolute ethanol (125 µL) and distilled water (120 µL), then 6.5 µL of nanoporous clay gel were added and stirred again for 15 minutes. Two different suspensions (20 µL) containing Valea Chioarului clay particles with the diameter below 20 µm and below 0.2 µm were deposited on the surface of two different GCEs and dried for 4 hours at 4°C.[243]

GCEs were provided by BAS Inc. (West Lafayette, USA) and were carefully washed with demineralized water and polished using diamond paste (BAS Inc.).

2.3 Results and discussions

The electrochemical behavior of several clay-modified electrodes was tested in the presence of some pharmaceutical compounds: acetaminophen, ascorbic acid, and riboflavin phosphate (Figure 11). The electrochemical behavior of these three selected redox probes (neutral, negatively and positively charged, respectively) is widely discussed in the literature on different electrode materials (Pt, carbon paste, glassy carbon, etc.) which enables the comparison between the resulting electrochemical performances with those described by other authors. Taking into consideration the adsorbent properties of the investigated clays, the study aimed to improve the oxidations and reductions potentials obtained on unmodified CPEs.

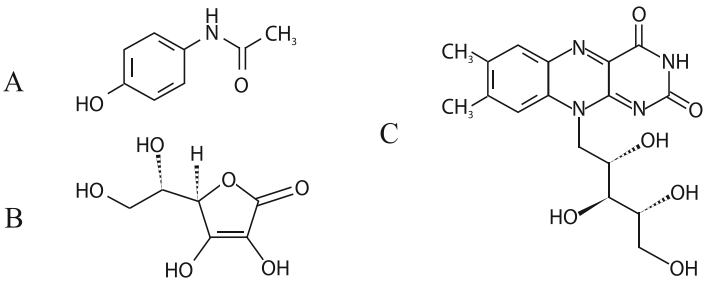

Figure 11 Chemical structures of investigated pharmaceuticals: (A) acetaminophen, (B) ascorbic acid, and (C) riboflavin[239]

Acetaminophen (N-acetyl-p-aminophenol) is one of the most commonly used analgesics in pharmaceutical formulations for the reduction of fever and also as a painkiller for the relief of mild to moderate pain associated with headache, backache, arthritis, and postoperative pain. Acetaminophen is metabolized primarily in the liver, into toxic and non-toxic products. The hepatic cytochrome P450 enzyme system metabolizes acetaminophen, resulting in a minor yet significant alkylating metabolite known as NAPQI (N-acetyl-p-benzo-quinone imine). NAPQI is then irreversibly conjugated with the sulfhydryl groups of glutathione:

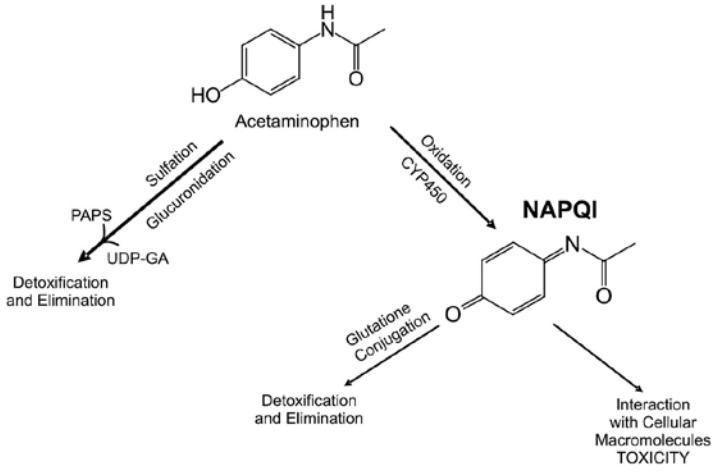

Ascorbic acid is a naturally occurring organic compound with antioxidant properties. As a mild reducing agent, it degrades upon exposure to air, converting the oxygen to water. The redox reaction is accelerated by the presence of metal ions and

light. Ascorbic acid can be oxidized by one electron to a radical state or doubly oxidized to the stable form called dehydroascorbic acid:

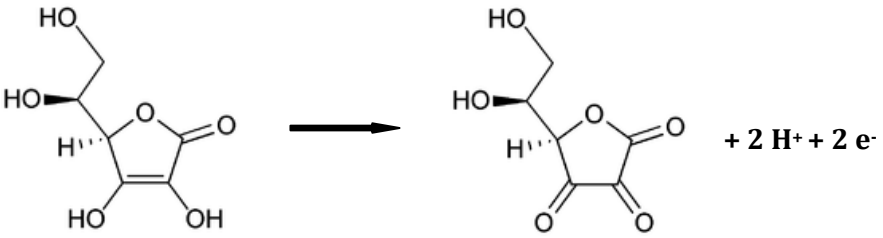

Riboflavin, also known as vitamin B_2, is a colored micronutrient, easily absorbed, with an important role in humans and animals health maintenance. This vitamin is the central component of the cofactors FAD and FMN, being therefore required by all flavoproteins. As such, vitamin B_2 is implied in a wide variety of cellular processes, playing a key role in energy metabolism, but also in the metabolism of fats, ketone bodies, carbohydrates, and proteins. The reversible oxidation and reduction processes of riboflavin take place as follows:

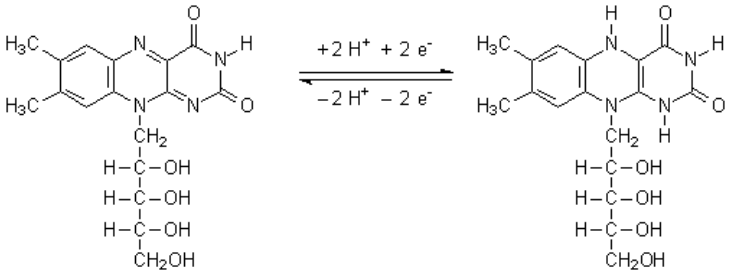

Acetaminophen and ascorbic acid (Figure 12A and 12B) showed relatively similar electrochemical behavior in CV investigations, one irreversible oxidation peak being obtained at 0.78 V and 150 μA for acetaminophen and 200 μA for ascorbic acid with 1% clay-modified CPEs (due to the two electron transfer described in the chemical reactions above). In both cases, the increase in the clay content was followed by an important shift of the oxidation potential towards lower values, 0.70 V for acetaminophen and 0.60 V for ascorbic acid, showing that the increasing clay concentration facilitates the oxidation process (ΔE = 100 - 150 mV).

In both cases, during the anodic potential sweep, voltammetric peaks were formed revealing that acetaminophen and ascorbic acid electrochemical oxidation

reactions are diffusion-controlled processes. Moreover, also in both cases, during the cathodic potential scan no significant currents were detected, thus both oxidation processes are irreversible.

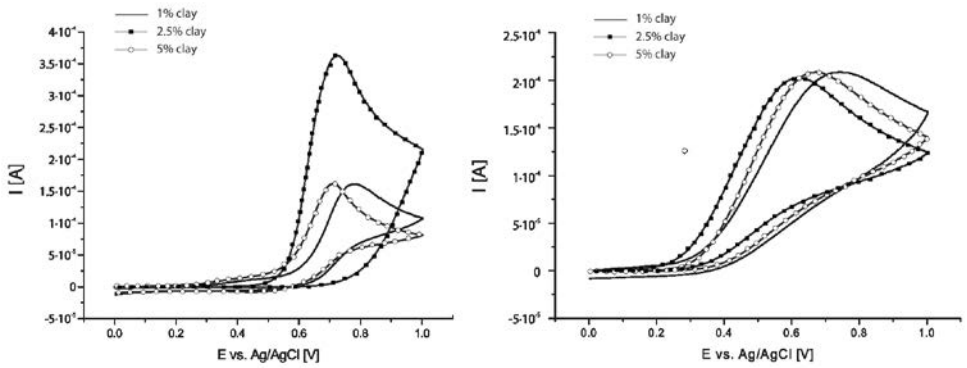

(A) (B)

Figure 12 Cyclic voltammograms of 10^{-3} M acetaminophen (A) and 10^{-3} M ascorbic acid (B) on 1% (solid line), 2.5% (square line), and 5% (dot line) Răzoare clay-modified CPEs (KCl 0.1 M, 100 mVs^{-1})[239]

In the case of acetaminophen, an increase in the current from 150 to 350 μA could be observed in the oxidation range at the 2.5 % clay-modified CPE, while for the 5 % clay-modified CPE the current had the same order of magnitude as the 1% clay-modified CPE (Figure 12A).

Ascorbic acid showed a different behavior, the increase in the clay content having no influence on the current range, but facilitating the oxidation reactions, proved by the above mentioned shift of the anodic potential towards lower values (Figure 12B). This can be attributed to the electrostatic repulsion between the negatively-charged clay sheet and the negatively-charged molecule.

Riboflavin phosphate exhibited a typical reversible cyclic voltammetric response at unmodified carbon paste electrode, with an oxidation peak at - 0.45 V and a reduction peak at - 0.60 V as presented in Figure 13. The electrostatic attraction between the positively-charged molecule and the negatively-charged clay sheets is very clear in this case.

Anodic currents increased proportionally with the clay content with about 5 nA and 10 nA for the 5% and the 10% clay-modified CPEs versus unmodified CPEs, respectively. The increase in the cathodic current was higher (20 nA) than the anodic current (10 nA) for the 10% clay-modified CPEs. Thus, it can be concluded that an increase in the clay concentration favors riboflavin detection. A significant difference could be observed when the 5% clay-modified CPE current was compared with the

current of the unmodified CPE. In the oxidation range, the current was 5 nA higher than the current measured at the unmodified electrode, while in the reduction range the value was about 10 nA lower than the one measured at the unmodified electrode. This proved that a lower concentration of clay was not enough for riboflavin detection.[239]

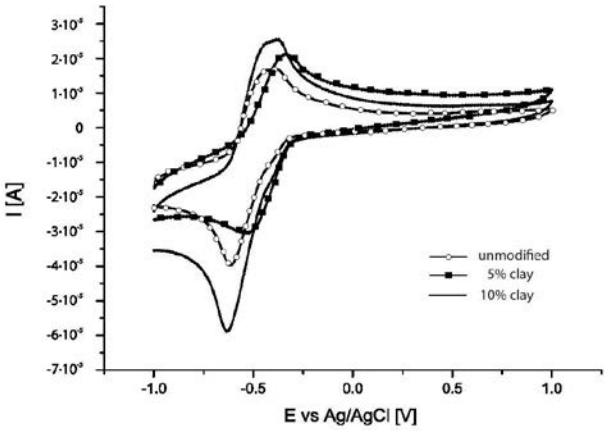

Figure 13 Cyclic voltammograms for 10^{-3} M riboflavin phosphate at unmodified CPE (dot line), at 5% (square line), and 10% (solid line) Răzoare clay-modified CPEs (KCl 0.1 M, 100 mVs^{-1})[239]

2.3.1 Biosensor for acetaminophen detection with Romanian clays and conductive polymers

Two types of transducers were studied (CPE and GCE) using two types of clay particles (under 20 μm and below 0.2 μm). CPE has been prepared by adding various amounts of clays (1, 2.5, 5, and 10 %). CPEs made by a mixture of graphite powder and solid paraffin are simple to prepare and offer a renewable surface essential for the electron transfer.[258] The use of CPEs in electroanalysis is due to their simplicity, minimal cost and the possibility of facile modification by adding other compounds thus giving the electrodes certain predetermined properties like high selectivity and sensitivity.[243, 259]

In order to realize a biosensor for the detection of acetaminophen, the electrochemical behavior of the doped CPEs was compared with the behavior of the thin PEI film GCEs. The thin PEI film deposited on the surface of a GCE exhibited a better mechanical stability in spite of its relative water solubility and an improved hydration layer, essential for the immobilization of the enzyme.

The difference between the two electrode configurations was clear. By CV recording of acetaminophen on modified CPE, only the oxidation process could be observed (Figure 12A). By comparison, the PEI film electrodes showed a reversible

oxidation and reduction process (Figure 14). The porosity of the clay film is obvious in this case, as it let the neutral acetaminophen species quite easily reach the electrode surface.

The current obtained on polymeric film electrodes was, however, lower (10-15 μA) than that obtained on clay-modified CPEs (100-350 μA).

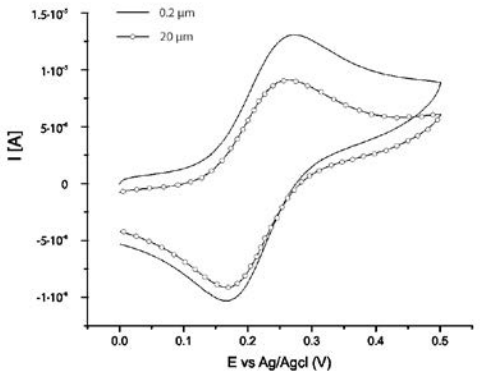

Figure 14 Cyclic voltammograms of 10^{-4} M acetaminophen solution using 20 μm (dot line) and 0.2 μm (solid line) Valea Chioarului clay immobilized in a 1 mg/mL PEI film (0.1 M phosphate buffer pH 7.4, 50 mVs^{-1})[243]

An increase of the current was noticed on different particle sizes of Valea Chioarului clay, the best response for acetaminophen being recorded for the 0.2 μm, due to the greater active surface (Figure 14).

In the human body, acetaminophen is metabolized to *N*-acetylbenzoquinonimine (NAPQI).[260] The same conversion can be achieved *in vitro* by HRP in the presence of hydrogen peroxide.

The amperometic studies (Figure 15) were made by recording the electrochemical reduction of the enzymatically generated electroactive oxidized species of acetaminophen (NAPQI) in the presence of hydrogen peroxide after stepwise addition of small amounts of 10^{-4} M acetaminophen solution.[243, 260]

$$\text{Acetaminophen} + H_2O_2 + 2H^+ + \text{HRP} \rightarrow \text{NAPQI} + 2H_2O$$

$$\text{NAPQI} + 2e^- + 2H^+ \rightarrow \text{Acetaminophen}$$

The linear range was calculated as the ratio of the standard deviation of the blank baseline (0.1 M phosphate buffer, pH 7.4), the noise and the biosensor's response to acetaminophen.[256] The amperometric assays were realized at -0.2V, which

represents the reduction potential of NAPQI. The HRP/clay/PEI/GCE biosensor had a sensitivity of 6.28×10^{-7} M and a linear range between 5.25×10^{-6} M and 4.95×10^{-5} M.

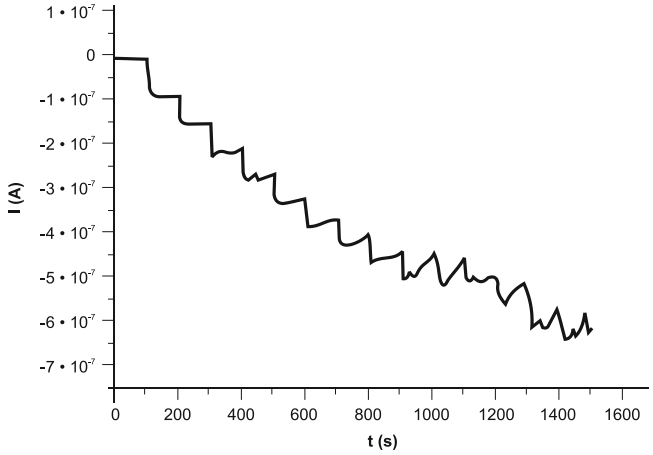

Figure 15 Amperometric response of the clay-modified electrode (0.2 µm Valea Chioarului clay in 1 mg/mL PEI /HRP/GCE) after successive additions of 50 µL of 10^{-4} M acetaminophen in phosphate buffer pH 7.4 and 0.2 mM H_2O_2[243]

The calibration curve equation of the amperometric biosensor was y= 0.0139x + 3×10^{-8} (R^2 = 0.996) and showed a linear range between 5×10^{-6} - 4.95×10^{-5} M. The reproducibility was also tested on the same electrode after 10 successive analyses in three different days. The RSDs of the slopes of the linear responses calculated by Line weaver-Burk method were less than 15%.[243]

The results are comparable with those recently presented in the literature:

Table 4 HRP amperometric biosensors for acetaminophen analysis

Electrode configuration	Enzyme/ Transducer	Sensitivity (µA M^{-1})	Linear range	LOD LOQ	References
Zr alcoxyde in PEI with HRP on GC	HRP/GC	1.17×10^{-7}	1.96×10^{-5}-2.55×10^{-4} M	*Not published*	Sima *et al.,* 2008
Nanoporous magnetic microparticles-HRP	HRP/Carbon paste with MMPs	*Not published*	2×10^{-6}- 5.7×10^{-5} M	*Not published*	Yu *et al.,* 2006
Zr alcoxyde in PEI with HRP on SPE	HRP/SPE	*Not published*	4.35×10^{-7}-4.98×10^{-6} M	6.21×10^{-8} M 2.07×10^{-7} M	Sima *et al.,* 2010
HRP/PEI/SWCT / GCE	HRP/GC	*Not published*	9.99 – 79.01µM	7.82×10^{-6} M	Tertis *et al.,* 2013
HRP/Ppy/SWCT / SPE	HRP/SPE	*Not published*	19.96 – 118.06 µM	8.09×10^{-6} M	Tertis *et al.,* 2013

2.4 Conclusions

New composite materials based on clay micro and nanoparticles for the development of electrochemical sensors were developed. The electrochemical behavior of acetaminophen and riboflavin phosphate was tested for the first time on clay-modified CPEs with different clay particle sizes using CV and new electrochemical methods were elaborated for their detection and applied in pharmaceutical analysis. The obtained results emphasized the great active surface, the adsorbent and ionic exchange properties and showed the advantages offered by Răzoare and Valea Chioarului clays for the development of novel modified electrodes applied in pharmaceutical analysis.[239] Carbon paste was chosen in this work because it is accessible, low cost, easy to manipulate, and it showed good electrochemical properties. It offered, in the meantime, a good entrapment for the clay at the electrode surface. The main disadvantage of the carbon paste was impossibility to quantify the clay at the electrode surface which comes in contact with the electrolyte and which is practically involved in the electrochemical measurements. Therefore, the results obtained in this study didn't present higher performances in comparison with the already existent methods.

A novel biosensor based on HRP immobilization in a PEI and clay porous gel film for acetaminophen was developed. When comparing the CV recording of acetaminophen on modified CPE and on PEI film electrodes, it was concluded that in the first case only the oxidation process could be observed, while in the second case reversible oxidation and reduction processes were visible. For the GCE modified electrode, the current response increased proportionally with the active surface area as a result of the decrease in the particle size.

The amperometric detection of acetaminophen was successfully achieved with a sensitivity of 6.28×10^{-7} M and a linear range between 5×10^{-6} M and 4.95×10^{-5} M. The clay offered both a good entrapping and a "protective" environment for the biocomponent. This immobilization strategy could be exploited in the development of other biomolecules for the detection of pharmaceuticals.[243]

These are preliminary results as these studies didn't aim at developing new analytical methods for the detection of the selected pharmaceutical probes (acetaminophen, ascorbic acid, and riboflavin), but to emphasize the specific properties of the Romanian clays employed which recommends them for further exploitation for electrodes modification and for the development of new composite materials applied in sensors and biosensors fabrication.

3 Tetrabutylammonium-modified clay film electrodes: characterization and application to the detection of metal ions

3.1 Introduction

Even their development has started a few decades ago, clay-modified electrodes (CLMEs) still represent a notable field of interest, especially for their applications in electroanalysis, as discussed in some reviews[2, 3, 21, 126, 249, 261] and illustrated in recent research papers where CLMEs have been used as sensors or biosensors (see examples, *e.g.*, from our group[239, 243, 262] and from those of Ngameni[68, 69, 73, 263-267], Mousty[268, 269], or some others[67, 270, 271]). Clay minerals used as electrode modifiers are primarily (but not only) phyllosilicates-layered hydrous aluminosilicates. An important characteristic of those minerals is their interlayer distance which depends on the number of intercalated water and exchangeable cations within the interlayer space[3]. They also exhibit attractive properties such as a relatively large specific surface area, ion exchange capacity, and the ability to adsorb and intercalate organic species. Smectites have been mostly used for CLMEs preparation in thin layer configuration, especially montmorillonite (MMT), due to a high cation exchange capacity (typically 0.80-1.50 mmol g^{-1}) and its thixotropy likely to generate stable and adhesive clay films on electrode surfaces.[3, 249]

One can remind here that clays are insulating materials so that their use in electrochemistry requires a close contact to an electrode surface, which can be achieved via either the dispersion of clay powders in a conductive composite matrix (*e.g.*, carbon paste electrode[272]) or the deposition of clay particles as thin films on solid electrode surfaces. An advantage of the clay film modified electrodes is that they are binder-free, thanks to the particular platelet morphology of clay particles bringing them self-adhesive properties toward polar surfaces[21], which ensure a better interaction with most electrode materials and, consequently, a more durable immobilization. Clay films can be attached to a solid electrode surfaces by physical means (through solvent casting, spin-coating, or layer-by-layer assembly[21, 249, 273], or electrophoretic deposition[18], by covalent bonding (via silane or alkoxysilane coupling agents)[10, 274], or, more recently, in the form of clay-silica composite films[275]. At the beginning, CLMEs were mainly prepared from bare (unmodified) clay materials[21, 249]

but recent advances have been mainly based on organically-modified clays (obtained either by intercalation or grafting of organic moieties in the interlayer region of the clay[276-279]) because they enable to tune, to control and to extend the clay properties, resulting therefore to better analytical performance in terms of selectivity and sensitivity[68, 69, 73, 263-267].

Dealing with sensitivity, preconcentration electroanalysis at modified electrodes (in which the analyte is firstly accumulated at open circuit and then electrochemically detected) has proven to be a powerful method to improve the performance of electrochemical sensors. In this respect, the ion exchange capacity of clays and the binding properties of organoclay have been exploited for the detection of metal ions using CLMEs (see examples in reviews[3, 126]). Till now, however, very few examples are based on the use of intercalated organoclay materials for that purpose[73, 265], in spite of the simpler modification procedure for intercalation than for grafting for instance (which requires the use of particular organoalkoxysilane reagents[69, 267]). Here, we have thus examined the interest of CLMEs based on clay particles intercalated with tetrabutylammonium (TBA^+) moieties for the preconcentration electroanalysis of some metal ions (i.e., Cd^{2+}, Pb^{2+} and Cu^{2+}). The choice of this tetraalkylammonium intercalation reagent was motivated by at least two features: (1) TBA^+ ions can be easily intercalated in the interlayer region of smectite clays by ion exchange[280], and (2) it modifies the packing configurations in the interlayer of the clay thus influencing the sorptive properties of the organoclay[281], notably with respect to adsorption of metal ions such as Cu^{2+} or Cd^{2+}[282, 283], which could be advantageously exploited here with CLMEs.

The present study describes the deposition of tetrabutylammonium modified clay particles (montmorillonite-rich natural clay from Romania) onto a glassy carbon electrode surface, subsequently covered with a dialysis tubing cellulose membrane, a configuration ensuring fast mass transport for analytes from the solution through the film to the electrode surface. The permeability properties of the novel thin clay films towards selected redox probes (cationic, neutral, and anionic) were characterized. The permeability properties and long-term operational stability of the modified electrodes are discussed regarding their physico-chemical characteristics.

Surprisingly, the fully doped tetrabutylammonium clay showed lower electrochemical performance towards cations than the unmodified clay. This is explained by the positive electrostatic barrier and the blockage of interlayer adsorption sites due to the tetrabutylammonium ion. In order to diminish the positive electrostatic barrier and also to create free adsorption sites, the partial removal of tetrabutylammonium ions was performed, thus improving the electrochemical performances of the modified clays.

Then, the modified electrode was applied to the detection of some metal ions chosen as relevant biological and environmental contaminants (Cd^{2+}, Pb^{2+} and Cu^{2+}). After optimization of various experimental parameters, a stable and reliable sensor was obtained.

3.2 Experimental

3.2.1 Clays, reagents, and electrochemical instrumentation

$NaNO_3$ (99%, Fluka), HCl (37%, Riedel de Haen), and tetrabutylammonium bromide (TBAB, 99%, Sigma) were used as received without further purification. The redox probes employed for permeability tests were of analytical grade: ferrocene dimethanol ($Fc(MeOH)_2$, Alfa Aesar); potassium hexacyanoferrate(III) ($K_3Fe(CN)_6$, Fluka); and hexaammineruthenium chloride ($Ru(NH_3)_6Cl_3$, Sigma-Aldrich). Single-component and multicomponent cation solutions were prepared daily by diluting standardized mother solutions (comprised of 1000 mg/l each metal ion, from Sigma–Aldrich). These standards were also used to certify copper(II) solutions prepared from $Cu(NO_3)_2 \cdot 3H_2O$ and 0.05 M HNO_3, lead(II) solutions prepared from $Pb(NO_3)_2$ and 0.5 M HNO_3 and cadmium(II) solutions prepared from $Cd(NO_3)_2 \cdot 4H_2O$ and 0.5 M HNO_3, Sigma-Aldrich), which were used to prepare diluted solutions for preconcentration studies (final pH in the electrolyte was 5.5 if not stated otherwise). The electrolyte employed was 0.1 M $NaNO_3$. All solutions were prepared with high purity water (18 MΩ cm^{-1}) from a Millipore milli-Q water purification system.

The clay sample used in this study was a natural Romanian clay from Valea Chioarului (Maramureş County), consisting mainly of MMT, with minor amounts of quartz. Its physico-chemical characterization is provided elsewhere[239]. The structural formula is $(Ca_{0.06}Na_{0.27}K_{0.02})_{\Sigma=0.35}(Al_{1.43}Mg_{0.47}Fe_{0.10})_{\Sigma=2.00}(Si_{3.90}Al_{0.10})\Sigma=4.00\ O_{10}(OH)_2 \cdot nH_2O$. It is characterized by a surface area (N_2, BET) of 190 $m^2\ g^{-1}$. Only the MMT-rich fine fraction of the clay (< 1 μm, as collected by sedimentation according to Stokes law, after the raw clay was suspended in water, ultrasonicated for about 15 min and allowed to settle, centrifugation and ultracentrifugation of the supernatant phase) was used here. This fine fraction has a CEC of 0.78 meq g^{-1} and was used before as template for an amperometric biosensor for acetaminophen detection[243]. Its XRD diffractogram showed a high content of MMT (with its characteristic peaks at 2θ: 6,94°; 19,96°; 21,82°; 28,63°; 36,14°; 62,01°) and also confirmed the almost negligible presence of other minerals.

3.2.2 Apparatus and characterization procedures

Electrochemical experiments were carried out using a PGSTAT-12 potentiostat (EcoChemie) equipped with the GPES software. A conventional three electrode cell configuration was employed for the electrochemical measurements. Film modified GCEs were used as working electrodes, with an Ag/AgCl/KCl 3M reference electrode

(Metrohm) and a platinum wire as reference and counter electrode. Cyclic voltammetry (CV) determinations were carried out respectively in 1 mM $K_3Fe(CN)_6$, 0.1 mM $Ru(NH_3)_6Cl_3$, and 5 mM $Fc(MeOH)_2$ (in 0.1 M $NaNO_3$). CV curves were typically recorded in multisweep conditions at a potential scan rate of 20 mV s^{-1} and used to qualitatively characterize accumulation/rejection phenomena and mass transport issues through the various films.

Accumulation-detection experiments were also performed using copper(II), lead(II), and cadmium(II) as model analytes. Typically, open-circuit accumulation was made from diluted cations solutions (5×10^{-7} - 10^{-6} M) at pH 5.5 and voltammetric detection was achieved after medium exchange to a cation-free electrolyte solution (0.1 M $NaNO_3$) by square wave voltammetry (SWV), at a scan rate of 5 mV s^{-1}, a pulse amplitude of 50 mV and a pulse frequency of 100 Hz.

The CNH elemental analysis was performed for the unmodified clay, for the TBAB fully doped MMT before and after the TBAB partial extraction, using an Elementar Vario Micro Cube, with the following experimental conditions: combustion temperature 950° C; reduction temperature 550° C; He flow 180 ml/min; O_2 flow 20 ml/min; pressure 1290 mbar.

The film structure was characterized by X-ray diffraction (XRD), FTIR and Raman Spectroscopy. XRD measurements were performed using a BRUKER D8 Advance X-ray diffractometer, with a goniometer equipped with a germanium monochromator in the incident beam, using Cu Kα1 radiation (λ = 1.5405Å) in the 2θ range 15-85°. The FTIR spectra were measured on a Jasco FT/IR-4100 spectrophotometer equipped with Jasco Spectra Manager Version 2 software (550-4000 cm^{-1}). The Raman spectra were acquired with a confocal Raman microscope (Alpha 300R from WiTec) using a WiTec Control software for data interpretation (-1000-3600 cm^{-1}, resolution > 0.5 cm^{-1}).

Electrochemical impedance spectroscopy (EIS) was used to characterize the electron transfer properties of the modified electrodes. The Nyquist plots were recorded with an Autolab potentiostat equiped with a FRA2 module and 4.9 version software.

3.2.3 Clay modification with TBAB

A MMT sample (10 g, particle size <1 μm) was suspended in ultrapure demineralized water (clay concentration in water 4%). A quantity of Na_2CO_3 equivalent to 100 mEg Na_2CO_3 per100 g clay was then added in the clay suspension and stirred for 30 minutes at 97°C. An aqueous solution of TBAB (corresponding quantitatively to 1.1 times montmorillonite cation exchange capacity (CEC_{MMT} = 0.78 mEq g^{-1}); 0.85 mEq g^{-1} of TBAB), was then added and the suspension was stirred for 30 more minutes at room temperature. The obtained solid was separated by

centrifugation and washed until it was free of any residual Br^-. The organoclay material was then dried for 48 h at 60° C. Depending on the analytical purpose, the TBAB was kept in the clay or partially solvent-extracted from the powder in an ethanol solution containing 0.1 M $NaClO_4$ for 30 min under moderate stirring.

3.2.4 Electrode assembly

Glassy carbon electrodes purchased from e-DAQ (GCEs, 1 mm in diameter) were first polished using 1 and 0.05 μm alumina powder and then washed with water and sonicated for 15 min in distilled water to remove any alumina trace, leading to an electrochemically active surface area of about $7.85 \cdot 10^{-3}$ cm^2. Clay or organoclay suspensions (5 mg/ml) were then prepared in distilled water stirred for 20 min, sonicated for 10 min, and left quiescent at room temperature.

The clay or organoclay film was deposited on GCE by spin-coating. A volume of 2.5 μl of the clay suspension (5 mg/ml) was deposited on the electrode surface and then stirred for 20 minutes at 2000 rotation per minute. The electrode was then dried at room temperature for 1 hour. The clay or organoclay film was covered with a dialysis tubing cellulose membrane (Sigma) fixed first with a rubber o-ring, and then with laboratory film to avoid the solution penetration under the membrane.

The five systems characterized in this study are: the bare glassy carbon electrode (GCE), the bare glassy carbon electrode with cellulose membrane (GCE/M), the unmodified MMT film coated on GCE with cellulose membrane (GCE+MMT/M), and the TBAB modified MMT film coated on GCE with cellulose membrane before (GCE+MMT+TBAB/M) and after TBAB partial extraction (GCE+MMT+TBAB(-TBAB)/M).

3.3 Results and discussions

3.3.1 Physical-chemical characterization of clays

XRD was first used to characterize the eventual structural changes of the smectite clay upon intercalation of TBAB. As expected, prior to surfactant entrapment, the clay film exhibited the same MMT characteristics as those reported for the raw clay particles in the experimental section (diffraction lines at 2θ values (°) of 6.9; 19.9; 21.8; 28.6; 36.1; 62.0, data not shown). The unit cell parameters and the profile discrepancy indices values (Table 5) indicate an expansion of the interlayer region between the clay sheets. As the clay was in contact with a TBAB solution, this expansion is certainly due to the incorporation of TBA^+ species in the clay interlayer (in agreement with a similar process described elsewhere for other surfactants such as cetyltrimethylammonium bromide (CTAB)[284].

After partial removal of the TBAB, the clay interlayer distance was found to maintain almost the same values obtained for the fully doped clay, MMT+TBAB (see Table 5).

Table 5 The unit cell parameters and profile (R_p) discrepancy indices calculated by Rietveld refinement analysis for the clay (MMT, clay with TBAB (MMT+TBAB) and clay with TBAB after TBAB removal (MMT+TBAB(-TBAB))

Samples	a [Å]	b [Å]	c [Å]	R_p
MMT	5.17	5.17	12.624	17.2
MMT+TBAB	5.24	5.24	15.487	18.6
MMT+TBAB(-TBAB)	5.23	5.23	15.475	17.6

The FTIR spectrum of Valea Chioarului clay (Figure 16, black line) presented the typical bands attributed to the characteristic groups of MMT, described elsewhere. [243, 244]

The FTIR spectrum of TBAB (Figure 16, blue line) presented at 739 cm^{-1} a band corresponding to the C-H alkanes rocking vibration. The band near 1020-1250 cm^{-1} can be assigned to the C-N stretching vibrations and the bands near 1450-1470 cm^{-1} are due to the C-H alkanes bending vibrations. The bands near 1350-1370 cm^{-1} correspond to the C-H alkanes rocking vibrations and the bands near 2969-2945 cm^{-1} to the C-H alkanes stretching vibrations. The bands near 600-1300 cm^{-1} can be assigned to the C-C aliphatic chain vibrations.[246]

For the fully dopped TBAB clay sample (Figure 16, red line), the peak at 3625 cm^{-1} attributed to the stretching vibration of the hydroxyl group, the band near 1637 cm^{-1} due to the bending vibration of H-O-H group and the broad band near 1000-1200 cm^{-1} assigned to the Si-O stretching vibration are common with MMT spectrum. In the same time, the bands near 2969-2945 cm^{-1} due to the C-H alkanes stretching vibrations, the bands near 1475 cm^{-1} can be assigned to the C-H alkanes bending vibrations, and the bands near 1350 cm^{-1} correspond to the C-H alkanes rocking vibrations, all indicating the presence of the surfactant in the clay. It can be assumed that the broad band at 1000-1200 cm^{-1} includes the C-N stretching vibrations.[243, 244, 246]

After the TBAB partial removal, the FTIR spectrum (Figure 16, green line) presents almost all the bands that were attributed to the surfactant, but with lower intensities.

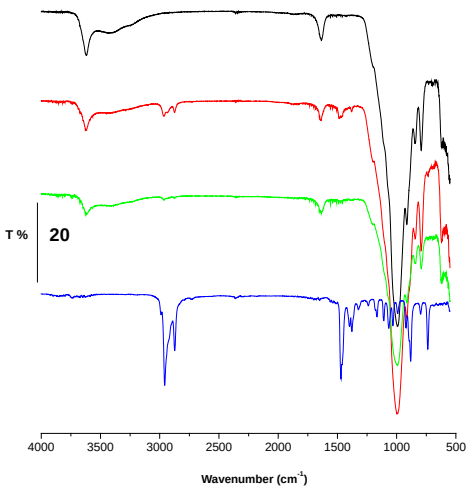

Figure 16 FTIR spectra of MMT samples, simple (black line) modified with TBAB (red line) and after the partial TBAB extraction (green line) compared with TBAB spectrum (blue line).

Raman spectrum of MMT is characterized by three strong bands near 200, 425 and 700 cm^{-1}, (Figure 17, black line).[285-287] The sharp Raman peak at 706 cm^{-1} is due to SiO_4 vibrations and the broader feature near 420 cm^{-1}has been assigned to M-OH bending vibrations[285, 287] and to Si-O-Si(Al) bending modes.[286, 287] The position of the strong band near 201 cm^{-1} varies depending on the clay mineral type[285, 287]; it is probably due to the SiO_4 and influenced by Al substitution and the dioctahedral or trioctahedral character. Weaker bands due to the OH bending vibration are observed near 850-920 cm^{-1}.[287]

In the case of TBAB spectra (Figure 17, blue line), the sharp Raman bands near 2800-3000 cm^{-1} are due to the C-H bending vibrations. The strong bands near 250-400 cm^{-1} can be assigned to the C-C aliphatic chains vibrations. The broader feature near 1380 cm^{-1} can be assigned to the CH_3 bending vibration, while the feature near 1460 cm^{-1} is due to the asymmetric CH_3 vibrations. The band near 1331 cm^{-1} corresponds to the C-N bending vibration and the weaker band near 1057 cm^{-1} is due to the C-C aliphatic chain vibrations.[288]

The Raman spectrum of the surfactant modified MMT shows, as expected, both characteristic bands of MMT and TBAB. At 705 cm^{-1} a sharp peak attributed to the SiO_4 vibrations, the broader feature near 421 cm^{-1} due to the M-OH bending vibrations, (Figure 17, red line)[285, 287] and to Si-O-Si(Al) bending modes[286, 287], and also the weaker bands due to the OH bending vibration observed near 850-920 cm^{-1}[287], all correspond to the MMT Raman spectrum. The sharp Raman bands near 2800-3000 cm^{-1} due to the C-H bending vibrations and the bands near 250-400 cm^{-1} assigned to the C-C aliphatic

chains vibrations, are common with the TBAB Raman spectrum. Also the feature near 1450 cm^{-1} due to the asymmetric CH_3 vibrations, the band near 1318 cm^{-1} corresponding to the C-N bending vibration, and the weaker band near 1058 cm^{-1} due to the C-C aliphatic chain vibrations[288] demonstrate clearly the incorporation of the surfactant in the clay. The data is a clear proof of the surfactant incorporation in the clay interlayer.

The assigned bands of TBAB are still present in the Raman spectrum (Figure 17, green line), but with lower intensities, after the partial removal of the surfactant from MMT, explaining thus, why the interlayer spaces were maintained (Table 2).

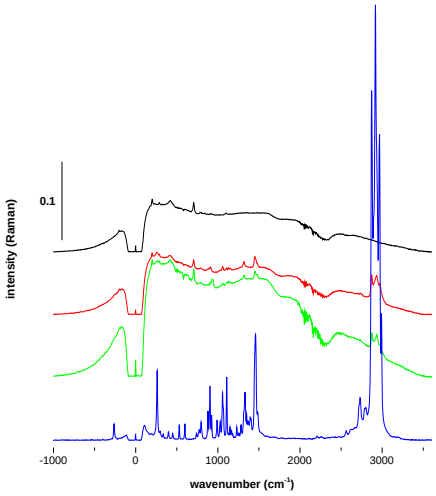

Figure 17 Raman spectra of MMT samples, simple (black line) modified with TBAB (red line) and after the partial TBAB extraction (green line) compared with TBAB spectrum (blue line).

X-ray diffraction, FTIR and Raman spectra data were confirmed by the elemental analysis results presented in Table 6.

The TBA^+ content, calculated using the N% values, as the doping agent is a quaternary ammonium salt, is 10.17 % for the fully doped clay, while after the surfactant partial extraction is decreasing to 2.07%.

Table 6 CNH elemental analysis for the modified clay before and after the TBAB partial extraction

Sample	C%	N%	H%	Assignment
MMT (unmodified)	0.14	0.14	2.839	Organic or/and inorganic impurities containing C and N, H_2O and Si-OH groups for H, respectively
MMT+TBAB (fully doped)	8.82	0.73	4.068	$TBAB^+$ and impurities
MMT+TBAB(-TBAB) (after extraction)	3.85	0.26	3.386	$TBAB^+$ and impurities

3.3.2 Clay film permeability

The MMT film presence at the GCE surface increases its voltammetric response in $Ru(NH_3)_6^{3+}$ (Figure 18C). This is possible due to the accumulation of the positively-charged electroactive probe by ion exchange in the clay film. For GCE+MMT/M, GCE+MMT+TBAB/M, and GCE+MMT+TBAB(-TBAB)/M, the stationary value of current intensity is reached after 30 potential scans at $0.020Vs^{-1}$ (Figures 18C, 18D, 18E). This behavior was observed for all the MMT samples used (unmodified or modified with different compounds) and corresponds to the diffusion from the solution/clay interface to the electrode surface, results in agreement with other authors[251]. This behavior proves the cation exchange capacity of modified clay and which can be exploited in ion exchange voltammetry (cations detection after preconcentration).

The first voltammetric cycles recorded with the MMT modified GCE shows less intense peaks than that obtained on bare GCE due to the fact that the clay film on the electrode surface reduces its active area. This fact was observed only when cycling potentials just after immersion of the electrode in the analyte solution. If the electrode was kept in electrolyte before testing it, the first voltammetric cycle showed peak currents comparable with those obtained on the bare electrode (data not shown).

The presence of TBA^+/TBAB in the clay is indicated by the lower response of the film to the $Ru(NH_3)_6^{3+}$ probe (lower accumulation possible by cation exchange, see Figure 18D). This signal decrease also tends to support the presence of some holes in the film (in the presence of a crack-free film the response to $Ru(NH_3)_6^{3+}$ would have been totally suppressed).

On the other hand, after surfactant partial removal, the accumulation response of $Ru(NH_3)_6^{3+}$ species upon continuous potential cycling is more marked (compare Figure 18E and 3C) due to the increase in the clay interlayer and also to the cation exchange in the clay.

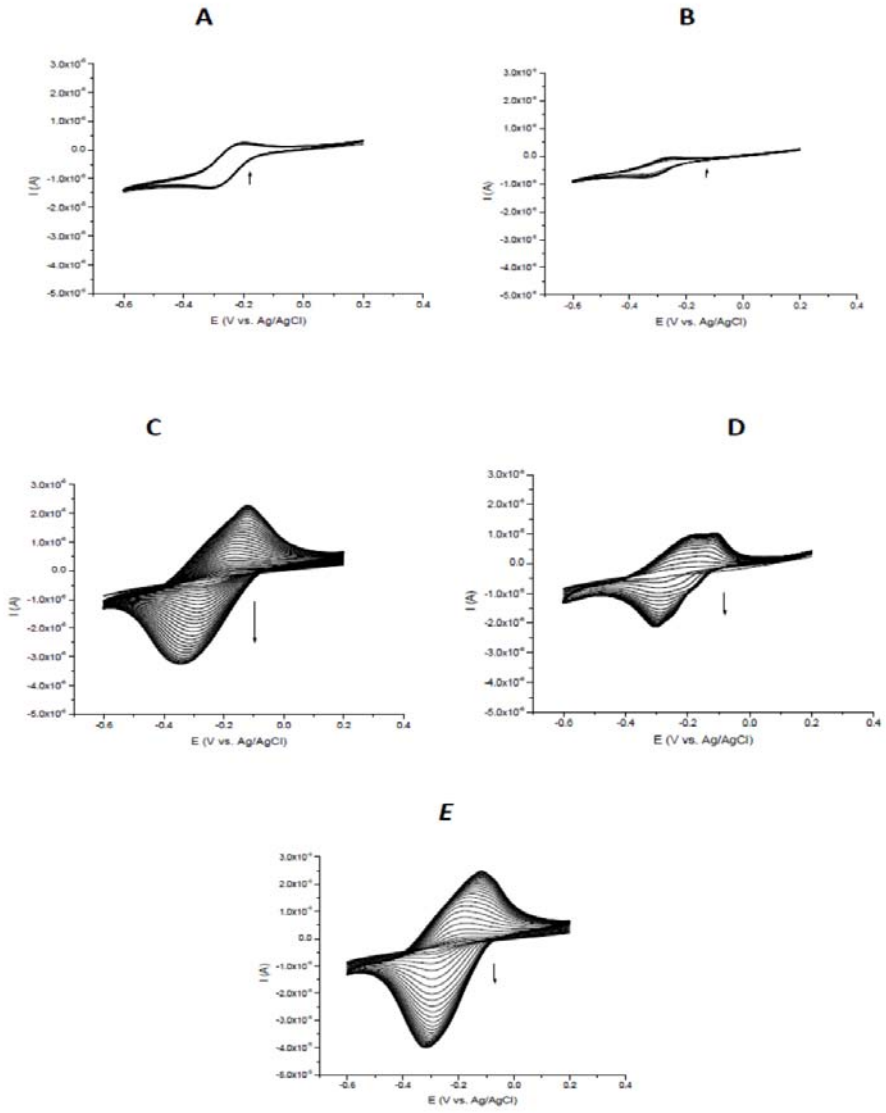

Figure 18 Multisweep cyclic voltammograms recorded in 10^{-3}M $Ru(NH_3)_6Cl_3$ in 0.1M $NaNO_3$ using: bare GCE (A) (10 cycles); GCE/M (10 cycles) (B); GCE+MMT/M (30 cycles) (C); GCE+MMT+TBAB/M (30 cycles) (D); and GCE+MMT+TBAB(-TBAB)/M (30 cycles) (E).

An important feature here is that extraction of the surfactant was made using ethanol and $NaClO_4$ (not the classically used ethanol/HCl mixture) to avoid any chemical degradation of the clay (i.e., acid hydrolysis of the aluminum sites in the

aluminosilicate) and to maintain its cation exchange capacity. These results indicate promising use of GCE+MMT+TBAB(-TBAB)/M for preconcentration electroanalysis of cationic analytes (see section 3.3 for confirmation).

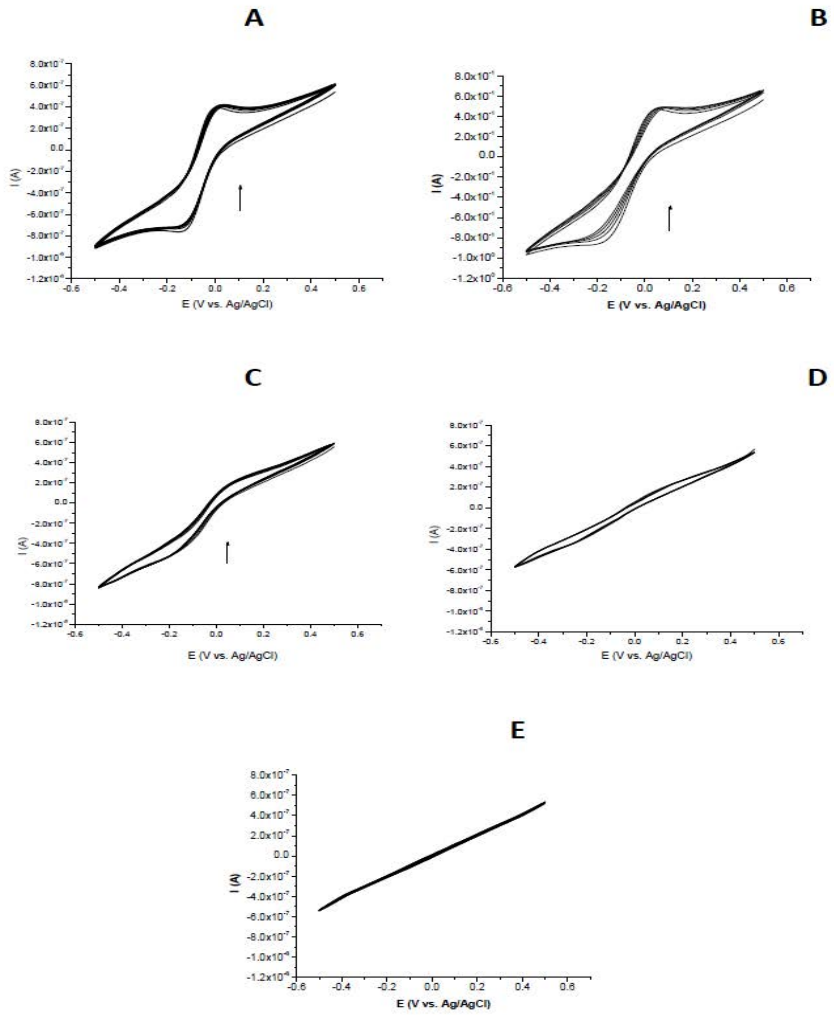

Figure 19 Multisweep CVs recorded in 10^{-3} M $[Fe(CN)_6]^{3-}$ (in 0.1M $NaNO_3$) using bare GCE (A) (5 cycles); GCE/M (10 cycles) (B); GCE+MMT/M (10 cycles) (C); GCE+MMT+TBAB/M (10 cycles) (D); and GCE+MMT+TBAB(-TBAB)/M (10 cycles) (E).

The negatively charged clay repulses the negatively charged $[Fe(CN)_6]^{3-}$ (Figure 19C) and the electrochemical signal is decreasing.

On the basis of the net negative charge of MMT clay, the negatively charged species would be expected to be totally rejected by the clay. Results in Figure 19 are also an indication that the MMT and the TBAB modified MMT films could present some cracks that permit the $[Fe(CN)_6]^{3-}$ diffusion to electrode surface. However, there are some studies in literature in which is mentioned that even cation-exchanging clays have been reported to accumulate somewhat the anionic species.[47, 54, 55, 251, 289, 290]

Prior to surfactant extraction, when using the $Fe(CN)_6^{3-}$ probe, a very small signal can be observed, yet clearly visible (see Figure 19D), slightly and continuously growing upon successive cycling. This behavior suggests some accumulation of the negatively-charged $Fe(CN)_6^{3-}$ species. This result can be attributed to the fact that tetrabutylammonium cation, TBA^+, is likely to accommodate the clay particles.[284]

It is known that when smectite type clays are treated with a cationic surfactant at a concentration ranging between 0.5 and 1.5 times the CEC of the clay, the surfactant molecules adopt a bilayer or pseudotrimolecular arrangement within the clay platelets, with both vertical and horizontal orientations of the alkylammonium chains.[291] Therefore, the aggregation of the organic cations occurs via both ion exchange and hydrophobic bonding which leads to the creation of positive charges in the clay layer and on the clay surface, inducing thereby possible uptake of anionic species by the clay composite via the formation of surface-anion complex.[292, 293] In the present case, the slight accumulation of redox species, as observed in Figure 19D, can be ascribed to the formation of ion pairs between TBA^+ cations and $Fe(CN)_6^{3-}$ anions. The accumulation effect is however much lower than that for classical surfactant-modified clay films (*e.g.,* smectite clay modified with hexadecyltrimethylammonium[265]), perhaps due to the presence of the cellulose membrane around the surfactant modified clay particles.

After surfactant partial removal, the absence of signal to negatively-charged $Fe(CN)_6^{3-}$ species (see Figure 19E) is again explained by electrostatic repulsions from the negatively-charged clay sheets. All the clay films used in this work greatly attenuate the current response in comparison to the bare GCE (about 70% signal suppression).

If the redox probe considered is the neutral $Fc(MeOH)_2$, the signal recorded on MMT modified GCE is quite similar with that obtain on bare GCE (compare Figure 20C and 20A) which proves that the clay film is still porous as it let the neutral $Fc(MeOH)_2$ species reach quite easily the electrode surface.

The reduction potential is shifted in negative direction in the presence of clay films, from 0.034 V in the case of bare GCE to -0.09 V in the case of MMT modified GCE and -0.02 V on GCE+MMT+TBAB(-TBAB)/M. In the case of the oxidation peak the potential is shifted to less positive values from 0.16 V in the case of bare GCE to 0.03 V for GCE+MMT/M.

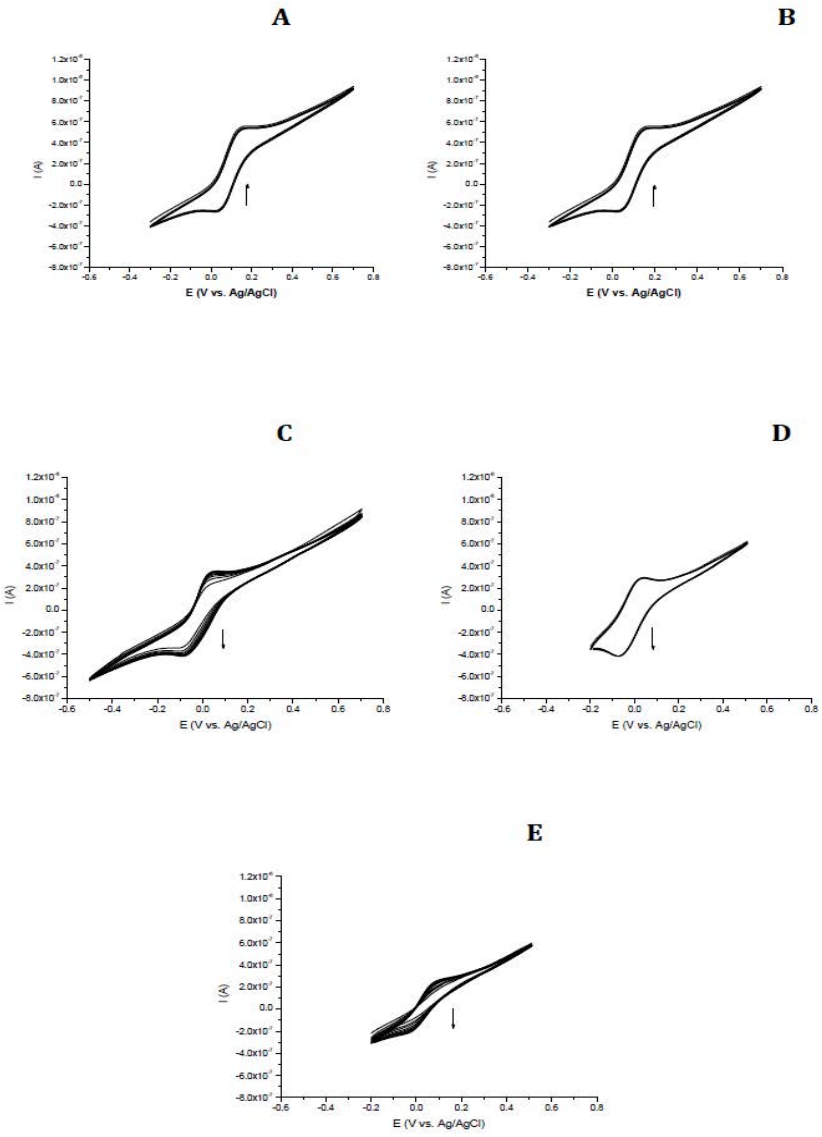

Figure 20 Multisweep cyclic voltammograms recorded in 10^{-3} M $Fc(MeOH)_2$ using bare GCE (A) (5 cycles); GCE/M (5 cycles) (B); GCE+MMT/M (10 cycles) (C); GCE+MMT+TBAB/M (10 cycles) (D); and GCE+MMT+TBAB(-TBAB)/M (10 cycles) (E).

The neutral $Fc(MeOH)_2$ probe is still detectable on the GCE+MMT+TBAB(-TBAB)/M film electrode but less easily than for GCE+MMT/M

(compare Figure 20E and 20C) because the increase in the interlayer clay makes it more difficult for the probe molecules to reach the underlying electrode surface.

3.3.3 EIS – determinations

EIS was employed to characterize the electron transfer properties of the modified electrodes (Figure 21). The typical Nyquist plot of EIS includes a semicircle and a linear zone, which correspond to the electron transfer limited process and the diffusion limited process, respectively.

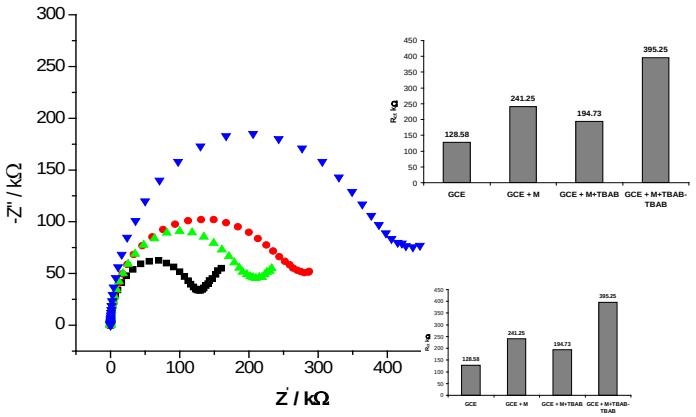

Figure 21 Nyquist plots for: GCE/M (e-Daq, d=1mm) (black); GCE+MMT/M (< 1 µm; 5 mg mL^{-1} suspension) (red); GC+MMT+TBAB/M (5 mg mL^{-1} suspension) (green); GC+MMT+TBAB(-TBAB)/M (5 mg mL^{-1} suspension) (blue); in 10 mM $K_3[Fe(CN)_6]$ in PBS (0.1M; pH7.4). Inset: R_{ct} variation with the electrode type. (5 mgmL^{-1} water suspensions; amplitude 0.005; begin frequency: 100 kHz; end frequency: 0.01 Hz; number of frequencies: 71).

The proposed circuit is R1(Q1[R2W1]) both for unmodified GCE and GCE modified with MMT (simple and with TBAB). The conventional C_{dl} is replaced by the constant phase element (CPE), representing the non uniform behavior of adsorbed species on irregular geometry and small electrode surface. The reaction seems to occur in single step and a combination of kinetic and diffusion processes with infinite thickness describe the whole process. The high frequency section of Nyquist curves describe an arc, the diameter of which displays the R_{ct} values (namely the electron transfer resistance), that increase in the presence of MMT from 128.58 Ω (GCE) to 395.25 Ω (GCE+MMT+TBAB(-TBAB)/M) due to the electrode surface coverage with non conductive clay films which obstruct the electron transfer. The best electrode surface coverage is achieved using TBAB modified MMT films after the surfactant extraction.

The experimental results of EIS confirmed that the clay films were fixed at the GCE surface and the clay's presence decrease the electron transfer rate of $[Fe(CN)_6]^{3-}$.

3.3.4 Optimization of experimental conditions

3.3.4.1 Supporting electrolyte for optimal metal ions detection

Different supporting electrolytes have been known to present different electroanalytical responses at CLMEs towards the detection of certain analytes by increasing/decreasing either the catalytic current response and/or lowering the detection potential. To choose the suitable detection medium, the electrochemical behavior of treated ions was studied using SWV on GCE+MMT+TBAB(-TBAB)/M in different buffer mediums (such as 0.1 M HCl; 0.2 M HNO_3; 0.1 M KCl (pH 4.0); 0.1 M $NaNO_3$ (pH 5.5 in ultrapure water). It appears that the current of Cu(II) oxidation peak is higher in the 0.2 M HNO_3 (Figure 22) and in this particular case the peak potential is shifted to less negative values (-0.17 V vs. Ag/AgCl). In the case of the 0.1 M $NaNO_3$, the peak potential appears at -0.22 V vs. Ag/AgCl, but the peak shape is more appropriate for analytical study, moreover an acidic medium might destroy the internal structure of the clay. Therefore, the 0.1 M $NaNO_3$ was used as supporting electrolyte in all subsequent electrocatalytical experiments of Cu(II) detection.

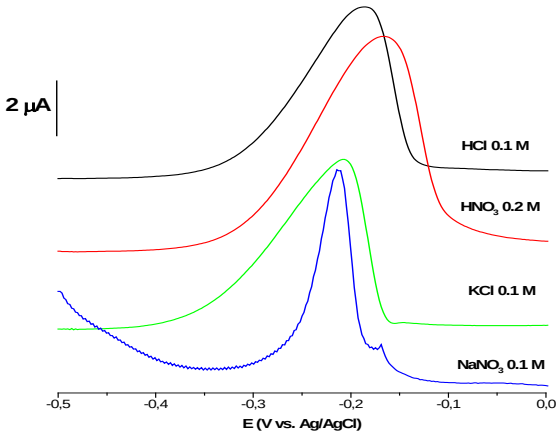

Figure 22 The electroanalytical response of Cu(II) in different electrolytes. SWVs were recorded using GCE+MMT+TBAB(-TBAB)/M, after 5 min accumulation at open-circuit in 10^{-5} M Cu(II) solution in ultrapure water. Detection performed in the supporting electrolyte after 180 s electrolysis at -0.6 V.

3.3.4.2 Accumulation time

The effect of accumulation time was studied in a range from 0 to 25 min in Cu^{2+} and Cd^{2+} solutions at different concentrations and the results are presented in Figure 23. The peak height (current) increases with the accumulation time both for Cu(II) and Cd(II) and, at higher concentrations, it reaches the steady-state after more than 15 min. This can be attributed to the saturation of the accessible adsorption sites in the clay film. The accumulation time was therefore set according to the amount of analytes in the solution.

For the analysis of Cu^{2+} and Cd^{2+} performed in solutions at lower cations concentration, a longer period may be required in order to sufficiently accumulate the metal ions at detectable levels. However, focusing on the most sensitive system (GCE+MMT+TBAB(-TBAB)/M), the relative large linear response range (from 0 to 20 – 25 minutes) demonstrated that is not easy for the system to be saturated with metal ions and requires longer accumulation periods. The variations are typical for preconcentration electroanalysis at modified electrodes. They involve an accumulation by analyte binding to active centers (a first linear increase of the signal followed by leveling off when reaching steady-state due to ion exchange equilibrium can be observed, together with the saturation of ion exchange sites). This is in agreement with previous observations made for copper (II) and cadmium(II) electroanalysis at other kind of modified electrodes[57, 191, 294, 295]. For the further determinations 5 to 10 minutes of preconcentration time were considered, depending on experiment type.

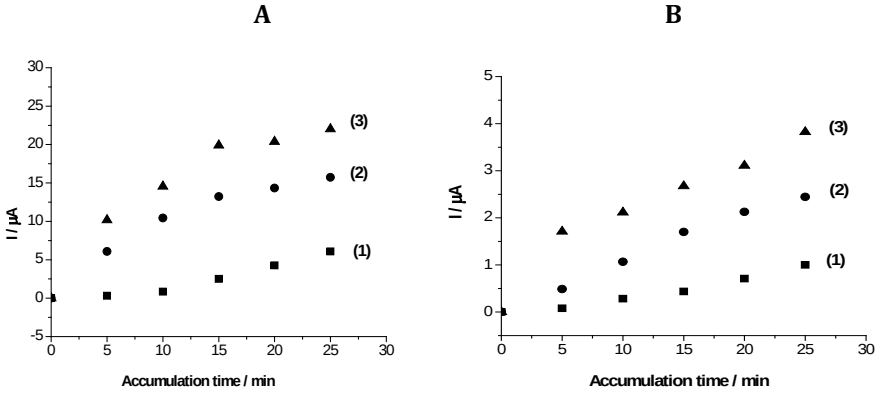

Figure 23 Variation of current peak intensity with accumulation time using GCE+MMT+TBAB(-TBAB)/M after open circuit accumulation of: Cu(II) (A) and Cd(II) (B) at different concentrations: (1) $5 \cdot 10^{-7}$ M; (2) 10^{-6} M; and (3) $5 \cdot 10^{-6}$ M. Detection performed in 0.1 M $NaNO_3$.

3.3.4.3 TBAB effect on montmorillonite

The effect of TBAB insertion in clay structure was studied both for Cu^{2+} and Cd^{2+} water solutions after 5 min accumulation at open-circuit. From Figure 24A and Figure 24B one can observe that the modification of MMT with TBAB (after surfactant removal) led to an increase of about two times the electroanalytical signal for all cations tested (compare curve a and b in Figure 24A and Figure 24B). This proves that the interlayer distance between the clay sheets was found to increase as a result of TBAB ion exchange.

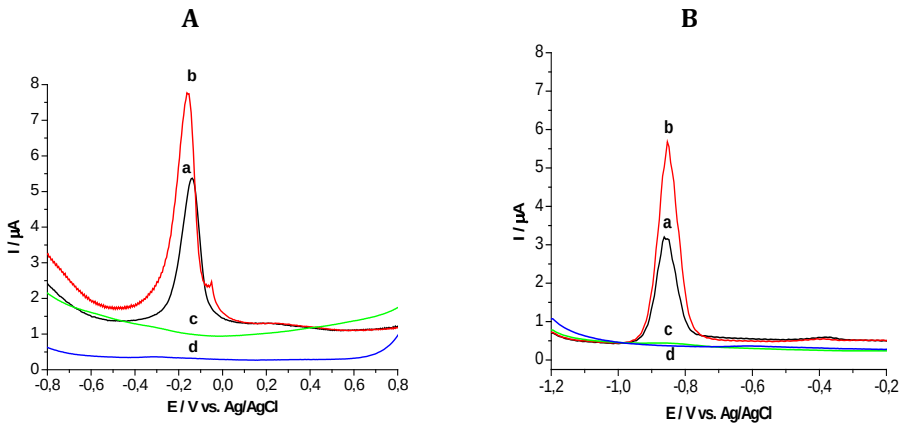

Figure 24 SWVs recorded using clay/GCE: (a) unmodified MMT; (b) GCE+MMT+TBAB(-TBAB) (after TBAB removal) after 5 min accumulation at open-circuit in 10^{-6} M Cu(II) (A) and Cd(II) (B) solutions in ultrapure water. Detection performed 0.1 M $NaNO_3$ after 180 s electrolysis at -0.6 and -1.0 V. Regeneration after 120 s magnetic stirring in 0.1M $NaNO_3$ solution ((c) and (d) represent the clay films regeneration curves).

Ten consecutive voltammetric measurements were performed using the same modified electrode in order to determine the system's stability towards the Cu^{2+} and Cd^{2+}, respectively. The MMT+TBAB(-TBAB)/M modified GCE shows good long-term operational stability for Cu^{2+} (Figure 25) and Cd^{2+} (Figure 26) and good reproducibility for successive preconcentration-detection steps on the same electrode (see some example signals in the inset of Figures 25 and 26). This can be ascribed to the durable mechanical immobilization of the clay material by the aid of the cellulose membrane. One can observe that both unmodified and TBAB modified MMT (tested after TBAB partial extraction) films present good stability, but clay modification improves the preconcentration properties toward Cu(II) and Cd(II) ions.

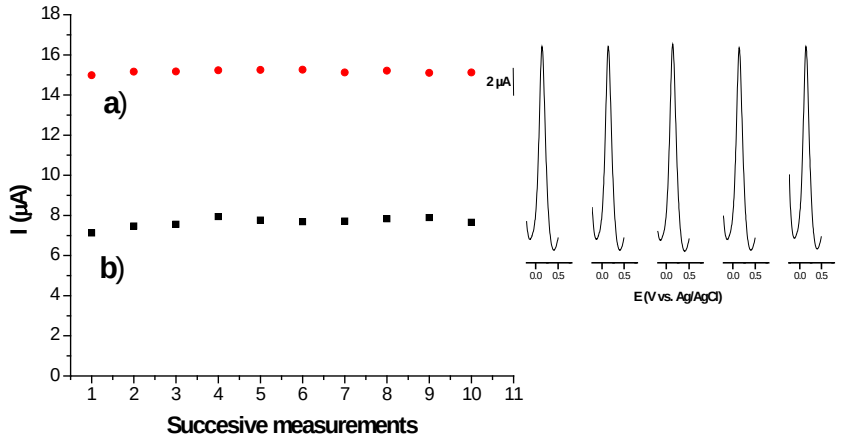

Figure 25 SWV responses obtained with (a) GCE+MMT/M and (b) GCE+MMT+TBAB(-TBAB)/M to successive preconcentration of 10^{-6} M Cu^{2+} solution (5 min accumulation at open circuit, detection in 0.1 M $NaNO_3$ after 180 s electrolysis at -0.6 V, regeneration after 120 s magnetic stirring in 0.1M $NaNO_3$ solution). The inset shows SWVs obtained using GCE+MMT+TBAB(-TBAB)/M after preconcentration in Cu^{2+} solution.

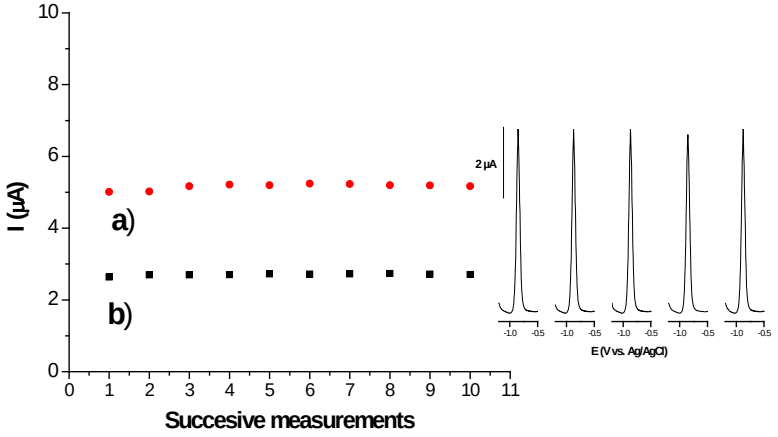

Figure 26 SWV responses obtained with (a) GCE+MMT/M and (b) GCE+MMT+TBAB(-TBAB)/M to successive preconcentration of 10^{-6} M Cd^{2+} solution (5 min accumulation at open circuit, detection in 0.1 M $NaNO_3$ after 180 s electrolysis at -0.6 V, regeneration after 120 s magnetic stirring in 0.1M $NaNO_3$ solution). The inset shows SWVs obtained using GCE+MMT+TBAB(-TBAB)/M after preconcentration in Cd^{2+} solution.

After each measurement, the regeneration of the modified electrode was achieved by immersing the electrode in 0.1 M $NaNO_3$ solution and washing under magnetic stirring for 2 minutes. The resulting relative standard deviation (RSD) is 0.37

% in the case of Cu(II) and 1.554% in the case of Cd(II) detection, indicating that the sensor obtained by fixing the clay film on the electrode with the cellulose membrane can be easily used for repetitive measurements.

3.3.4.4 Calibration data

SWV was used to determine the relationship between the analyte concentration (Cu(II) and Cd(II)) and the peak current intensity in the oxidation field of potentials, by using GCE+MMT+TBAB(-TBAB)/M.

As shown in Figure 27 and Figure 28, there are no anodic peaks when the experiments were performed in Cu(II) and Cd(II) free solutions. In the case of Cu(II), an anodic peak appears at about 0.1 V vs. Ag/AgCl after accumulation at open-circuit in Cu^{2+} solution and the peak current increases with the cation concentration. The oxidation peak potential is slightly shifted to higher positive values with the increase in the analyte concentration in preconcentration solution.

The LOD values were estimated on the basis of a signal-to-noise ratio of 3,[267] while the LOQ values were estimated on the basis of a signal-to-noise ratio of 10.

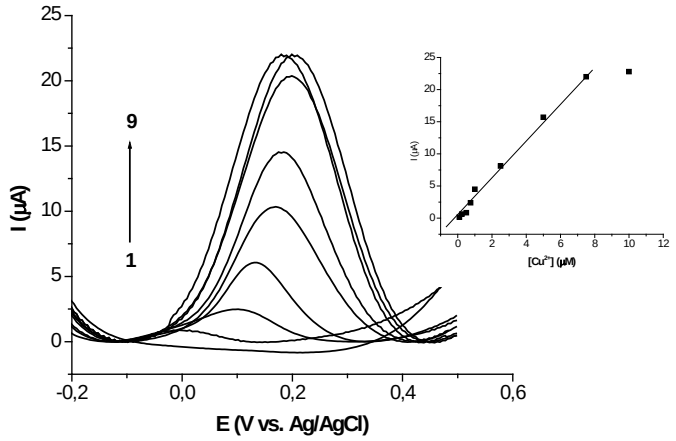

Figure 27 Variation of current intensity on GCE+MMT+TBAB(-TBAB)+M for Cu(II) at different concentration: 0 (1); 0.25 (2); 0.50 (3); 0.75 (4); 1 (5); 2.5 (6); 5 (7); 7.5 (8) and 10 μM (9) in 0.1M $NaNO_3$ solution. Inset: the calibration curve for Cu(II) obtained under optimized conditions. Experimental conditions: 10 min accumulation at open-circuit in Cu^{2+} solutions in ultrapure water; detection performed in 0.1M $NaNO_3$ solution, after 180 s electrolysis at -0.6 V; regeneration after 120 s magnetic stirring in 0.1M $NaNO_3$ solution.

The relationship between Cu(II) concentration and current intensity obtained with SWV was linear in a range from 1.2×10^{-7} M to 7.5×10^{-6} M, according to the equation I (μA) = 2.9823±0.1077 × $[Cu^{2+}]$ (μM) + 0.2333±0.03601 with a correlation coefficient of 0.9922 (8 points considered for the linear plotting). In the case of Cu(II), the LOD was estimated at 3.62×10^{-8} M and LOQ = 10.86×10^{-8} M.

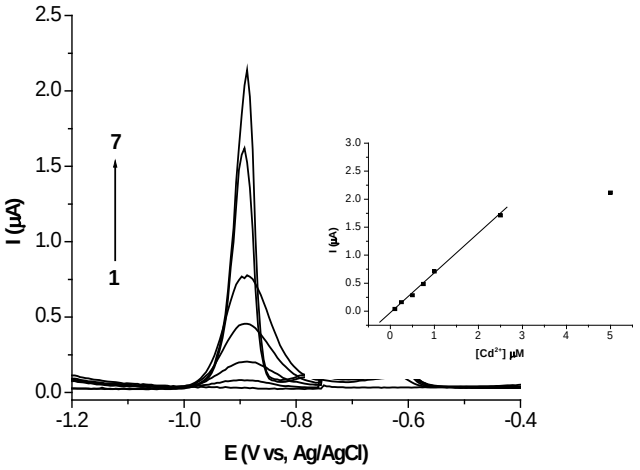

Figure 28 Variation of current intensity on GCE+MMT+TBAB(-TBAB)+M for Cd(II) at different concentration: 0 (1); 0.25 (2); 0.50 (3); 0.75 (4); 1 (5); 5 (6); 7.5 μM (7) in 0.1M $NaNO_3$ solution. Inset: the calibration curve for Cd(II) obtained under optimized conditions. Experimental conditions: 10 min accumulation at open-circuit in Cd^{2+} solutions in ultrapure water; detection performed in 0.1M $NaNO_3$ solution, after 180 s electrolysis at -1.1 V; regeneration after 120 s magnetic stirring in 0.1M $NaNO_3$ solution.

In the case of Cd(II), an anodic peak appears at about -0.9 V/Ag/AgCl after accumulation at open-circuit in Cd^{2+} solution and the peak current increases with the cation concentration. No oxidation peak potential shift was observed when increasing Cd^{2+} concentration in preconcentration solution.

The relationship between Cd(II) concentration and current intensity obtained with SWV was linear in a range from 2.16×10^{-7} M to 2.5×10^{-6} M , according to the equation I (μA) = 0.69791±0.0144 × $[Cd^{2+}]$ (μM) - 0.0277±0.0167 with a correlation coefficient of 0.9983 (6 points considered for the linear plotting). Cd(II) detection limit was estimated at 7.2×10^{-8} M, while LOQ calculated value was 21.6×10^{-8} M.

3.3.4.5 Simultaneous determination of multicomponent cations solutions

Figure 29 shows the voltammetric response of a multi-component solution of Cd^{2+}, Pb^{2+}, and Cu^{2+} registered on GCE+MMT+TBAB(-TBAB)/M after 5 min preconcentration using a 10^{-5} M solution of each metal ion, in comparison with the signals obtained for monocomponent solutions determined in the same conditions. One can see that the interactions between the three cations is minimal in terms of peak current intensity, but the peak potential is shifted to less negative values in the case of Cd(II) signal, while in the case of Cu(II) the sift takes place to more negative values. The position of the Pb(II) peak is less affected by the presence of the other metal ions.

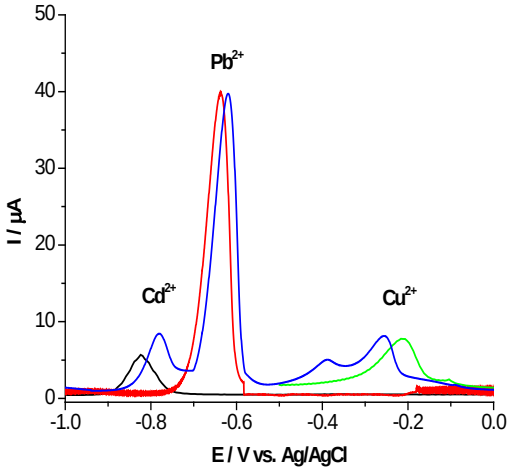

Figure 29 SWVs recorded using GCE+MMT+TBAB(-TBAB)/M, after 5 min accumulation at open-circuit in 10^{-5} M: Cd^{2+} (black), Pb^{2+} (red), Cu^{2+} (green) and a mixture of these three cations (blue) solutions in ultrapure water. Detection performed in 0.1M $NaNO_3$ solution, after 180 s electrolysis at -1.1 V (frequency: 100 Hz; amplitude: 0.05 V; potential step: 0.02; counter electrode: Pt/Ti; reference electrode: Ag/AgCl without internal solution).

3.3.4.6 Interference study

The selectivity of the MMT based sensor for Cu^{2+} and Cd^{2+} was evaluated in the presence of some common metal ions expected to influence the electrochemical sensors signals: Pb^{2+}, Co^{2+}, Ni^{2+}, Zn^{2+}, Ba^{+}, Na^{+}, and K^{+} tested at the same concentration. 10^{-6} M solutions of Cu^{2+} and Cd^{2+}, and of the possible interfering ions were tested by SWV using the GCE+MMT+TBAB(-TBAB)+M system.

The current intensity was measured for each determination and the results are presented in Table 7. The presence of Pb^{2+}, Co^{2+}, Zn^{2+}, Ba^{+}, Na^{+}, and K^{+} does not influence the electrochemical signal of Cu^{2+} and Cd^{2+} in a significant way, but an

important decrease (12 – 16%) in current intensity could be observed in the presence of Ni^{2+} at the same concentration as the main analytes.

To avoid the interferences appearance, for real sample analysis, a dilution of the samples before experimental determination is recommended if samples contain high concentration of cations.

Table 7 Interference study

Interfering ion	Analyte signal (%)	
	Cu^{2+}	**Cd^{2+}**
Cu^{2+}	-	98.89
Cd^{2+}	99.59	-
Co^{2+}	100.03	99.54
Pb^{2+}	101.22	99.76
Ni^{2+}	84.45	88.59
Zn^{2+}	97.28	93.19
Ba^{+}	99.36	99.10
Na^{+}	98.88	99.32
K^{+}	100.47	99.05

3.4 Conclusions

This work demonstrates that low-cost pillared clay is attractive to be used as the electrode modifier for electrochemical sensors.

The effective grafting and functionalization of MMT with TBAB were confirmed by XRD, FT-IR, FT-Raman, and EIS determinations.

TBAB modified montmorillonite was prepared. After partial removal of the surfactant, the resulting material preserved the basic properties of the clay (i.e., cation exchange) and exhibited excellent permeability issues and long-term mechanical stability, which could be notably exploited in preconcentration electroanalysis.

The selectivity of the MMT based sensor for Cu^{2+} and Cd^{2+} was not significantly influenced by the presence of Pb^{2+}, Co^{2+}, Zn^{2+}, Ba^{+}, Na^{+}, and K^{+} ions.

The detection limits were estimated at 3.62×10^{-8} M for Cu^{2+} and 7.2×10^{-8} M for Cd^{2+}, respectively.

The new material exhibited good permeability properties towards selected redox probes (cationic, neutral, and anionic).

The partial removal of TBA^+ ions minimized the positive electrostatic barrier towards cations adsorption and created free adsorption sites, improving thus the electrochemical performances of the new sensor material.

To conclude, the obtained sensor was easily fabricated and showed linear response ranges and good reproducibility being a promising electrode modifier for the accumulation of other cationic toxic species. This low-cost device will be a useful alternative in environmental monitoring of highly toxic contaminants.

4 Clay–mesoporous silica composite films generated by electro-assisted self-assembly

4.1 Introduction

Structuration of electrode surfaces with inorganic thin films has become a well established field of interest, notably for applications in electroanalysis.[3, 116, 121, 123, 126, 128, 160, 249, 253, 262, 296-306] Various materials have been used for that purpose, including zeolites[128, 297-299], clays[3, 126, 249, 262, 300] and layered double hydroxides[300, 301], silica[128, 253, 302] and silica-based organic-inorganic hybrids[121, 302], sol-gel materials[121, 123, 303, 304] and, more recently, ordered mesoporous materials.[116, 128, 160, 305, 306] The driving force to select one or another of these electrode modifiers often relies on the particular properties (ion exchange, selective recognition, hosting capacity, size selectivity, redox activity, permselectivity, etc) which can be useful to the final application (preconcentration electroanalysis, electrocatalysis, permselective coatings, biosensors, ...).

As most of these materials are electronic insulators, their use in connection to electrochemistry requires a close contact to an electrode surface, which can be basically achieved via dispersion of as-synthesized powdered materials in a conductive composite matrix (e.g., CPEs[272]) or deposited as thin films on solid electrode surfaces. In the latter case, a critical point is the uniformity and long-term mechanical stability of the thin coatings, which might be challenging when attempting to deposit particulate materials onto electrodes, requiring often the use of an additional polymeric binder. [307] This is especially the case of zeolite film modified electrodes, the situation being somewhat less problematic for clay film modified electrodes because of the particular platelet morphology of clay particles and their self-adhesive properties toward polar surfaces[21] ensuring better interaction with most electrode materials and consequently more durable immobilization. Nevertheless, besides the classical physical attachment of a clay film to a solid electrode surface (through solvent casting, spin-coating or layer-by-layer assembly as the mainstream techniques[21, 249, 273], or electrophoretic deposition[18]), other strategies based on covalent bonding (via silane or alkoxysilane coupling agents) have been also developed.[10, 274]

On the other hand, the versatility of the sol-gel process makes it especially suitable to coat electrode surfaces with uniform deposits of metal or semimetal oxides (mainly silica) and organic-inorganic hybrid thin films of controlled thickness, composition and porosity. The method is intrinsically simple and exploits the fluidic character of a sol (typically made of alkoxysilane precursors for silica-based materials) to cast it on the surface of a solid electrode, allowing gelation, and drying to get a xerogel film[121, 123, 303, 304]. The driving force for film formation is thus solvent evaporation and this approach is often sufficient to yield high quality films of flat surfaces[308], including the ordered mesoporous ones generated by evaporation induced self-assembly in the presence of surfactant templates[139]. Sol-gel thin films can be also generated onto electrode surfaces by electrolytic deposition. The method involves the immersion of the electrode into a hydrolyzed sol solution (i.e., typically in moderate acidic medium) and the application of a suitable cathodic potential likely to generate hydroxyl ions locally at the electrode/solution interface, such local pH increase contributing to catalyze the precursors polycondensation and the growth of the silica film on the electrode surface.[150, 309, 310] This approach can be extended to the generation of organically-functionalized silica films[152, 153] or to the co-deposition of sol-gel/metal nanocomposites[311] or conductive polymer-silica hybrids[312], and is compatible with the encapsulation of biomolecules to build bioelectrocatalytic devices.[313, 314] When applied in the presence of surfactant template (i.e., CTAB), the method enables the deposition of highly ordered mesoporous silica films with mesopore channels oriented normal to the underlying support[148, 149], a configuration ensuring fast mass transport for analytes from the solution through the film to the electrode surface, thus offering great promise for the elaboration of sensitive electroanalytical devices[182]. Moreover, contrary to the evaporation method, the electro-assisted generation approach enables to get uniformly deposited sol-gel layers onto electrode surfaces of complex geometry or complex conductive patterns (i.e., gold CD-trodes[153], macroporous electrodes[315], metal nanofibers[316] or printed circuits[317]) or at the local scale using ultramicroelectrodes[318, 319]. The method was also proven to be suited to the generation of sol-gel materials through nano- or micro-objects deposited onto electrode surfaces, such as nanoparticles[320] or bacteria[321], thus acting somewhat as a template for film growing.

In the present study, we have further extended the electro-assisted deposition method to generate clay-mesoporous silica composite films and characterized their permeability properties towards selected redox probes (cationic, neutral, and anionic). The synthesis procedure involves at first the deposition of clay particles (montmorillonite-rich natural clay from Romania) onto a glassy carbon electrode surface, and the subsequent electro-assisted self-assembly of a surfactant-templated mesoporous silica around the clay particles. The use of a cationic surfactant (i.e., CTAB) in the synthesis medium was driven by at least two points, the fact that it contributes

to template the silica film (which exhibits distinct permeability properties before and after extraction[148, 149, 182]), and its possible incorporation into the interlayer region of the clay by cation exchange (which is known to modify the interlayer spacing between the clay sheets[284]). Even if some silica-clay composites have been described in the literature[322-324], including two as thin layers on electrode[325, 326], the present work provides, to the best of our knowledge, the first example of electrogenerated clay-mesoporous silica composite films. Their permeability properties and long-term operational stability of the modified electrodes are discussed regarding their physico-chemical characteristics.[275]

4.2 Experimental

4.2.1 Reagents and materials

Tetraethoxysilane (TEOS, 98%, Alfa Aesar), ethanol (95-96%, Merck), $NaNO_3$ (99%, Fluka), HCl (37%, Riedel de Haen), and CTAB (99%, Acros) were used as received for sol-gel films synthesis. The redox probes employed for permeability characterization were analytical grade: ferrocene dimethanol ($Fc(MeOH)_2$, Alfa Aesar); potassium hexacyanoferrate(III) ($K_3Fe(CN)_6$, Fluka); and hexaammineruthenium chloride ($Ru(NH_3)_6Cl_3$, Sigma-Aldrich); they were typically used in 0.1 M $NaNO_3$ solution. A certified copper (II) standard solution (1000 ± 4 mg L^{-1}, Sigma-Aldrich) was used to prepare diluted solutions for preconcentration studies. The electrolytes KCl (99.8%) and HCl (36% solution) were obtained from Reactivul Bucureşti. All solutions were prepared with high purity water (18 MΩ cm^{-1}) from a Millipore Milli-Q water purification system.

The clay sample used in this study was natural Romanian clay from Valea Chioarului (Maramureş County), which consisted mainly of smectite, with minor amounts of quartz. Its physico-chemical characterization is provided elsewhere[239]. The structural formula is $(Ca_{0.06}\ Na_{0.27}\ K_{0.02})_{\Sigma=0.35}\ (Al_{1.43}\ Mg_{0.47}\ Fe_{0.10})_{\Sigma=2.00}\ (Si_{3.90}\ Al_{0.10})_{\Sigma=4.00}\ O_{10}(OH)_2 \cdot nH_2O$. It is characterized by a surface area (N_2, BET) of 190 $m^2\ g^{-1}$. Only the montmorillonite-rich fine fraction of the clay (< 0.2 μm, as collected by sedimentation according to Stockes law, after the raw clay was suspended in water, ultrasonicated for about 15 min and allowed to settle, centrifugation and ultracentrifugation of the supernatant phase) was used here. This fine fraction has a cation exchange capacity (CEC) of 0.78 meq g^{-1}. Its XRD diffractogram showed a high content of montmorillonite (with its characteristic peaks at 2θ: 6.94°; 19.96°; 21.82°; 28.63°; 36.14°; 62.01°) and also confirmed the almost negligible presence of other minerals.[275]

4.2.2 Preparation of the clay-mesoporous silica films

Glassy carbon electrodes (GCE, 5 mm in diameter) were first polished on wet silicon carbide paper using 1 and 0.05 μm Al_2O_3 powder sequentially and then washed

in water and ethanol for a few minutes, respectively. GCE were afterwards coated with a clay film, which was prepared by depositing a 10 µL aliquot of an aqueous clay suspension (5 mg mL^{-1}) by spin-coating onto the GCE surface, as in[251]. The film was dried for 1 h at room temperature prior to any further use. This electrode is denoted below as "GCE-clay". A mesoporous silica film was then electrogenerated through this film, around the clay particles, onto the electrode surface under potentiostatic conditions. This was typically achieved from a precursor solution containing 20 mL ethanol, 20 mL aqueous solution of 0.1 M $NaNO_3$ and 0.1 M HCl, to which 13.6 mmol TEOS and 4.35 mmol CTAB were added under stirring (optimized conditions as in[148, 149, 182]) and the resulting sol was aged for 2 h prior to use. The GCE-clay electrode was then immersed in this sol solution and electro-assisted deposition was performed by applying -1.3 V for 10 s. The electrode was then quickly removed from the solution, rinsed with water, and dried/aged overnight in an oven at 130°C. The resulting composite film electrode is denoted "GCE-clay-mesopSiO_2". It can be used as such or after template removal; in this latter case, the CTAB template is solvent-extracted with an ethanol solution containing 0.1 M $NaClO_4$ for 5 min under moderate stirring. For comparison purposes, a template-free silica film was also deposited onto the GCE-clay electrode, exactly under the same aforementioned conditions but in the absence of CTAB in the starting sol. It is denoted "GCE-clay-SiO_2".[275]

4.2.3 Apparatus and characterization procedures

All electrochemical experiments were performed using a PGSTAT-12 potentiostat (EcoChemie) monitored by the GPES software. A conventional three electrode cell configuration was employed for the electrochemical measurements. Film modified GCEs were used as working electrodes, with a saturated Ag/AgCl (Metrohm) and a platinum wire as reference and counter electrode, respectively. CV measurements were carried out respectively in 5 mM $Fc(MeOH)_2$, 1 mM $K_3Fe(CN)_6$, or 0.1 mM $Ru(NH_3)_6Cl_3$ (in 0.1 M $NaNO_3$). CV curves were typically recorded in multisweep conditions (ca. 20 cycles) at a potential scan rate of 20 mV s^{-1} and used to qualitatively characterize accumulation/rejection phenomena and mass transport issues through the various films. Accumulation-detection experiments were also performed using copper (II) as a model analyte. Typically, open-circuit accumulation was made from diluted copper(II) solutions (10^{-7} – 10^{-6} M) at pH 5.5, and voltammetric detection was achieved after medium exchange to a copper(II)-free electrolyte solution (0.1 M KCl + 0.1 mM HCl) by SWV, at a scan rate of 5 mV s^{-1}, a pulse amplitude of 50 mV and a pulse frequency of 100 Hz.

The films morphology was observed by scanning electron microscopy (SEM) and micrographs were recorded with a Hitachi FEG S-4800 apparatus. The film structure was characterized by X-ray diffraction (XRD) in Bragg-Brentano geometry using a Panalytical X'Pert Pro diffractometer operating with a copper cathode ($\lambda_{K\alpha}$ = 1.54056

Å). Atomic force microscopy (AFM, apparatus Thermomicroscope Explorer Ecu+, Veeco Instruments SAS) was also used to evaluate the film thickness.[275]

4.3 Results and discussions

4.3.1 Films preparation and permeability properties evaluated by cyclic voltammetry

The various electrode configurations investigated here are schematically represented in Figure 30. In the raw clay modified electrode (GCE-clay, Figure 3a), the clay particles are expected to lie randomly onto the electrode surface[21, 249]. Then, the non occupied volume between these particles is filled upon electro-assisted generation of the surfactant-templated silica material (GCE-clay-mesopSiO_2) or the non templated silica layer (GCE-clay-SiO_2). It was proven previously that electro-assisted deposition of sol-gel films implies a mechanism involving the generation of hydroxyl ions under potential control, leading to a pH increase at the electrode/solution interface, catalyzing thereby the sol-gel film deposition[148-150, 152, 182, 309, 310, 320]. The method is thus conceptually different from the direct electrodeposition of composites such as clay-metallic films (i.e., using the clay particles as quasi-templates[327]) or conductive polymer-clay films[328], for which the deposited matter is that resulting from the direct electrochemical transformation of the precursors (reduction of metal ions or electropolymerization of monomers), thus leading film growing obligatory from the underlying electrode surface. In the present case, the electron transfer reaction does not contribute to the electrochemical transformation of the precursors but it generates the catalyst (i.e., hydroxyl ions) that induces the precursors polycondensation and formation of the silica network. These catalytic species are expected to be present in a rather thick region at the electrode/solution interface (i.e., the diffusion layer) so that the gelification process can occur simultaneously in the whole non occupied volume between the clay particles to form the clay-mesoporous silica film (GCE-clay-mesopSiO_2, Figure 30b-c) or clay-silica composite films (GCE-clay-SiO_2, Figure 30d). Actually, it has been reported that electro-assisted deposition of mesoporous silica through an assembly of microparticles deposited onto an electrode surface happened in a multi-step process, the material starting to deposit around the particles (in agreement to faster gelification onto solid surfaces in comparison to bulk gelification from homogeneous sols[329]) and then tended to fill all the interstitial volume to give the final composite films[320]. The schemes in Figure 30, though simplified, provide thus a realistic view of the different systems studied here. No real morphology difference is expected to occur between GCE-clay-mesopSiO_2 electrodes before and after surfactant extraction, except that mesoporosity would be revealed after template removal.[148]

The cyclic voltammetry characterization of these 4 film electrodes (GCE-clay, GCE-clay-mesopSiO_2 before and after surfactant extraction, and the non templated

GCE-clay-SiO_2 film), using three relevant redox probes ($Fe(CN)_6^{3-}$, $Fc(MeOH)_2$, $Ru(NH_3)_6^{3+}$), is summarized in Figure 31. Several observations and conclusions can be drawn from these data.

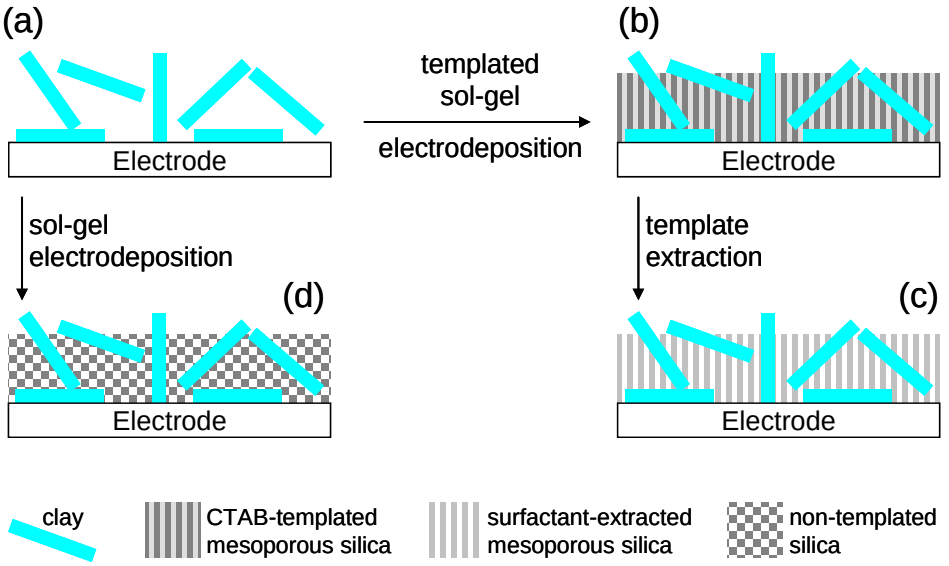

Figure 30 Schematic view of the various electrode configurations used in this work

First, the raw clay deposit acts as a barrier to the negatively-charged $Fe(CN)_6^{3-}$ species (see part B1 in Figure 31), as a result of electrostatic repulsions of the negatively-charged clay sheets. Nevertheless, the clay film is still porous as it let the neutral $Fc(MeOH)_2$ species quite easily reach the electrode surface, which resulted in almost similar CV response as on bare GCE, at least when reaching steady-state after 20 cycles (compare parts B2 and A2 in Figure 31).

Finally, the CV signal of the positively-charged $Ru(NH_3)_6^{3+}$ species was found to be larger than at the bare electrode (compare parts B3 and A3 in Figure 31) and was found to continuously grow upon multiple successive potential scanning (see part B3 in Figure 31) owing to the preconcentration of these $Ru(NH_3)_6^{3+}$ species by cation exchange in the clay particles. Overall, this behavior is consistent with previous observations on similar systems[251] and the preconcentration capacity was exploited in ion exchange voltammetry.[330]

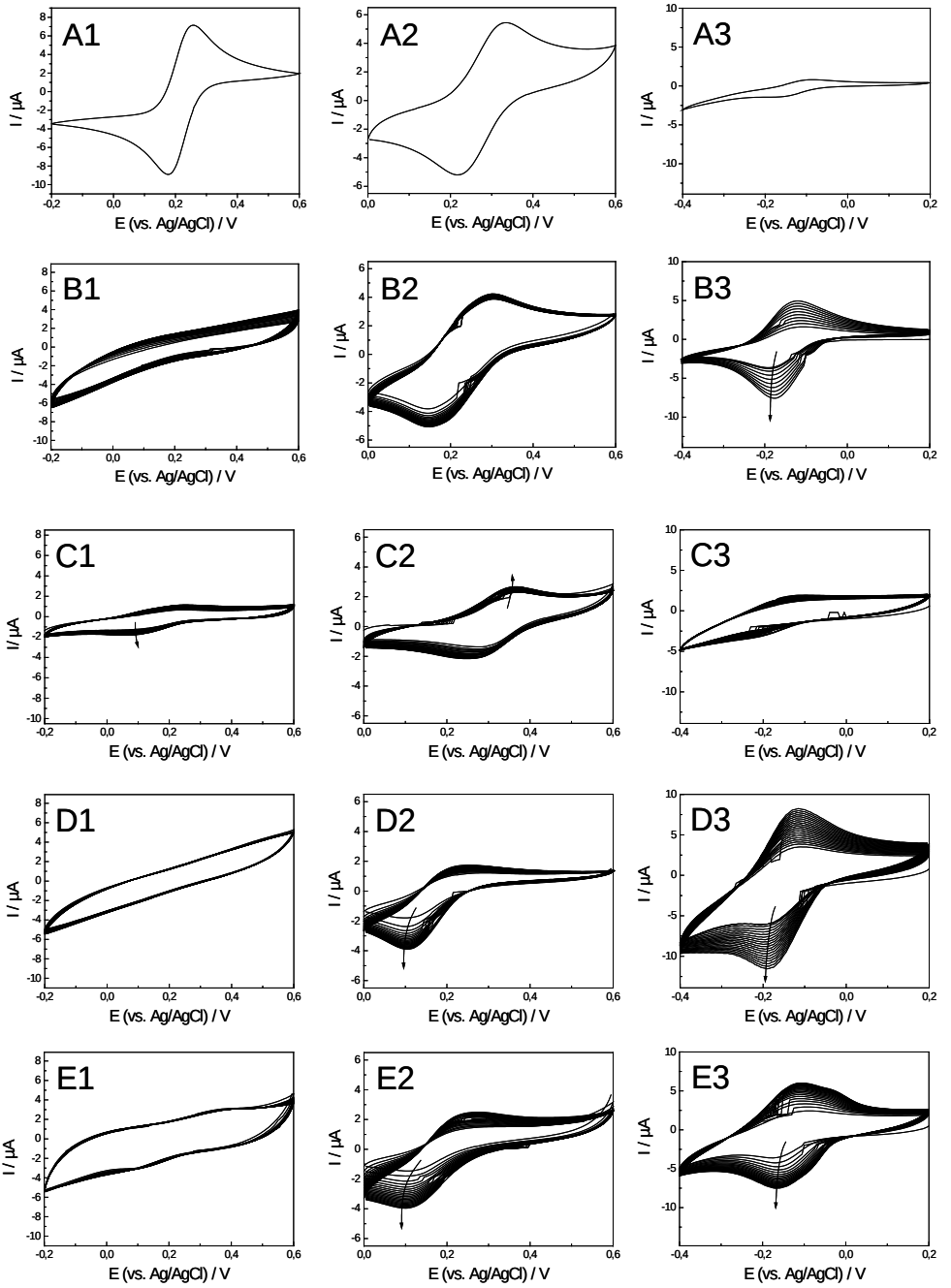

Figure 31 Cyclic voltammetric curves recorded at 20 mV s^{-1} for 20 successive cycles using (A) bare GCE, (B) GCE-clay, (C, D) GCE-clay-mesopSiO_2 respectively before (C) and after (D) surfactant removal, and (E) GCE-clay-SiO_2 electrodes, for three redox probes (1: $Fe(CN)_6^{3-}$; 2: Fc(MeOH)2; 3: $Ru(NH_3)_6^{3+}$) in 0.1 M $NaNO_3$

The situation was definitely different for the GCE-clay-mesopSiO_2 electrode. Let's first consider the case prior to surfactant extraction. Using the $Fe(CN)_6^{3-}$ probe resulted in a very small signal, yet clearly visible (see part C1 in Figure 31), slightly and continuously growing upon successive cycling. This behavior suggests some accumulation of the negatively-charged $Fe(CN)_6^{3-}$ species. To interpret this result, one has to remind that sol-gel electro-assisted deposition was performed in the presence of CTAB in the solution (at ca. 0.1 M), and that the cetyltrimethylammonium cation, CTA^+, is likely to accommodate the clay particles.[284] Actually, when smectite type clays are treated with a cationic surfactant at a concentration ranging between 0.5 and 1.5 times the CEC of the clay, the surfactant molecules adopt a bilayer or pseudotrimolecular arrangement within the clay platelets, with both vertical and horizontal orientations of the alkylammonium chains.[291] The aggregation of the organic cations thus occurs via both ion exchange and hydrophobic bonding which leads to the creation of positive charges in the clay layer and on the clay surface, inducing thereby possible uptake of anionic species by the clay composite via the formation of surface-anion complex.[292, 293] In the present case, even if it is impossible to quantitatively determine the amount of surfactant molecules in the clay, one can reasonably ascribe the slight accumulation of redox species, as observed in part C1 in Figure 31, to the replacement of the weakly retained counterions (Br^-) of the surfactant in the clay by the $Fe(CN)_6^{3-}$ probe, leading to the formation of ion pairs between CTA^+ cations and $Fe(CN)_6^{3-}$ anions. The accumulation effect is however much lower than that for classical surfactant-modified clay films (e.g., smectite clay modified with hexadecyltrimethylammonium[265]) because of the presence of the surfactant-templated mesoporous materials around the clay particles in the present case. An additional indication of the presence of CTA^+/CTAB in the clay is the almost totally suppressed response of the film to the $Ru(NH_3)_6^{3+}$ probe (no more accumulation possible by cation exchange, see part C3 in Figure 31). This signal suppression also tends to support a good coverage of the whole electrode surface with a crack-free clay-mesoporous silica composite film (the presence of some holes would have resulted in noticeable CV response). Finally, the response to the neutral $Fc(MeOH)_2$ species was lower than previously, but still significant (40 % of the intensity on bare GCE), and shifted by ca. 0.1 V towards more anodic potentials (compare parts B2 and C2 in Figure 31). This is explained by the solubilization of the neutral probe in the surfactant phase, as previously reported for electrodes covered with surfactant-templated mesoporous silica films[141, 148].

After surfactant removal, the GCE-clay-mesopSiO_2 electrode exhibited again a distinct behavior (compare parts C1-3 and D1-3 in Figure 31). Note that extraction of the surfactant template was made using ethanol and $NaClO_4$ (not the classically used ethanol/HCl mixture) to avoid any chemical degradation of the clay (i.e., acid hydrolysis of the aluminum sites in the aluminosilicate) and to maintain its cation exchange capacity. The voltammetric characteristics of the surfactant-extracted GCE-

clay-mesopSiO_2 electrode resembles somewhat to those observed for the raw clay film electrode (GCE-clay), yet with some differences, as it can be seen by comparing parts B1-3 and D1-3 in Figure 31. The absence of signal to negatively charged $Fe(CN)_6^{3-}$ species (see part D1 in Figure 31) is again explained by electrostatic repulsions from both the negatively-charged clay sheets and the negatively-charged silica surface (as also evidenced for pure mesoporous silica films[141]). The neutral $Fc(MeOH)_2$ probe is still detectable on the GCE-clay-mesopSiO_2 film electrode but less easily than for GCE-clay (compare parts D2 and B2 in Figure 31) because the probe molecules have now to cross the mesoporous silica binder to reach the underlying electrode surface. On the other hand, the accumulation response of $Ru(NH_3)_6^{3+}$ species upon continuous potential cycling is more marked (compare parts D3 and B3 in Figure 31) due to the synergistic properties of the composite film (cation exchange in the clay and favorable electrostatic interactions with the negatively charged silica surface; this last phenomena was previously demonstrated for the accumulation of both $Ru(NH_3)_6^{3+}$ and $Ru(bpy)_3^{2+}$ at mesoporous silica modified electrodes[141, 148]). These results indicate promising use of GCE-clay-mesopSiO_2 for preconcentration electroanalysis of cationic analytes (see section 3.3 for confirmation).

Some control experiments have been also performed using a non templated GCE-clay-SiO_2 composite film electrode. The results indicate comparable behavior as for GCE-claymesopSiO_2 (suppressed response to $Fe(CN)_6^{3-}$; significant signal for $Fc(MeOH)_2$, suggesting the existence of some porosity; good response to the positively-charged $Ru(NH_3)_6^{3+}$ species, in agreement with previous observations made for sol-gel derived clay-silicate film electrodes using $Fe(CN)_6^{3-}$ and methylviologen as redox probes[325]), but a less effective accumulation of the $Ru(NH_3)_6^{3+}$ probe in comparison to the templated composite film (compare parts E3 and D3 in Figure 31).[275]

4.3.2 Physico-chemical characterization

XRD was first used to characterize the eventual structural changes of the smectite clay upon entrapment within the CTAB-templated mesoporous silica film. As expected, prior to sol-gel electrodeposition, the clay film exhibited the same montmorillonite characteristics as those reported for the raw clay particles in the experimental section (diffraction lines at 2θ values (°) of 6.9; 19.9; 21.8; 28.6; 36.1; 62.0, data not shown). Focusing on the low angles range (Figure 32), corresponding to the d001 reflection, one can see what happened as a result of the various treatments (electro-assisted deposition in the presence of CTAB and template removal, respectively). Prior to any treatment, the d001 reflection appears at 2θ = 6.9° (see curve "a" in Figure 32), which corresponds to a *d* spacing of 12.9 Å (i.e., a classical interlayer distance for montmorillonite clays[331, 332]). After electro-assisted deposition of the mesoporous silica, this line at 2θ = 6.9° almost disappears, to be replaced by new lines at much lower 2θ values (i.e., 4.59° and 2.19°, see curve "b" in Figure 32). This

indicates an expansion of the interlayer region between the clay sheets. As the clay was in contact with a CTAB solution prior to and during electro-assisted deposition of the mesoporous silica material, this expansion is certainly due to the incorporation of CTA^+ and CTAB species in the clay interlayer (a process which is known elsewhere[284, 333, 334]). Actually, the XRD pattern (curve "b" in Figure 32) is very similar to those previously observed for montmorillonite treated with CTAB at a concentration at least 3 times higher than the clay cation exchange capacity (which is the case here), indicating the existence of a CTAB-clay material with the surfactant in a paraffin-bilayer configuration (i.e., with surfactant binding to the clay by ion exchange and via hydrophobic interactions).[284] This result supports the above interpretation of CV data obtained for the $Fe(CN)_6^{3-}$ probe at GCE-clay-mesopSiO_2 (part C1 in Figure 31) for which the observed small increase of the voltammetric signal was attributed to the formation of ion pairs between CTA^+ cations immobilized in/on the clay particles and $Fe(CN)_6^{3-}$ anions. After removal of the surfactant template from GCE-clay-mesopSiO_2, the clay interlayer distance was found to recover almost its initial value (see curve "c" in Figure 32), with a *d* spacing of 13.2 Å (i.e., close to the 12.9 Å value measured for the raw clay). This indicates that the CTAB loading/removal from the clay is reversible and that no silica condensation occurred in the interlayer of the clay (as might occur in porous clay heterostructures[335, 336]). The control XRD measurements performed for samples prepared without clay or without CTAB (see curves "d" and "e" in Figure 32) further confirmed the above discussed phenomena.

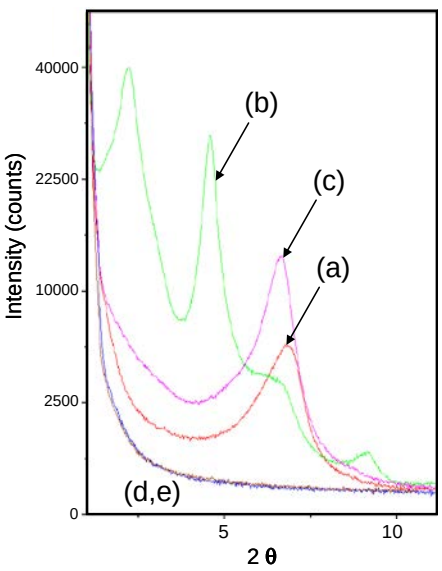

Figure 32 X-Ray diffractograms for (a) GCE-clay, (b, c) GCE-clay-mesopSiO_2 respectively before (b) and after (c) surfactant removal, (d) GCE-clay-SiO_2 and (e) GCE-mesopSiO_2.

SEM characterization of similar films as those analyzed in XRD provided additional information on their texture. Both top-view and cross-sectional views are shown (Figure 33). Clay particles are clearly visible on the cross-sectional view of the spin-coated clay film (Figure 33B). At the opposite, the composite material prepared by electro-assisted deposition of mesoporous silica with CTAB is characterized by a more homogeneous texture, which can be explained by a rather good filling of the inter-particle region of the clay film with the surfactant-templated silica matrix (Figure 33D). Some increase in the film thickness can be also evidenced (as also confirmed by AFM measurements in Figure 34), consistent with the expansion of the clay in the presence of CTAB. On the other hand, the composite sample prepared from electroassisted deposition of silica from a CTAB-free sol solution leads to a texture (Figure 33F) quite comparable to the one observed with the initial clay film. This is explained by the much slower electro-assisted deposition of silica in the absence of CTAB[148], resulting in lesser amounts of silica binder deposited around the clay particles. Note that SEM top views did not show different film features between the initial clay film and the composite material prepared by electro-assisted deposition of mesoporous silica with CTAB (compare parts A and C in Figure 33), which is also supported by AFM imaging (Figure 34), indicating that mesoporous silica deposition was essentially restricted to the clay layer.

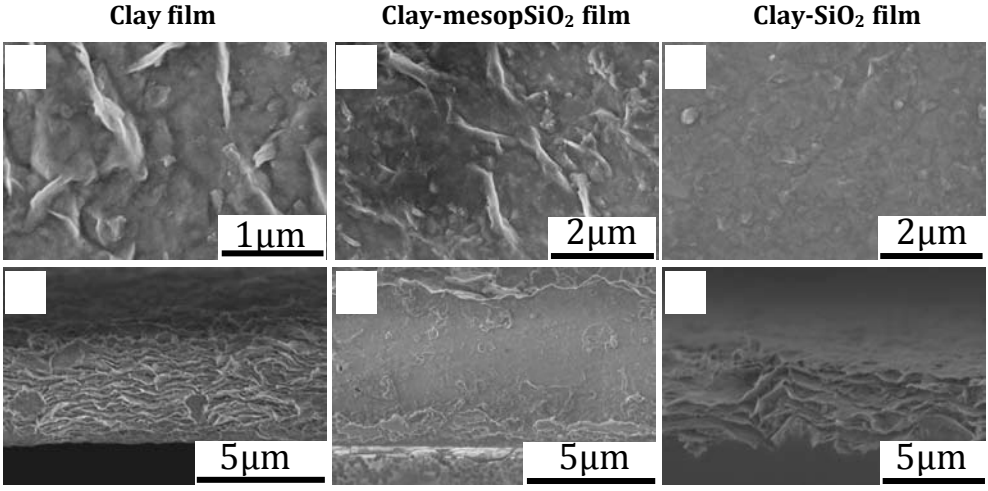

Figure 33 SEM images of a spin-coated clay film (A,B) and composite materials obtained by electro-assisted deposition of surfactant-templated silica around the clay (clay-mesopSiO$_2$: C,D) and non-templated composite materials (E,F). Both top views (A, C, and E) and cross-sections (B, D, and F) are shown.

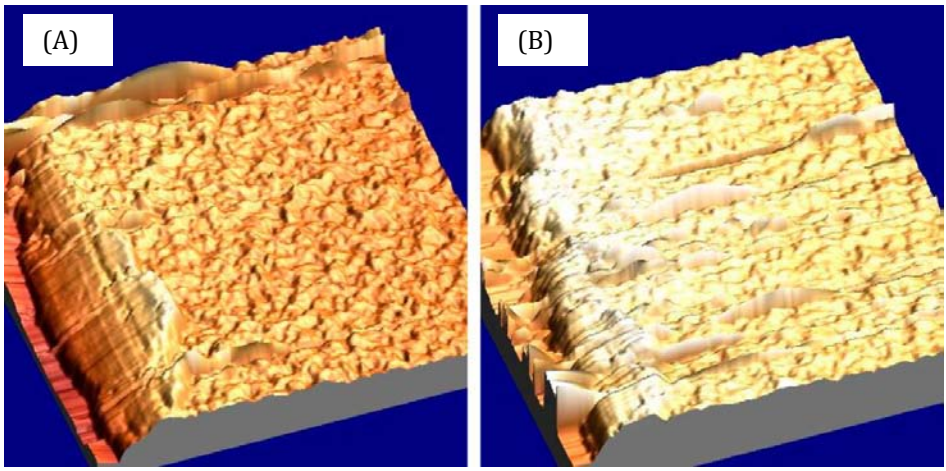

Figure 34 AFM images of a spin-coated clay film (A) and a clay-mesopSiO_2 film (B)

It can be concluded that electro-assisted deposition of a surfactant-templated mesoporous silica matrix through a clay film electrode allows the fabrication of a composite material displaying a good homogeneity in the whole thickness of the composite film, which confirms the above voltammetric behavior and suggests possibly good mechanical stability, as discussed below on the basis of successive uses in preconcentration electroanalysis. [275]

4.3.3 Effect on copper(II) preconcentration and detection

To further characterize the novel composite films and to discuss their potential interest for voltammetric sensing, the modified electrodes were subject to preconcentration analysis using copper(II) as a model analyte. The accumulation was made at open-circuit from an unbuffered copper(II) solution and detection was made by SWV after medium exchange to a slightly acidic chloride solution (pH 4) likely to desorb the previously accumulated copper(II) species; actually the detection sensitivity was highly pH-dependent (signal intensity increasing continuously when decreasing pH from 5 to 1) but, as far as multiple analyses with the same electrode are concerned, too acidic media have to be avoided to maintain the chemical integrity of the clay (i.e., ion exchange capacity), so that pH 4 was chosen as the best compromise between sufficient sensitivity and good reusability. In these conditions, well-defined SWV curves can be obtained and the peak intensity was dependent on the electrode type, growing from GCE-clay-SiO_2 to GCE-clay and to surfactant-extracted GCE-clay-mesopSiO_2, in agreement with the trend observed in their CV response to the cationic

$Ru(NH_3)_6^{3+}$ redox probe (Figure 31C). Focusing on the most sensitive system (GCE-clay-mesopSiO_2), one can see in Figure 35 that the SWV response was function of both copper(II) concentration in the accumulation medium and preconcentration time. The variations were as expected for preconcentration electroanalysis at modified electrodes involving an accumulation by analyte binding to active centers (i.e., a first linear increase of the signal followed by leveling off when reaching steady-state (ion exchange equilibrium or saturation of ion exchange sites), in agreement with previous observations made for copper(II) electroanalysis at other kind of modified electrodes.[191, 294, 295] Interestingly, the time response was very fast (the voltammetric response of the electrode increased linearly as a function of accumulation time from the early accumulation times) contrary to some delay that can be observed to get a detectable signal, e.g., in case of restricted diffusion rates or slow binding processes.[191, 294] Such good performance can be explained by the highly porous structure of the composite film after surfactant extraction.

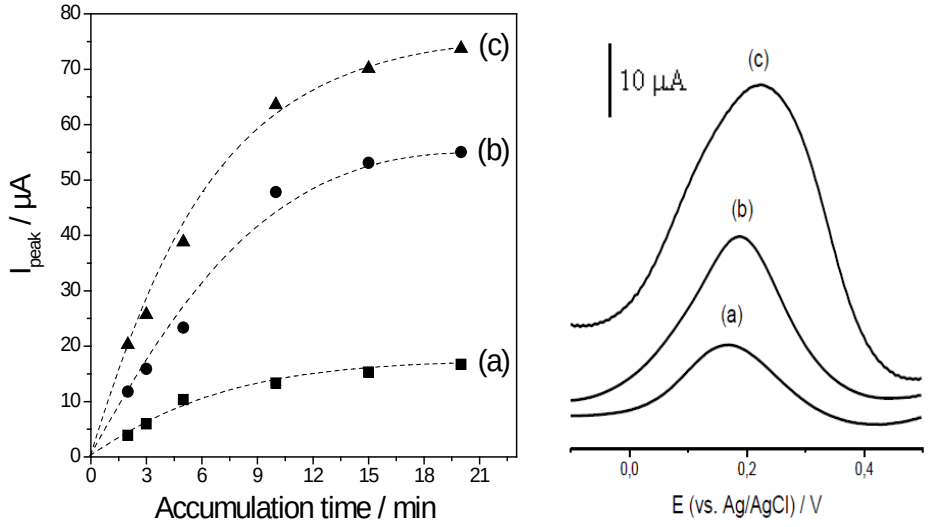

(A) (B)

Figure 35 (A) Variation of SWV peak currents recorded using GCE-clay-mesopSiO_2 after open circuit accumulation of Cu^{2+} at various concentrations: (a) 10^{-7} M, (b) $5 \cdot 10^{-7}$ M, and (c) 10^{-6} M. Detection medium composition: 0.1 M KCl + 0.1 mM HCl. (B) Typical SWV curves obtained at the above different concentrations of Cu2+ but at the same preconcentration time (5 min).

Another attractive feature is the rather good long-term operational stability of the GCE-clay-mesopSiO_2, as illustrated in Figure 36 (curve "b") and the good reproducibility observed for successive preconcentration-detection steps with the same electrode (see some typical signals in the inset of Figure 36). This can be ascribed to the durable immobilization of the clay material by physical entrapment in the surrounding mesoporous silica matrix. By contrast, the response of GCE-clay to successive experiments was found to rapidly decrease to almost zero (see curve "a" in Figure 36), probably as a result of progressive leaching of the clay particles in the solution due to rather poor mechanical stability in stirred medium (it should be reminded here that preconcentration was performed in stirred solution to facilitate mass transport of the analyte). Finally, it is noteworthy that a clay-free GCE-mesopSiO_2 electrode gave also rise to stable signals upon successive preconcentration-detection experiments (see curve "c" in Figure 36), but with much lower sensitivity as a result of poor Cu^{2+} preconcentration efficiency of the mesoporous silica matrix, confirming again the interest of the clay-mesoporous silica composite material developed here.

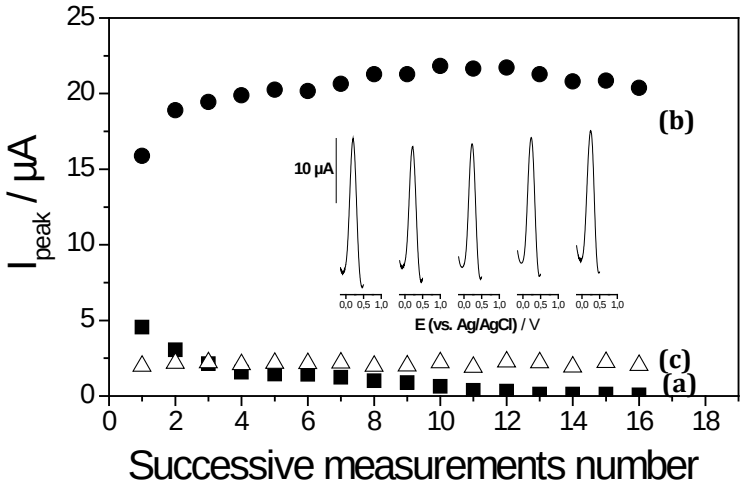

Figure 36 SWV responses obtained with (a) GCE-clay, (b) GCE-clay-mesopSiO_2 after surfactant removal, and (c) GCE-mesopSiO_2, to successive preconcentration of 10^{-6} M Cu^{2+} (2 min accumulation at open circuit; detection in 0.1 M KCl + 0.1 mM HCl). The inset shows some typical curves obtained with GCE-clay-mesopSiO_2 after surfactant removal (corresponding to data in part "b" of the figure).

The modified electrode developed here offers good performance in terms of sensitivity and long-term stability but, of course, not in terms of selectivity as the Cu^{2+} recognition processes ion exchange, which is obviously not so selective with respect to other metal ions. Anyway, the method could be applied to generate composite films

based on other clay materials, such as organically-grafted clays, which are known to exhibit much better selectivity towards target metal ions depending on the nature of the organo-functional groups used to modify the clay.[69, 251, 267, 275]

4.4 Conclusions

This work has demonstrated the possible electro-assisted generation of clay-mesoporous silica composite films on electrodes by combining the electro-assisted self-assembly process[148, 149] with the spin-coated clay films. After surfactant removal, the resulting materials kept the basic properties of the clay (i.e., cation exchange) and exhibited excellent permeability issues and long-term mechanical stability, which could be notably exploited in preconcentration electroanalysis. A particular feature of the developed method was the reversible intercalation/exchange of the cationic surfactant in the interlayer region of the clay (with concomitant variation in the interlayer distance), which avoided any deposition of silica between the clay sheets and probably also ensured fast mass transport through the film by creating high porosity upon surfactant extraction. The method appears rather general and could be applied, for example, to the preparation of organically-functionalized clay-mesoporous silica materials by adding suitable organosilanes in the synthesis medium, which would lead to multifunctional composite films.[275]

5 Final conclusions

The high demand for simple, fast, accurate, and sensitive detection methods in pharmaceutical and environmental analysis has led to the development of novel electrochemical sensors. Due to their ion exchange capacity and adsorbent properties, clay modified electrodes are likely to be used for this application.

Montmorillonite-rich indigenous Romanian clays were employed for the modification of different types of electrodes in order to develop sensors applied in the detection of heavy metals from matrices of biopharmaceutical and biomedical interest and biosensors for the detection of different pharmaceuticals.

Bentonites obtained from Răzoare and Valea Chioarului deposits (Maramureş County, Romania) were refined and characterized by X-ray diffraction, transmission electron microscopy, FTIR, and thermodifferential analysis. The ion exchange capacity of purified clays was determined by replacing the compensatory ions with NH_4^+ ions. All physico-chemical studies revealed montmorillonite as the main component of their structure.

The electrochemical behavior of acetaminophen, ascorbic acid, and riboflavin phosphate was tested by cyclic voltammetry on clay-modified CPEs with different clay particle sizes. Resulting CPEs revealed either better electroanalytical signals or oxidation at lower potential values. These results recommend the application of the new clay-modified sensors in pharmaceutical analysis.

The development of a biosensor based on the immobilization of HRP within a Romanian clay-polyethylenimine film at GCEs surface for acetaminophen detection is described. In this case, HRP was immobilized on the surface of the GCE by retention in a polyethylenimine and clay porous gel film, a technique that offered good entrapping and a protective environment for the biocomponent due to the hydration properties of the immobilization layer. The amperometric detection of acetaminophen was successfully achieved with a sensitivity of 6.28×10^{-7} M and a linear range between 5.25×10^{-6} M and 4.95×10^{-5} M.

The use of a low-cost pillared clay as electrode modifier for electrochemical sensors development is also demonstrated in this work. For this, montmorillonite was modified with TBAB. By partial removal of the surfactant, the resulting material

preserved the basic properties of the clay (i.e., cation exchange) and could be therefore exploited in the development of sensors able to detect the cationic toxic species (e.g., Cu(II), Cd(II)) from different matrices with good reproducibility and sensitivity.

Finally, this thesis reveals the electro-assisted generation of clay-mesoporous silica composite films onto GCEs. The method involved the deposition of clay particles by spin-coating on GCE and the subsequent growing of a surfactant-templated silica matrix around these particles by EASA. EASA typically consisted in applying a cathodic potential to the electrode immersed into a hydrolyzed sol (containing TEOS as the silica source, and CTAB as surfactant) in order to generate the necessary hydroxyl catalysts inducing the formation of the mesoporous silica. In such conditions, alongside the silica deposition process, the interlayer distance between the clay sheets was found to increase as a result of CTAB ion exchange. After removal of the surfactant template, the composite film became highly porous (i.e., to redox probes) and the clay recovered its pristine interlayer distance and cation exchange properties. This made it promising for application in preconcentration electroanalysis, as pointed out here using copper(II) as a model analyte, especially because it offered much better long-term operational stability than the conventional (i.e., without silica binder) clay film electrode. This is the first example of electrogenerated clay-mesoporous silica composite films in the literature and the promising applications of these new composite materials are also discussed here.

The rather general methods presented in this thesis can be further exploited to develop new reliable methods for environmental and pharmaceutical monitoring of highly toxic contaminants with improved selectivity.

6 Originality of the thesis

This thesis aims at developing new composite materials by exploring the ion exchange and adsorbent properties of two montmorillonite-rich Romanian natural clays (from Răzoare and Valea Chioarului deposits, Maramureş County) for sensors and biosensors construction. I believe that the results of these studies will have important impact on the pharmaceutical and environmental fields as they:

1) Present for the first time the applications of Romanian clays in electroanalysis for heavy metal detection and for development of biosensors with applications in pharmaceutical analysis;

2) Describe for the first time the complete structural characterization of Răzoare and Valea Chioarului bentonites;

3) Establish new performances for the existent sensor devices as the developed systems show good long-term operational stability and good reproducibility (e.g., GCE-clay-mesopSiO_2);

4) Provide new approaches for the determination of heavy metals in various matrices;

5) Give the first example of electrogenerated clay-mesoporous silica composite films with promising applications;

6) Acetaminophen and riboflavin phosphate was tested for the first time on clay-modified CPEs and new electrochemical methods are proposed to be applied for their detection in pharmaceutical analysis.

This study describes reliable methods for environmental monitoring of highly toxic contaminants. The methods presented here are rather general and could be further exploited to generate composite films based on other clay materials with improved selectivity.

REFERENCES

1. Stetter J, Penrose WR, Yao S. Sensors, chemical sensors, electrochemical sensors, and ECS. J Electrochem Soc. 2003;150:511 - 6.
2. Mousty C. Sensors and biosensors based on clay-modified electrodes—new trends. Appl Clay Sci. 2004;27:159-77.
3. Navrátilová Z, Kula P. Clay modified electrodes: present applications and prospects. Electroanalysis. 2003;15:837- 46.
4. Lee SM, Tiwari D. Organo and inorgano-organo-modified clays in the remediation of aqueous solutions: An overview. Appl Clay Sci. 2012;59-60:84-102.
5. Bedioui F. Zeolite-encapsulated and clay-intercalated metal porphyrin, phthalocyanine and Schiff-base complexes as models for biomimetic oxidation catalysts: an overview. Coordination Chemistry Reviews. 1995; 144:39-68.
6. Layer Charge Characteristiscs of 2:1 Silicate Clay Minerals. Mermut AR, editor. Boulder: The Clay Minerals Society,USA; 1994.
7. Vaccari A. Preparation and catalytic properties of cationic and anionic clays. Catal Today. 1998;41:53- 71.
8. Vaccari A. Clays and catalysis: a promising future. Appl Clay Sci. 1999;14:161- 98.
9. Gianfreda L, Rao M A, Sannino F, Saccomandi F, Violante A. Enzymes in soil: properties, behavior and potential applications. Dev Soil Sci. 2002;28B:301- 27.
10. Rong D, Kim YI, Mallouk TE. Electrochemistry and photoelectrochemistry of pillared clay-modified-electrodes. Inorg Chem. 1990;29:1531-5.
11. Hotta Y, Inukai K, Taniguchi M, Yamagishi A. Electrochemical behavior of hexa-ammineruthenium (III) cations in clay-modified-electrodes prepared by the Langmuir-Blodgett method. J Electroanal Chem. 1997;429:107-14.
12. Okamoto K, Tamura K, Takahashi M, Yamagishi A. Preparation of a clay-metal complex hybrid film by the Langmuir-Blodgett method and its application as an electrode modifier. Colloids Surf, A Physicochem Eng Asp. 2000;169:241- 9.
13. He J, Kobayashi K, Takahashi M, Villemure G, Yamagishi A. Preparation of hybrid films of an anionic Ru(II) cyanide polypytidyl complex with layered double hydroxides by the Langmuir-Blodgett method and their use as electrode modifiers. Thin Solid Films. 2001;397:255- 65.
14. He J, Kobayashi K, Chen YM, Villemure G, Yamagishi A. Electrocatalytic response of GMP on an ITO electrode modified with a hybrid film of Ni(II)-Al(III) layered double hydroxide and amphiphilic Ru(II) cyanide complex. ElectrochemCommum 2001;3:473-7.
15. He J, Sato H, Yang, P. Creation of stereoselective solid surface by self-assembly of a chiral metal complex onto a nanothick clay film. Electrochem Commun. 2003;5:388-91.
16. He J, Sato H, Yang P, Yamagishi A., . Preparation of a novel clay/metal complex hybrid film and its catalytic oxidation to chiral 1,1'-binaphtol. J Electroanal Chem. 2003;560:169- 74.
17. Shirtcliffe N. Deposition of clays onto a rotating electrochemical quartz crystal microbalance. Colloids Surf, A Physicochem Eng Asp. 1999;155:277-85.
18. Song C, Villemure G. Preparation of clay-modified electrodes by electrophoretic deposition of clay films. J Electroanal Chem. 1999;462:143- 9.

19. Baker MD, Senaratne C. Electrochemistry with clays and zeolites. In: Lipkowski J, Ross, P.N., editor. Electrochemistry of Novel Materials. New York: Frontiers of Electrochemistry. VCH; 1994. p. 339-80.
20. Bard AJ, Mallouk T. Electrodes modified with clays, zeolites and related microporous solids. In: Murray RW, editor. Molecular Design of Electrodes Surfaces, Techniques of Chemistry. 22. New York: Wiley and Sons; 1992. p. 271- 312.
21. Macha SM, Fitch A. Clays as architectural units at modified-electrodes. Mikrochim Acta. 1998; 128:1 -18.
22. Therias S, Mousty C. Electrodes modified with synthetic anionic clays. Appl Clay Sci. 1995;10:147- 62.
23. Yao K, Shimazu K, Nakata M, Yamagishi A. Clay-modified electrodes as studied by the quartz crystal microbalance: adsorption of ruthenium complexes. J Electroanal Chem. 1998;442:235-42.
24. Yao K, Shimazu K, Nakata M, Yamagishi A. Clay-modified electrodes as studied by the quartz crystal microbalance: redox processes of ruthenium and iron complexes. J Electroanal Chem. 1998;443:253- 61.
25. Yao K, Taniguchi M, Nakata M, Shimazu K, Takahashi M, Yamagishi A. Mass transport on an anionic claymodified electrode as studied by a quartz crystal microbalance. J Electroanal Chem. 1998;457:119-28.
26. Carrero H, León L E. Electrochemically active films of negatively charged molecules, surfactants and synthetic clays. Electrochem Commun. 2001; 3:417- 20.
27. Falaras P, Lezou F, Pomonis P, Ladavos, A. Al-pillared acid activated montmorillonite modified electrodes. J Electroanal Chem 2000;486:156-65.
28. Qiu J, Villemure G. Anionic clay modified electrodes: electron transfer mediated by electroactive nickel, cobalt or manganese sites in layered double hydroxide films. J Electroanal Chem 1997; 428:165- 72.
29. Xiang Y, Villemure G. Electron transport in clay-modified electrodes: study of electron transfer between electrochemically oxidized tris(2,2'-bipyridyl)iron cations and clay structural iron(II) sites. Can J Chem 1992;70:1833-7.
30. Xiang Y, Villemure G. Electrodes modified with synthetic clay minerals: evidence of direct electron transfer from structural iron sites in the clay lattice. J Electroan Chem. 1995;381:21-7.
31. Xiang Y, Villemure G. Electrodes modified with synthetic clay minerals: electron transfer between adsorbed tris(2,2'-bipyridyl) metal cations and electroactive cobalt centers in synthetic smectites. J Phys Chem. 1996;100:7143- 7.
32. Xiao J, Villemure G. Preparation, characterization and electrochemistry of synthetic copper clays. Clays Clay Miner. 1998;46:195-203.
33. Rudzinski WE, Figueroa, C, Hoppe C, Kuromoto T Y, Root D. Polypyrrole-clay modified electrodes. J Electroanal Chem 1988;243:367- 78.
34. Faguy PW, Ma W, Lowe J A, Pan W P, Brown T. Conducting polymer-clay composites for electrochemical applications. J Mater Chem. 1994; 4:771- 2.
35. Anaissi F, Demets GJF, Toma HE, Coelho ACV. Modified electrode based on mixed bentonite vanadium (V) oxide xerogels. J Electroanal Chem. 1999;464:48- 53.
36. Lei C, Wollenberger U, Jung C, Scheller FW. Clay-bridged electron transfer between cytochrome $P450_{cam}$ and electrode. Biochem Biophys Res Commun 2000;268:740- 4.
37. Sallez Y, Bianco P, Lojou E. Electrochemical behavior of c-type cytochromes at clay-modified carbon electrodes: a model for the interaction between proteins and soils. J Electroanal Chem 2000;493:37- 49.
38. Bianco P. Protein modified and membrane electrodes: strategies for the development of biomolecular sensors Rev Mol Biotechnol. 2002;82:393-409.
39. Scheller F, Wollenberger U, Lei C, Jin W, Ge B, Lehmann C, Lisdat F, Fridman V. Bioelectrocatalysis by redox enzymes at modified electrodes. Rev Mol Biotechnol. 2002; 82:411 - 24.

40. Dai Z, Xiao Y, Yu X, Mai Z, Zhao X, Zou X. Direct electrochemistry of myoglobin based on ionic liquid-clay composite films. Biosens Bioelectron. 2009 24:1629-34.
41. http://soil-environment.blogspot.ro/2009/07/heavy-metals-and-their-health-effects.html.
42. Wang J, Martinez T. Trace analysis at clay-modified carbon paste electrodes. Electroanalysis. 1989;1:167- 72.
43. Kalcher K, Grabec I, Raber G, Cai X, Tavcar G, Ogorevc, B. The vermiculite-modified carbon paste electrode as a model system for preconcentrating mono and divalent cations. J Electroanal Chem 1995;386:149- 56.
44. Kula P, Navrátilová Z. Voltammetric Study of Clay Minerals Properties. Acta Universitatis Carolinae Geologica. 1994;38:295.
45. Kula P, Navrátilová Z. Voltammetric copper (II) determination with a montmorillonite-modified carbon paste electrode. Fresenius' J Anal Chem. 1996;354:692-5.
46. Švegl I, Kolar M, Ogovevc B, Pihlar B. Vermicullite clay mineral as an effective carbon paste electrode modifier for the preconcentration and voltammetric determination of Hg(II) and Ag(I) ions. Fresenius' J Anal Chem. 1998;361:358- 62.
47. Navrátilová Z, Kula P. Cation and anion exchange on clay modified electrodes. J Solid State Electrochem. 2000;4:342- 7.
48. Švegl I, Ogorevc B, Hudnik V. A methodological approach to the application of a vermiculite modified carbon paste electrode in interaction studies: Influence of some pesticides on the uptake of Cu(II) from a solution to the solid phase. Fresenius' Journal of Analytical Chemistry. 1996;354:770-3.
49. Švegl I, Ogorevc B. Soil-modified carbon paste electrode: a useful tool in environmental assessment of heavy metal ion binding interactions. Fresenius' J Anal Chem 2000;367:701-6.
50. Ogorevc B, Cai X, Grabec I. Determination of traces of copper by anodic stripping voltammetry after its preconcentration via an ion-exchange route at carbon paste electrodes modified with vermiculite. Anal Chim Acta. 1995;305:176-82.
51. Shaw B, Creasy KE. Carbon composite electrodes containing alumina, layered double hydroxides, and zeolites. J Electroanal Chem. 1988;243:209.
52. El Murr N, Kerkeni M , Sellami A, Taarit YB. The zeolite-modified carbon paste electrode. J Electroanal Chem. 1988;246:461.
53. Zen J, Chen HP, Kumar AS. Disposable claycoated screen-printed electrode for amitrole analysis. Anal Chim Acta. 2001;449:95- 102.
54. Kula P, Navrátilová Z., Kulová P, Kotoucek M. Sorption and determination of Hg(II) on clay modified carbon paste electrodes. Anal Chim Acta. 1999;385:91- 101.
55. Navratilova Z, Kula P. Determination of gold using clay modified carbon paste electrode. Fresenius J Anal Chem. 2000;367:369-72.
56. Kula P, Navrátilová Z. . Anion exchange of gold chloro complexes on carbon paste electrode modified with montmorillonite for determination of gold in pharmaceuticals. Electroanalysis. 2001;13:795- 8.
57. Marchal V, Barbier F, Plassard F, Faure R, Vittori O. Determination of cadmium in bentonite clay mineral using a carbon paste electrode. Fresenius' J Anal Chem. 1999;363:710-2.
58. Barančok D, Cirák J, Tomčík P, Gmucová K. Surface modified microelectrodes for selective electroanalysis of metal ions in environmental components. Bioelectrochemistry. 2002;55:153-5.
59. Wang S, Chou T-C. Immobilized ionophore calcium ion sensor modified by montmorillonite. Electroanalysis. 2000;12:468- 70.
60. Zen J, Lai YY, Yang HH, Kumar AS. Multianalyte sensor for the simultaneous determination of hypoxanthine, xanthine and uric based on a preanodized nontronite-coated screen-printed electrode. Sens Actuat B-Chem. 2002;84:237-44.
61. Navrátilová Z, Vaculíková L. Electrodeposition of mercury film on electrodes modified with clay minerals. Chem Pap. 2006;60:348-52.

62. Issa A, Al-Degs YS, Al-Rabady NA. Deposition of two natural clays on a Pt surface using potentiostatic and spin-coating techniques: a comparative study. Clay Miner. 2008;43:501-10.
63. Luo L, Wang X, Ding Y, Li Q, Jia J, Deng D. Voltammetric determination of Pb^{2+} and Cd^{2+} with montmorillonite-bismuth-carbon electrodes. Appl Clay Sci. 2010;50:154-7.
64. Mohammadi H, Amine A, Cosnier S , Mousty C. Mercury–enzyme inhibition assays with an amperometric sucrose biosensor based on a trienzymatic-clay matrix. Anal Chim Acta. 2005;543:143-9.
65. Yariv S. Organo-clay complexes and interactions. In: Yariv S, Cross H, editor. Introduction to Organo-Clay Complexes and Interactions. New York: Marcel Dekker; 2002. p. 39-112.
66. Tonlé I, Ngameni E, Njopwouo D, Carteret C, Walcarius A. Functionalization of natural smectite-type clays by grafting with organosilanes: physicochemical characterization and application to mercury(II) uptake. Phys Chem Chem Phys. 2003;5:4951-61.
67. Dias Filho N, do Carmo DR. Study of an organically modified clay: Selective adsorption of heavy metal ions and voltammetric determination of mercury(II). Talanta. 2006;68:919–27.
68. Jieumboué-Tchinda A, Ngameni E, Walcarius A. Thiol-functionalized porous clay heterostructures (PCHs) deposited as thin films on carbon electrode: Towards mercury(II) sensing. Sens Actuat B-Chem. 2007;121:113-23.
69. Tonlé I, Ngamenia E, Walcarius A. Preconcentration and voltammetric analysis of mercury(II) at a carbon paste electrode modified with natural smectite-type clays grafted with organic chelating groups. Sens Actuat B-Chem. 2005;110:195-203.
70. Stathi P, Litina K, Gournis D, Giannopoulos TS, Deligiannakis Y. Physicochemical study of novel organoclays as heavy metal ion adsorbents for environmental remediation. J Colloid Interf Sci. 2007;316:298-309.
71. Rezaei B, Ghiaci M, Sedaghat ME. A selective modified bentonite-porphyrin carbon paste electrode for determination of Mn(II) by using anodic stripping voltammetry. Sens Actuat B-Chem. 2008;131:439–47.
72. Yuan S, Chen W, Hu S. Simultaneous determination of cadmium (II) and lead (II) with clay nanoparticles and anthraquinone complexly modified glassy carbon electrode. Talanta. 2004;64:922-8.
73. Bouwe R, Tonlé IK, Letaief S, Ngameni E, Detellier C. Structural characterisation of 1,10-phenanthroline-montmorillonite intercalation compounds and their application as low-cost electrochemical sensors for Pb(II) detection at the sub-nanomolar level. Appl Clay Sci. 2011;52:258-65.
74. Besombes J, Cosnier S, Labbé P, Reverdy G. Improvement of analytical characteristic of an enzyme electrode for free and total cholesterol via laponite clay additives. Anal Chim Acta 1995;317:275- 80.
75. Besombes J, Cosnier S, Labbé P., . Improvement of poly(amphiphilic pyrrole) enzyme electrodes via the incorporation of synthetic laponite-clay-nanoparticles. Talanta. 1997; 44(2209- 2215).
76. Cosnier S, Gondran C, Senillou A, Grätzel M., Vlachopoulos, N. Mesoporous TiO_2 films: new catalytic electrode materials for fabricating amperometric biosensors based on oxidases. Electroanalysis. 1997; 9:1387-92.
77. Shan D, Mousty C, Cosnier S, Mu S. A new polyphenol oxidase biosensor mediated by Azure B in laponite clay matrix. Electroanalysis 2003;15:1506- 12.
78. Poyard S, Jaffrezic-Renault N, Martelet C, Cosnier, S, Labbé P,Besombes JL. A new method for the controlled immobilization of enzyme in inorganic gels (laponite) for amperometric glucose biosensing. Sens Actuat B-Chem. 1996;33:44- 9.
79. Shyu S, Wang CM. Characterization of iron containing clay modified electrodes and their applications for glucose sensing. J Electrochem Soc 1998;145:134-58.
80. Zen J, Lo CW. A glucose sensor made of an enzymatic clay modified electrode and methyl viologen mediator

Anal Chem 1996;68:2635- 40.
81. Coche-Guérente L, Deprez V, Labbé P. Characterization of organosilasesquioxane-intercalated-laponite-clay modified electrodes and (bio)electrochemical applications. J Electroanal Chem. 1998;458:73- 86.
82. Coche-Guérente L, Desprez V, Labbé P, Therias S. Amplification of amperometric biosensor responses by electrochemical substrate recycling: Part II. Experimental study of the catechol-polyphenol oxidase system immobilized in a laponite clay matrix. J Electroanal Chem 1999;470:61- 9.
83. Coche-Guérente L, Labbé P, Mengeaud V. Amplification of amperometric biosensor response by electrochemical substrate recycling. 3. Theoretical and experimental study of phenol-polyphenol oxidase system immobilized in laponite hydrogels and layer-by-layer self-assembled structures. Anal Chem 2001;71:3206- 18.
84. Poyard S, Jaffrezic-Renault N, Martelet C, Cosnier S, Labbe P. Optimization of an inorganic/bio-organic matrix for the development of new glucose biosensor membranes. Anal Chim Acta 1998;364:165-72.
85. Poyard S, Martelet C, Jaffrezic-Renault N, Cosnier, S, Labbé P. Association of a poly(4-vinylpyridine-costyrene) membrane with an inorganic/organic mixed matrix for the optimization of glucose biosensors. Sens Actuat B-Chem. 1999;58: 380- 3.
86. Ohsaka T, Yamaguchi Y, Oyama N. A new amperometric glucose sensor based on bilayer film coating of redox-active clay film and glucose oxidase enzyme film. Bull Chem Soc Jpn. 1990;63:2646-52.
87. Ouyang C, Wang CM. Clay-enhanced electrochemiluminescence and its application in the detection of glucose. J Electrochem Soc. 1998;145:2654-9.
88. Mousty C, Cosnier S, Shan D, Mu S. Trienzymatic biosensor for the determination of inorganic phosphate. Anal Chim Acta. 2001;443:1- 8.
89. Hu S, Xu C, Luo J, Luo J, Cui D. Biosensor for detection of hypoxanthine based on xanthine oxidase immobilized on chemically modified carbon paste electrode. Anal Chim Acta. 2000;412:55-61.
90. Lei C, Deng J. Hydrogen peroxide sensor based on coimmobilized methylene green and horseradish peroxidase in the same montmorillonite-modified bovine serum albuminglutaraldehyde matrix on a glassy carbon electrode surface. Anal Chem. 1996;68:3344-9.
91. Zen J, Chen PJ. A selective voltammetric method for uric acid and dopamine detection using clay-modified electrodes. Anal Chem. 1997;69:5087-93.
92. Zen J, Lo CW, Chen PJ. An enzymatic clay modified electrode for aerobic glucose monitoring with dopamine as mediator. Anal Chem 1997;69:1669- 73.
93. Cosnier S, Lambert F, Stoytcheva M. A composite clay glucose biosensor based on an electrically connected HRP. Electroanalysis. 2000; 12:356- 60.
94. Shan D, Cosnier S, Mousty C. HRP wiring by redox active layered double hydroxides: application to the mediated H_2O_2 detection. Anal Lett 2003;36:909- 22.
95. Cosnier S, Le Lous K. A new strategy for the construction of amperometric dehydrogenase electrodes based on laponite gel-methylene blue polymer as the host matrix. J Electroanal Chem. 1996;406:243- 6.
96. Cosnier S, Le Lous K. Amperometric detection of pyridine nucleotide via immobilized viologen-accepting pyridine nucleotide oxidoreductase or immobilized diaphorase. Talanta. 1996;43:331- 7.
97. Cosnier S, Fontecave M, Innocent C, Niviere V. An original electroenzymatic system: flavin reductase-riboflavin for the improvement of dehydrogenase-based biosensors. Application to the amperometric detection of lactate. Electroanalysis. 1997;9:685- 8.
98. Shan D, Mousty C, Cosnier S, Mu S. A composite poly azure B-Clay-enzyme sensor for the mediated electrochemical determination of phenols. J Electroanal Chem. 2002;537:103- 9.

99. Shan D, Cosnier S, Mousty C. Layered double hydroxides: an attractive material for electrochemical biosensor design. Anal Chem 2003;75:3872- 9.
100. Shan D, Mousty C, Cosnier S. Subnanomolar cyanide detection at polyphenol oxidase/anionic clay biosensors. Anal Chem. 2004;76:178- 83.
101. Qian D-I, Nakamura C, Wenk SO, Ishikawa H, Zorin N, Miyake J. A hydrogen biosensor made of clay, poly(butylviologen) and hydrogenase sandwiched on a glass carbon electrode. Biosens Bioelectron. 2002;17:789-96.
102. Lei C, Zhang Z, Liu H, Deng J. Studies on employing tetrathiofulvalene as an electron shuttle incorporated in a montmorillonite-modified immobilization matrix for an enzyme electrode. J Electroanal Chem. 1996;419:93- 8.
103. Hsu H, Jehng JM, Liu YC. . Synthesis and characterization of carbon nanotubes synthesized over NiO/Na-montmorillonite catalyst and application to a hydrogen peroxide sensor. Mater Chem Phys. 2009;113:166–71.
104. Shan D, Li Q-B, Ding S-N , Xu J-Q, Cosnier S, Xu H-G. Reagentless biosensor for hydrogen peroxide based on self-assembled films of horseradish peroxidase/laponite/chitosan and the primary investigation on the inhibitory effect by sulfide. Biosens Bioelectron. 2010;26:536–41.
105. Chen X, Hu N, Zeng Y, Rusling JF, Yang J. Ordered electrochemically active films of hemoglobin, didodecyldimethylammonium ions, and clay. Langmuir. 1999;15:7022- 30.
106. Lei C, Listad F, Wollenberger U, Scheller FW. Cytochrome c/clay modified electrodes. Electroanalysis. 1999;11:274- 6.
107. Lei C, Wollenberger U, Bistolas N, Guiseppi-Elie A, Scheller FW. Electron transfer of hemoglobin at electrodes modified with colloidal clay nanoparticles. Anal Bioanal Chem Pap. 2002;372:235-9.
108. Fan C, Zhuang Y, Li G, Zhu J, Zhu D. Direct electrochemistry and enhanced catalytic activity for hemoglobin in a sodium montmorillonite film. Electroanalysis 2000;12:1156- 8.
109. Zhou Y, Hu N, Zeng Y, Rusling JF. Heme protein clay films: direct electrochemistry and electrochemical catalysis. Langmuir. 2002;18:211- 9.
110. Shi Q, Li Q, Shan D, Fan Q, Xue H. Biopolymer-clay nanoparticles composite system (Chitosan-laponite) for electrochemical sensing based on glucose oxidase. Mater Sci Eng: C. 2008;28:1372–5.
111. Mignani A, Scavetta E, Guadagnini L, Tonelli D. Comparative study of protective membranes for glucose biosensors based on electrodeposited hydrotalcites. Sensor Actuat B-Chem. 2009;136:196–202.
112. Shan D, Li QB, Ding SN, Xu JQ, Cosnier S, Xue H-G. Colloidal laponite nanoparticles: Extended application in direct electrochemistry of glucose oxidase and reagentless glucose biosensing. Biosens Bioelectron. 2010;25:1427–33.
113. Fan Q, Shan D, Xue H, He Y, Cosnier S. Amperometric phenol biosensor based on laponite clay–chitosan nanocomposite matrix. Biosens Bioelectron. 2007;22: 816–21.
114. Sanchez-Paniagua López M, López-Cabarcos E, López-Ruiz B. Influence of the host matrix of the enzyme in the performance of amperometric biosensors. Sens Actuat B-Chem. 2012;171-172:387–97.
115. Zanini V, López de Mishima B, Solís V. An amperometric biosensor based on lactate oxidase immobilized in laponite–chitosan hydrogel on a glassy carbon electrode. Application to the analysis of L-lactate in food samples. Sens Actuat B-Chem. 2011;155:75–80.
116. Walcarius A. Mesoporous materials and electrochemistry. Chem Soc Rev. 2013;42:4098-140.
117. Kresge C, Leonowicz ME, Roth WJ, Vartuli JC, Beck JS. Ordered mesoporous molecular sieves synthesized by a liquid-crystal template mechanism. Nature. 1992;359:710-2.
118. Beck J, Vartuli JC, Roth WJ, Leonowicz ME, Kresge CT, Schmitt KD, Chu CTW, Olson DH,Sheppard EW. A new family of mesoporous molecular sieves prepared with liquid crystal templates. J Am Chem Soc. 1992;114:10834-43.

119. Beck J, Vartuli JC. Recent advances in the synthesis, characterization and applications of mesoporous molecular sieves. Curr Opin Solid-State Mater Sci. 1996;1:76-87.
120. Brinker C. Porous inorganic materials. Curr Opin Solid-State Mater Sci. 1996;1 798-805.
121. Walcarius A, Mandler D, Cox J, Collinson MM, Lev O. Exciting new directions in the intersection of functionalized sol–gel materials with electrochemistry. J Mater Chem. 2005;15:3663-89.
122. Walcarius A, Collinson MM. Analytical chemistry with silica sol-gel: traditional routes to new materials for chemical analysis. Annu Rev Anal Chem. 2009;2:121-43.
123. Lev O, Wu Z, Bharathi S, Glezer V, Modestov A, Gun J, Rabinovich L, Sampath S. Sol–Gel Materials in Electrochemistry. Chem Mater 1997; 9:2354-75.
124. Audebert P, Walcarius A. Electrochemistry of Sol-Gel Derived Hybrid Materials. In: Sanchez PG-RaC, editor. Functional Hybrid Materials. Weinheim: Wiley-VCH; 2004. p. 172-209.
125. Lev O, Sampath S. Sol-gel electrochemistry: Silica and silicates. In: Bard A, Zoski CG. , editor. Electroanalytical Chemistry: A Series of Advances. 232010. p. 211.
126. Mousty C. Biosensing applications of clay-modified electrodes: a review. Anal Bioanal Chem. 2010;396:315-25.
127. Walcarius A. In: Auerbach S, Carrado KA, Dutta PK, editor. Handbook of Zeolite Science and Technology. New York: Marcel Dekker; 2003. p. 721-83.
128. Walcarius A. Electroanalytical applications of microporous zeolites and mesoporous (organo) silicas: Recent trends. Electroanalysis. 2008;20:711-38.
129. Guo Y-G, Hu J-S, Wan L-J. Nanostructured materials for electrochemical energy conversion and storage devices. Adv Mater. 2008;20:2878-87.
130. Li C, Bai H, Shi G. Conducting polymer nanomaterials: electrosynthesis and applications. Chem Soc Rev. 2009; 38: 2397-409.
131. Liu R, Duay J, Lee SB. Heterogeneous nanostructured electrode materials for electrochemical energy storage. Chem Commun. 2011;47:1384-404.
132. Rawolle M, Niedermeier MA, Kaune G, Perlich J, Lellig P, Memesa M, Cheng Y-J, Gutmann JS, P. Müller-Buschbaum P. Fabrication and characterization of nanostructured titania films with integrated function from inorganic-organic hybrid materials. Chem Soc Rev. 2012; 41:5131-42.
133. Joshi R, Schneider JJ. Assembly of one dimensional inorganic nanostructures into functional 2D and 3D architectures. Synthesis, arrangement and functionality. Chem Soc Rev. 2012; 41:5285-312.
134. Oskam G. Dye-Sensitized, Nanostructured Metal Oxide Photoelectrodes for Solar Energy Conversion. Curr Top Electrochem. 2004;10:141.
135. Su B-L, Léonard A, Yuan Z-Y. Highly ordered mesoporous CMI-n materials and hierarchically structured meso–macroporous compositions. C R Chim. 2005;8:713-26.
136. Soler-Illia G, Sanchez C, Lebeau B,Patarin J. Chemical strategies to design textured materials: from microporous and mesoporous oxides to nanonetworks and hierarchical structures. Chem Rev. 2002;102:4093-138.
137. Soler-Illia G, Crepaldi EL, Grosso D, Sanchez C. Block copolymer-templated mesoporous oxides. Curr Opin Colloid Interface Sci. 2003;8:109.
138. Lu Y, Ganguli R, Drewien CA, Anderson MT, Brinker CJ, Gong W, Guo Y, Soyez H, Dunn B, Huang MH, Zink JI. Continuous formation of supported cubic and hexagonal mesoporous films by sol-gel dip-coating. Nature. 1997;389:364-8.
139. Grosso D, Cagnol F, Soler-Ilia GJAA, Crepaldi EL, Amenitsch H, Brunet-bruneau A, Bourgeois A, Sanchez C. Fundamentals of mesostructuring through evaporation-induced self-assembly. Adv Funct Mater. 2004;14:309-22.
140. Song C, Villemure G. Electrode modification with spin-coated films of mesoporous molecular sieve silicas. Microporous Mesoporous Mater. 2001;44-45: 679-89.
141. Etienne M, Quach A, Grosso D, Nicole L, Sanchez C, Walcarius A. Molecular Transport into Mesostructured Silica Thin Films: Electrochemical Monitoring and Compa rison between p6m, P63/mmc, and Pm3n Structures. Chem Mater. 2007;19:844-56.

142. Lytle J, Stein A. Recent progress in syntheses and applications of inverse opals and related macroporous materials prepared by colloidal crystal templating. Annu Rev Nano Res. 2006;1:1-79.
143. Zhao B, Collinson MM. Well-Defined Hierarchical Templates for Multimodal Porous Material Fabrication. Chem Mater. 2010;22:4312-9.
144. Yiu H, Wright PA. Enzymes supported on ordered mesoporous solids: a special case of an inorganic-organic hybrid. J Mater Chem. 2005;15:3690-700.
145. Hudson S, Cooney J, Magner E. Proteins in Mesoporous Silicates. Angew Chem, Int Ed. 2008;47:8582.
146. Hartmann M. Ordered mesoporous materials for bioadsorption and biocatalysis. Chem Mater. 2005;17:4577-93.
147. Vinu A, Gokulakrishnan N, Mori T, Ariga K. Imobilization of biomolecules on mesoporous structured materials. In: Ruiz-Hitzky E, Ariga K, Lvov Y., editor. Bio-Inorganic Hybrid Nanomaterials. Weinheim, Germany: Wiley-VCH Verlag GmbH & Co. KGaA; 2008. p. 113-57.
148. Walcarius A, Sibottier E, Etienne M, Ghanbaja J. Electrochemically assisted self-assembly of mesoporous silica thin films. Nat Mater. 2007;6:602-8.
149. Goux A, Etienne M, Aubert E, Lecomte C, Ghanbaja J, Walcarius A. Oriented mesoporous silica films obtained by electro-assisted self-assembly (EASA). Chem Mater. 2009;21:731-41.
150. Shacham R, Avnir D, Mandler D. Electrodeposition of Methylated Sol-Gel Films on Conducting Surfaces. Adv Mater. 1999;11:384-8.
151. Collinson M, Moore N, Deepa PN, Kanungo M. Electrodeposition of Porous Silicate Films from Ludox Colloidal Silica. Langmuir. 2003;19:7669-72.
152. Sayen S, Walcarius A. Electro-assisted generation of functionalized silica films on gold. Electrochem Commun. 2003;5:341-8.
153. Sibottier E, Sayen S, Gaboriaud F, Walcarius A. Factors affecting the preparation and properties of electrodeposited silica thin films functionalized with amine or thiol groups. Langmuir. 2006;22:8366-73.
154. Brinker C, Dunphy DR. Morphological control of surfactant-templated metal oxide films. Curr Opin Colloid Interface Sci. 2006;11:126-32.
155. Wang X, Xiong R, Wei G. Preparation of mesoporous silica thin films on polystyrene substrate by electrochemically induced sol-gel technique. Surf Coat Technol. 2010;204:2187.
156. Walcarius A, Etienne M, Bessière J. Rate of Access to the Binding Sites in Organically Modified Silicates. 1. Amorphous Silica Gels Grafted with Amine or Thiol Groups. Chem Mater. 2002;14:2757-66.
157. Walcarius A, Etienne M, Lebeau B. Rate of Access to the Binding Sites in Organically Modified Silicates. 2. Ordered Mesoporous Silicas Grafted with Amine or Thiol Groups. Chem Mater. 2003;15(2161-2173).
158. Melde B, Johnson BJ, Charles PT. Mesoporous Silicate Materials in Sensing. Sensors. 2008;8:5202-28.
159. Hasanzadeh M, Shadjou N, de la Guardia M, Eskandani M, Sheikhzadeh P. Mesoporous silica-based materials for use in biosensors. TrAC, Trends Anal Chem. 2012;33:117-29.
160. Walcarius A, Kuhn A. Ordered porous thin films in electrochemical analysis. Trends Anal Chem. 2008;27:593-603.
161. Walcarius A. Template-directed porous electrodes in electroanalysis. Anal Bioanal Chem. 2010;396:261-72.
162. Fattakhova Rohlfing D, Rathouský J, Rohlfing, Y, Bartels O, Wark M. Functionalized Mesoporous Silica Films as a Matrix for Anchoring Electrochemically Active Guests. Langmuir. 2005;21:11320-9.
163. Li L, Li W, Sun C, Li L. Fabrication of carbon paste electrode containing 1:12 phosphomolybdic anions encapsulated in modified mesoporous molecular sieve MCM-41 and its electrochemistry. Electroanalysis. 2002;14:368-75.

164. Li W, Li L, Wang Z, Cui A, Sun C,Zhao J. 12-tungstophosphoric heteropolyacid anions encapsulated in chemically modified mesoporous silica FSM-16 and its electrocatalytic reduction for nitrite. Mater Lett. 2001;49:228-34.
165. Xie F, Li W, He J, Yu S, Fu T, Yang H. Directly immobilize polycation bearing Os complexes on mesoporous material MAS-5 and its electrocatalytic activity for nitrite. Mater Chem Phys. 2004;86:425-9.
166. Pal M, Ganesan V. Zinc phthalocyanine and silver/gold nanoparticles incorporated MCM-41 type materials as electrode modifiers. Langmuir. 2009;25:13264-72.
167. Walcarius A, Despas C, Trens P, Hudson MJ, Bessière J. Voltammetric in situ investigation of an MCM-41-modified carbon paste electrode-a new sensor. J Electroanal Chem. 1998;453:249-52.
168. Zhang H-X, Cao A-M, Hu J-S, Wan L-J, Lee S-T. Electrochemical sensor for detecting ultratrace nitroaromatic compounds using mesoporous SiO_2-modified electrode. Anal Chem. 2006;78:1967-71.
169. Wang F, Yang J, Wu K. Mesoporous silica-based electrochemical sensor for sensitive determination of environmental hormone bisphenol A. Anal Chim Acta. 2009;638:23-8.
170. Sun D, Zhang Y, Wang F, Wu K, Chen J, Zhou Y. Electrochemical sensor for simultaneous detection of ascorbic acid, uric acid and xanthine based on the surface enhancement effect of mesoporous silica. Sens Actuat B-Chem. 2009;141:641-5.
171. Zhou C, Liu Z, Dong Y, Li D. Electrochemical behavior of o-nitrophenol at hexagonal mesoporous silica modified carbon paste electrodes. Electroanalysis. 2009;21:853-8.
172. Sun D, Li X, Zhang H, Xie X. An electrochemical sensor for p-aminophenol based on the mesoporous silica modified carbon paste electrode. Int J Environ Anal Chem. 2012;92:324-33.
173. Zhao J, Huang W, Zheng X. Mesoporous silica-based electrochemical sensor for simultaneous determination of honokiol and magnolol. J Appl Electrochem. 2009;39:2415-9.
174. Sun D, Wang F, Wu K, Chen J, Zhou Y. Electrochemical determination of hesperidin using mesoporous SiO_2 modified electrode. Microchim Acta. 2009;167:35-9.
175. Wan C, Zhang Y, Lin H, Wu K, Chen J, Zhou Y. Electrochemical determination of p-chlorophenol based on the surface enhancement effects of mesoporous TiO_2-modified electrode. J Electrochem Soc. 2009;156:F151-F4.
176. Walcarius A, Bessière J. Electrochemistry with mesoporous silicaselective mercury(II) binding. Chem Mater. 1999;11:3009-11.
177. Walcarius A, Mercier L. Mesoporous organosilica adsorbents: nanoengineered materials for removal of organic and inorganic pollutants. J Mater Chem. 2010;20:4478-511.
178. Etienne M, Delacôte C, Walcarius A. In: Nunez M, editor. Progress in Electrochemistry Research, Inc, Hauppauge. New York: Nova Science Publishers; 2005. p. 145-84.
179. Yantasee W, Lin Y, Li X, Fryxell GE, Zemanian TS,Viswanathan VV. Nanoengineered electrochemical sensor based on mesoporous silica thin-film functionalized with thiol-terminated monolayer. Analyst. 2003;128:899-904.
180. Walcarius A, Etienne M, Sayen S, Lebeau B. Grafted silicas in electroanalysis: amorphous versus ordered mesoporous materials. Electroanalysis. 2003;15:414-21.
181. Yantasee W, Charnhattakorn B, Fryxell GE, Lin Y, Timchalk C, Addleman RS. Detection of Cd, Pb, and Cu in non-pretreated natural waters and urine with thiol functionalized mesoporous silica and Nafion composite electrodes. Anal Chim Acta. 2008;620: 55-63.
182. Etienne M, Goux A,Sibottier E, Walcarius A. Oriented mesoporous organosilica films on electrode: a new class of nanomaterials for sensing. J Nanosci Nanotechnol. 2009;9:2398-406.
183. Walcarius A, Ganesan V. Ion-exchange properties and electrochemical characterization of quaternary ammonium-functionalized silica microspheres obtained by the surfactant template route. Langmuir. 2006;22:469-77.
184. Ganesan V, Walcarius A. Surfactant templated sulfonic acid functionalized silica microspheres as new efficient ion exchangers and electrode modifiers. Langmuir. 2004;20:3632-40.

185. Yantasee W, Fryxell GE, Conner MM, Lin Y. Nanostructured electrochemical sensors based on functionalized nanoporous silica for voltammetric analysis of lead, mercury, and copper. J Nanosci Nanotechnol. 2005;5:1537-40.
186. Yantasee W, Fryxell GE, Lin Y. Voltammetric analysis of europium at screen-printed electrodes modified with salicylamide self-assembled on mesoporous silica. Analyst. 2006;131:1342-6.
187. Walcarius A, Sayen S, Gérardin C, Hamdoune F, Rodehuser L. Dipeptide-functionalized mesoporous silica spheres. Colloids Surf A 2004;234:145-51.
188. Yantasee W, Lin Y, Fryxell GE, Busche BJ. Simultaneous detection of cadmium, copper, and lead using a carbon paste electrode modified with carbamoylphosphonic acid self-assembled monolayer on mesoporous silica (SAMMS). Anal Chim Acta. 2004;502:207-12.
189. Cesarino I, G. Marino G, do Rosario Matos J, Cavalheiro ETG. Using the organofunctionalised SBA-15 nanostructured silica as a carbon paste electrode modifier: determination of cadmium ions by differential anodic pulse stripping voltammetry. J Braz Chem Soc. 2007;18:810-7.
190. Popa D, Mureseanu M, Tanase IG. Organofunctionalized mesoporous silica carbon paste electrode for simultaneously determination of copper, lead and cadmium. Rev Chim (Bucharest). 2012;63:507-12.
191. Goubert-Renaudin S, Etienne M, Rousselin Y, Denat F, Lebeau B, Walcarius A. Cyclam-functionalized silica-modified electrodes for selective determination of Cu (II). Electroanalysis. 2009;21:280-9.
192. Goubert-Renaudin S, Moreau M, Despas C, Meyer M, Denat F, Lebeau B, Walcarius A. . Voltammetric detection of lead(II) using amide-cyclam- functionalized silica-modified carbon paste electrodes. Electroanalysis. 2009;21:1731-42.
193. Xu X, Liu Z, Zhang X, Duan S, Xu S, Zhou C. β-Cyclodextrin functionalized mesoporous silica for electrochemical selective sensor: Simultaneous determination of nitrophenol isomers. Electrochim Acta. 2011;58:142-9.
194. Morante-Zarcero S, Sanchez A, Fajardo M, Hierro I, Sierra I. Voltammetric analysis of Pb(II) in natural waters using a carbon paste electrode modified with 5-mercapto-1-methyltetrazol grafted on hexagonal mesoporous silica. Microchim Acta. 2010;169:57-64.
195. Sanchez A, Walcarius A. Surfactant-templated sol-gel silica thin films bearing 5-mercapto-1-methyl-tetrazole on carbon electrode for Hg(II) detection. Electrochim Acta. 2010;55:4201-7.
196. Zhang P, Dong S,Gu G, Huang T. Simultaneous determination of Cd^{2+}, Pb^{2+}, Cu^{2+} and Hg^{2+} at a carbon paste electrode modified with oonic liquid-functionalized ordered mesoporous silica. Bull Korean Chem Soc. 2010;31:2949-54.
197. Etienne M, Cortot J, Walcarius A. Preconcentration electroanalysis at surfactant-templated thiol-functionalized silica thin films. Electroanalysis. 2007;19:129-38.
198. Yantasee W, Lin Y, Fryxell GE, Wang Z. . Carbon paste electrode modified with carbamoylphosphonic acid functionalized mesoporous silica: A new mercury-free sensor for uranium detection. Electroanalysis. 2004;16:870-3.
199. Goubert-Renaudin S, Etienne M, Brandès S, Meyer M, Denat F, Lebeau B, Walcarius A. Factors affecting copper(II) binding to multiarmed cyclam-grafted mesoporous silica in aqueous solution. Langmuir. 2009; 25:9804-13.
200. Wang Y, Yang Y, Xu L, Zhang J. Bisphenol A sensing based on surface molecularly imprinted, ordered mesoporous silica. Electrochim Acta. 2010;56:2105-9.
201. Zhang X, Duan S, Xu X, Xu S, Zhou C. Electrochemical behavior and simultaneous determination of dihydroxybenzene isomers at a functionalized SBA-15 mesoporous silica modified carbon paste electrode. Electrochim Acta. 2010;56:1981.
202. Liu X, Hua Y, Villemure G. Preparation and characterization of thin films of amine functionalised mesoporous silica having cubic pore structures and their use for electrode surface modifications. Microporous Mesoporous Mater. 2009;117:317-25.

203. Fattakhova-Rohlfing D, Wark M, Rathouský J. Ion-permselective pH-switchable mesoporous silica thin layers. Chem Mater. 2007;19:1640-7.
204. Fattakhova-Rohlfing D, Wark M, Rathouský J. Electrode layers for electrochemical applications based on functionalized mesoporous silica films. Sens Actuat B-Chem. 2007;126:78-81.
205. Zhang X, Wang J, Wu W, Qian S, Man Y. Immobilization and electrochemistry of cytochrome c on amino-functionalized mesoporous silica thin films. Electrochem Commun. 2007;9:2098-104.
206. Wang Y, Qian K, Guo K, Kong J, Marty J-L, Yu C, Liu B. Electrochemistry and biosensing activity of cytochrome c immobilized in macroporous materials. Microchim Acta. 2011;175:87-95.
207. Liu Y, Xu Q, Feng X, Zhu J-J, Hou W. Immobilization of hemoglobin on SBA-15 applied to the electrocatalytic reduction of H_2O_2. Anal Bioanal Chem. 2007; 387:1553-9.
208. Jia N, Wen Y, Yang G, Lian Q, Xu C, Shen H. Direct electrochemistry and enzymatic activity of hemoglobin immobilized in ordered mesoporous titanium oxide matrix. Electrochem Commun. 2008;10:774-7.
209. Dai Z, Xu X, Ju H. Direct electrochemistry and electrocatalysis of myoglobin immobilized on a hexagonal mesoporous silica matrix. Anal Biochem. 2004;332:23-31.
210. Teng Y, Wu X, Zhou Q, Chen C,Zhao H, Lan M. Direct electron transfer of myoglobin in mesoporous silica KIT-6 modified on screen-printed electrode. Sens Actuat B-Chem. 2009;142:267-72.
211. Li J, Xiong Z, Zhou L, Han X, Liu H. Effects of pore structure of mesoporous silicas on the electrochemical properties of hemoglobin. Microporous Mesoporous Mater. 2010;130:333-7.
212. Zhang L, Zhang Q, Li J. Direct electrochemistry and electrocatalysis of hemoglobin immobilized in bimodal mesoporous silica and chitosan inorganic–organic hybrid film. Electrochem Commun. 2007;9:1530-5.
213. Li Y, Zeng X, Liu X, Liu X, Wei W, Luo S. Direct electrochemistry and electrocatalytic properties of hemoglobin immobilized on a carbon ionic liquid electrode modified with mesoporous molecular sieve MCM-41. Colloids Surf B. 2010;79:241-5.
214. Xian Y, Xian Y, Zhou LH, Wu FH, Ling Y, Jin LT. . Encapsulation hemoglobin in ordered mesoporous silicas: Influence factors for immobilization and bioelectrochemistry. Electrochem Commun. 2007;9:142-8.
215. Zhang Q, Zhang L, Liu B, Lu X, Li J. Assembly of quantum dots-mesoporous silicate hybrid material for protein immobilization and direct electrochemistry. Biosens Bioelectron. 2007;23:695-700.
216. Wu S, Ju H, Liu Y. Conductive mesocellular silica-carbon nanocomposite foams for immobilization, direct electrochemistry, and biosensing of proteins. Adv Funct Mater. 2007;17:585-92.
217. Dai Z, Ni J, Huang XH, Lu GF, Bao JC. Direct electrochemistry of glucose oxidase immobilized on a hexagonal mesoporous silica-MCM-41 matrix. Bioelectrochem. 2007;70:250-6.
218. Dai Z, Ju H, Chen H. Mesoporous materials promoting direct electrochemistry and electrocatalysis of horseradish peroxidase. Electroanalysis. 2005;17:862-8.
219. Bai Y, Yang H, Yang W, Li Y, Sun C. Gold nanoparticles-mesoporous silica composite used as an enzyme immobilization matrix for amperometric glucose biosensor construction. Sens Actuat B-Chem. 2007;124:179-86.
220. Chen C-C, Do J-S, Gu Y. Immobilization of HRP in mesoporous silica and its application for the construction of polyaniline modified hydrogen peroxide biosensor. Sensors. 2009;9:4635-48.
221. Xu Q, Zhu JJ, Hu XY. Ordered mesoporous polyaniline film as a new matrix for enzyme immobilization and biosensor construction. Anal Chim Acta. 2007;597:151-6.
222. Dai Z, Xu X, Wu L, Ju H. Detection of trace phenol based on mesoporous silica derived tyrosinase-peroxidase biosensor. Electroanalysis. 2005;17:1571-7.

223. Stefanakis D, Margellou A, Psarouli A, Chaniotakis N, Ghanotakis DF. Immobilization of glucose oxidase and 2-hydroxybiphenyl 3-monooxygenase in mesoporous silica: Characterization studies and construction of an amperometric glucose biosensor. Anal Lett. 2010;43:2582-97.
224. Yang M, Li H, Javadi A, Gong S. Multifunctional mesoporous silica nanoparticles as labels for the preparation of ultrasensitive electrochemical immunosensors. Biomater. 2010;31:3281-6.
225. Lu J, Liu S, Ge S, Yan M, Yu J, Hu X. Ultrasensitive electrochemical immunosensor based on Au nanoparticles dotted carbon nanotube-graphene composite and functionalized mesoporous materials. Biosens Bioelectron. 2012; 33:29-35.
226. Liu S, Lin Q, Zhang X, He X, Xing X, Lian W, Li J, Cui M, Huang J. Electrochemical immunosensor based on mesoporous nanocomposites and HRP-functionalized nanoparticles bioconjugates for sensitivity enhanced detection of diethylstilbestrol. Sens Actuat B-Chem. 2012;166-167:562-8.
227. Cui Z, Cai Y, Wu D, Yu H, Li Y, Mao K, Wang H, Fan H, Wie Q, Du B. An ultrasensitive electrochemical immunosensor for the detection of salbutamol based on Pd@SBA-15 and ionic liquid. Electrochim Acta. 2012; 69:79-85.
228. Lin J, Wei Z, Mao C. A label-free immunosensor based on modified mesoporous silica for simultaneous determination of tumor markers. Biosens Bioelectron. 2011; 29:40-5.
229. Lin J, Wei Z, Chu P. A label-free immunosensor by controlled fabrication of monoclonal antibodies and gold nanoparticles inside the mesopores. Anal Biochem. 2012;421:97-102.
230. Wu D, Li R, Wang H, Liu S, Wang H, Wei Q, Du B. Hollow mesoporous silica microspheres as sensitive labels for immunoassay of prostate-specific antigen. Analyst. 2012;137:608-13.
231. Guo S, Du Y, Yang X, Dong S, Wang E. Solid-state label-free integrated aptasensor based on graphene-mesoporous silica-gold nanoparticle hybrids and silver microspheres. Anal Chem. 2011;83:8035-40.
232. Du Y, Guo S, Qin H, Dong S, Wang E. Target-induced conjunction of split aptamer as new chiral selector for oligopeptide on graphene-mesoporous silica-gold nanoparticle hybrids modified sensing platform. Chem Commun. 2012;48:799-801.
233. Du Y, Guo S, Dong S, Wang E. An integrated sensing system for detection of DNA using new parallel-motif DNA triplex system and graphene-mesoporous silica-gold nanoparticle hybrids. Biomaterials. 2011;32:8584-92.
234. Font J, de March P, Busque F, Casas E, Benitez M, Teruel L, Garcia H. Periodic mesoporous silica having covalently attached tris(bipyridine)ruthenium complex: synthesis, photovoltaic and electrochemiluminescent properties. J Mater Chem. 2007;17:2336-43.
235. Innocenzi P, Martucci A, Guglielmi M, Bearzotti A, Traversa E. Electrical and structural characterisation of mesoporous silica thin films as humidity sensors. Sens Actuat B-Chem. 2001;76:299-303.
236. Bertolo J, Bearzotti A, Falcaro P, Traversa E, Innocenzi P. Sensoristic Applications of Self-assembled Mesostructured Silica Films. Sensor Lett. 2003;1:64-70.
237. Yuliarto B, Zhou HS, Yamada T, Honma I, Katsumura Y, Ichihara M. Effect of tin addition on mesoporous silica thin film and its application for surface photovoltage NO_2 gas sensor. Anal Chem. 2004;76:6719-26.
238. Laberty-Robert C, Vallé K, Pereira F, Sanchez C Design and properties of functional hybrid organic-inorganic membranes for fuel cells. Chem Soc Rev. 2011;40:961-1005.
239. Maghear A, Cristea C, Marian A, Marian IO, Săndulescu R. Physico-chemical and electroanalytical characterization of two Romanian clays with possible applications in pharmaceutical analysis. Farmacia. 2013;61:648-57.
240. Anthony J, Bideaux RA, Bladh KW, Nichols MC. Handbook of Mineralogy. II (Silica, Silicates). America MSo, editor. Chantilly, VA, US2011.
241. http://pubs.usgs.gov/of/2001/of01-041/htmldocs/clays/smc.htm: U. S. Geological Survey Open-File Report 01-041.

242. Tanner C, Jackson ML. Nomographs of sedimentation times for soil particles under gravity or centrifugal acceleration. Soil Science Society of America Proceedings: 12; 1947. p. 60-5.
243. Maghear A, Cristea C, Marian A, Marian IO, Săndulescu R. A novel biosensor for acetaminophen detection with Romanian clays and conductive polymeric films. Farmacia. 2013;61:1-11.
244. Marian A, Marian IO, Cristea C, Săndulescu R, Vasilie G. Study of some clay minerals used in electrode making with application in environment chemistry. Studia UBB, Ambientum. 2009;LIV:67-75.
245. Kaeeble E. Handbook of X-rays. New York: McGraw-Hill; 1967.
246. Socrates G. Infrared and Raman characteristic group frequencies: Tables and charts: John Wiley and Sons; 2001.
247. Lucas J, Tranth N. Bulletin du service cartographique et géologique de l´Alsace et Lorraine1965. 4 p.
248. Todor D. Analiza termicã a mineralelor. Editura Tehnica. Bucureşti1972.
249. Fitch A. Clay-modified electrodes: a review. Clays Clay Miner. 1990;38:391-400.
250. Lipkowski J, Ross PN. The electrochemistry of novel materials. New York: VCH Publishers Inc.; 1994.
251. Tonlé I, Ngameni E, Walcarius A. From clay to organoclay-film modified electrodes: Tuning charge selectivity in ion exchange voltammetry. Electrochim Acta. 2004;49:3435-43.
252. Walcarius A. Zeolite-modified electrodes: Analytical applications and prospects. Electroanalysis. 1996; 8:971-86.
253. Walcarius A. Analytical applications of silica - modified electrodes – a comprehensive review. Electroanalysis. 1998;10:1217-35.
254. Walcarius A, Lefevre G, Rapin JP, Renaudin G, Francois, M. Voltammetric detection of iodide after accumulation by Friedel's salt. Electroanalysis. 2001;13:313-20.
255. Lee Y, Mutharasan R. Biosensors. In: Wilson J, editor. Sensor Technology Handbook: Elsevier; 2005.
256. Sima V, Cristea C, Lăpăduş F, Marian IO, Marian A, Săndulescu R. Electroanalytical properties of a novel biosensor modified with zirconium alcoxide porous gels for the detection of acetaminophen. J Pharm Biom Anal. 2008;48:1195-200.
257. Sima V, Cristea C, Bodoki E, Duţu G, Săndulescu R. Screen-printed electrodes modified with HRP-zirconium alcoxide film for the development of a biosensor for acetaminophen detection. Cent Eur J Chem. 2010;8:1034-40.
258. Săndulescu R, Mirel S, Oprean R. The development of spectrophotometricand electroanalytical methods for ascorbic acid and acetaminophen and their applications in the analysis of effervescent dosage forms. J Pharm Biom Anal. 2000;23:77-87.
259. Grygar T, Marken F, Schröder U, Scholz F. Electrochemical Analysis of Solids. A Review. Collection of Czechoslovak Chemical Communications. 2002;67:163-70.
260. Yu D, Renedo OD, Blankert B, Sima V, Sandulescu R, Arcos J, Kauffmann JM. A peroxidase-based biosensor supported by nanoporous magnetic silica microparticles for acetaminophen biotransformation and inhibition studies. Electroanalysis. 2006;18:1637-42.
261. Zen J-M, Kumar AS. Peer Reviewed: The Prospects of Clay Mineral Electrodes. Anal Chem. 2004;76:205A-11A.
262. Maghear A, Cernat A, Cristea C, Marian A, Marian IO,Săndulescu R. New electrochemical sensors based on clay and carbon micro and nanoparticles for pharmaceutical and environmental analysis. Technical Proceedings of the 2012 NSTI Nanotechnology Conference and Expo. 1. Santa Clara, CA: NSTI-Nanotech; 2012.
263. Kemmegne-Mbouguen J, Ngameni E, Walcarius A. Organoclay-enzyme film electrodes. Anal Chim Acta. 2006;578:145-55.

264. Kemmegne-Mbouguen J, Tonlé IK, Walcarius A, Ngameni E. Electrochemical response of ascorbic and uric acids at organoclay film modified glassy carbon electrodes and sensing applications. Talanta. 2011;85:754-62.
265. Ngameni E, Tonlé IK, Apohkeng JT, Bouwé RGB, Jieumboué-Tchinda A, Walcarius A. Permselective and preconcentration properties of a surfactant- intercalated clay modified electrode. Electroanalysis. 2006;18:2243-50.
266. Tonlé I, Ngameni E, Tcheumi HL, Tchieda V, Carteret C, Walcarius A. Sorption of methylene blue on an organoclay bearing thiol groups and application to electrochemical sensing of the dye. Talanta. 2008;74:489-97.
267. Tonlé I, Letaief S, Ngameni E, Detellier C. Square wave voltammetric determination of lead (II) ions using a carbon paste electrode modified by a thiol-functionalized kaolinite. Electroanalysis. 2011;23:245-52.
268. Charmantray F, Touisni N, Hecquet L, Mousty C. Amperometric biosensor based on galactose oxidase immobilized in clay matrix. Electroanalysis. 2013; 25:630-5.
269. Charradi K, Forano C, Prévot V, Ben Haj Amara A, Mousty C. Direct electron transfer and enhanced electrocatalytic activity of hemoglobin at iron-rich clay modified electrodes. Langmuir 2009;25:10376-83.
270. Chen H, Zhang Z, Cai D, Zhang S, Zhang B, Tang J, Wu Z. Direct electrochemistry and electrocatalytic behavior of horseradish peroxidase on attapulgite clay modified electrode. Anal Sci. 2011;27:613-6.
271. Demir B, Seleci M, Ag D, Cevik S, Yalcinkaya EE, Demirkol DO, Anik U, Timur S. Amine intercalated clay surfaces for microbial cell immobilization and biosensing applications. RSC Adv. 2013;3:7513-9.
272. Svancara I, Kalcher K, Walcarius A, Vytras K. Electroanalysis with Carbon Paste Electrodes. Boca Raton, FL, USA: Analytical Chemistry Series, CRC Press,Taylor and Francis Group; 2012.
273. Zhou C-H, Shen Z-F, Liu L-H, Liu S-M. Preparation and functionality of clay-containing films. J Mater Chem. 2011;21:15132-53.
274. Coche-Guérente L, Cosnier S, Desprez V, Labbé P, Petridis D. Organosilasesquioxane-laponite clay sols: a versatile approach for electrode surface modification. J Electroanal Chem. 1996;401:253-6.
275. Maghear A, Etienne M, Tertiş M, Sandulescu R ,Walcarius A. Clay–mesoporous silica composite films generated by electro-assisted self-assembly. Electrochim Acta 2013;112:333-41.
276. Carrado K. Synthetic organo-and polymer–clays: preparation, characterization, and materials applications. Appl Clay Sci. 2000;17:1-23.
277. Wypych F. Chemical modification of clay surfaces. Interface Sci Technol. 2004;1:1-56.
278. Jaber M, Miehé-Brendlé J. Organoclays: preparation, properties and applications. In: Valtchev V, Mintova S, Tsapatsis M. , editor. Ordered Porous Solids: Recent Advances and Prospects: Elsevier, Stevenson Ranch; 2009. p. 31-9.
279. He H, Tao Q, Zhu J, Yuan P, Shen W, Yang S. Silylation of clay mineral surfaces. Appl Clay Sci. 2013;71:15-20.
280. Akçay M. Characterization and adsorption properties of tetrabutylammonium montmorillonite (TBAM) clay: thermodynamic and kinetic calculations. J Coll Interface Sci. 2006;296:16-21.
281. Chun Y, Sheng G, Boyd SA. Sorptive characteristics of tetraalkylammonium-exchanged smectite clays. Clays Clay Miner. 2003;51:415-20.
282. Bhattacharyya K, Sen Gupta S. Kaolinite, montmorillonite and their modified derivatives as adsorbents for removal of Cu(II) from aqueous solution. Sep Purif Technol. 2006; 50:388-97.
283. Sen Gupta S, Bhattacharyya KB. Removal of Cd(II) from aqueous solution by kaolinite, montmorillonite and their poly(oxo zirconium) and tetrabutylammonium derivatives. J Hazard Mater. 2006;128:247-57.

284. Xue W, He H, Zhu J, Yuan P. FTIR investigation of CTAB–Al–montmorillonite complexes. Spectrochim Acta A. 2007;67:1030-6.
285. Loh E. Optical vibrations in sheet silicates. J Phys C: Solid State phys. 1973;6:1091-104.
286. Frost R, Rintoul L. . Lattice vibrations of montmorillonite: An FT Raman and X-ray diffraction study. Appl Clay Sci. 1996;11:171-83.
287. Bishop J, Murad EJ. Characterization of minerals and biogeochemical markers on Mars: A Raman and IR spectroscopic study of montmorillonite. Raman Spectrosc. 2004;35:480-6.
288. http://www.horiba.com/fileadmin/uploads/Scientific/Documents/Raman/bands.pdf.
289. Kaviratna P, Pinnavaia TJ. Electroactive $Ru(NH_3)_6^{3+}$ gallery cations in clay-modified electrodes. J Electroanal Chem. 1992;332:135-45.
290. Navratilova Z, Kula P. Anion exchange of gold chloro complexes on carbon paste electrode modified with montmorillonite for determination of gold in pharmaceuticals Electroanalysis. 2001;13:795-8.
291. Chen B, Zhu L, Zhu J, Xing B. Configurations of the bentonite-sorbed myristylpyridinium cation and their influences on the uptake of organic compounds. Environ Sci Technol. 2005;39: 6093-100.
292. Zhao H, Jaynes WF, Vance GF. Sorption of the ionizable organic compound, dicamba (3,6-dichloro-2-methoxy benzoic acid), by organo-clays. Chemosphere. 1996; 33:2089-100.
293. Krishna B, Murty DSR, Prakash BSJ. Thermodynamics of chromium (IV) anionic species sorption onto surfactant-modified montmorillonite clay. J Coll Interf Sci. 2000;229:230-6.
294. Walcarius A, Barbaise T, Bessière J. Factors affecting the analytical applications of zeolite-modified electrodes preconcentration of electroactive species. Anal Chim Acta. 1997;340:61-76.
295. Sayen S, Gérardin C, Rodehüser L, Walcarius A. Electrochemical detection of copper (II) at an electrode modified by a carnosine–silica hybrid material. Electroanalysis. 2003;15:422-30.
296. Cox J, Jaworski RK, Kulesza PJ. Electroanalysis with electrodes modified by inorganic films. Electroanalysis. 1991;3:869-77.
297. Walcarius A. Zeolite-modified electrodes in electroanalytical chemistry. Anal Chim Acta. 1999;384:1-16.
298. Walcarius A. Electrochemistry with micro- and mesoporous silicates. In: Valtchev V MS, Tsapatsis M., editor. Ordered Nanoporous Solids: Recent Advances and Prospects: Elsevier, Stevenson Ranch; 2008. p. 523-57.
299. Muresan L. Zeolite-modified electrodes with analytical applications. Pure Appl Chem 2011;83:325-43.
300. Tonelli D, Scavetta E, Giorgetti M. Layered-double-hydroxide-modified electrodes: electroanalytical applications. Anal Bioanal Chem. 2013;405:603-14.
301. Mousty C, Prévot V. Hybrid and biohybrid layered double hydroxides for electrochemical analysis. Anal Bioanal Chem. 2013;405:3513-23.
302. Walcarius A. Electroanalysis with pure, chemically modified and sol-gel-derived silica-based materials. Electroanalysis. 2001;13:701-18.
303. Wang J. Sol–gel materials for electrochemical biosensors. Anal Chim Acta. 1999;399:21-7.
304. Aurobind S, Amirthalingam KP, Gomathi H. . Sol-gel based surface modification of electrodes for electro analysis Adv Coll Interf Sci. 2006;121:1-7.
305. Hasanzadeh M, Shadjou N, Eskandani M, de la Guardia M. Mesoporous silica-based materials for use in electrochemical enzyme nanobiosensors. Trends Anal Chem 2012;40:106-18.
306. Yantasee W, Lin Y, Fryxell GE. Electrochemical sensors based on nanomaterials for environmental monitoring. In: Fryxell G, Cao G., editor. Environmental Applications of Nanomaterials. Singapore: World Scientific Publishing; 2012. p. 523-59.
307. Walcarius A. Electrochemistry of silicate-based nanomaterials. In: Nalwa H, editor. Encyclopedia of Nanoscience and Nanotechnology. 2. Stevenson Ranch, California: American Scientific Publishers; 2004. p. 857-93.

308. Mitzi D. Thin-film deposition of organic-inorganic hybrid materials. Chem Mater. 2001;13:3283-98.
309. Deepa P, Kanungo M, Claycomb G, Sherwood PMA, Collinson MM. Electrochemically deposited sol–gel-derived silicate films as a viable alternative in thin-film design. Anal Chem. 2003;75:5399.
310. Collinson M. Electrochemistry: An important tool to study and create new sol–gel-derived materials. Acc Chem Res. 2007;40:777-83.
311. Toledano R, Shacham R, Avnir D, Mandler, D. Electrochemical co-deposition of sol–gel/metal thin nanocomposite films. Chem Mater. 2008;20:4276-83.
312. Raveh M, Liu L, Mandler, D. Electrochemical co-deposition of conductive polymer–silica hybrid thin films. Phys Chem Chem Phys. 2013;15:10876-84.
313. Nadzhafova O, Etienne M, Walcarius A. Direct electrochemistry of hemoglobin and glucose oxidase in electrodeposited sol–gel silica thin films on glassy carbon. Electrochem Commun. 2007;9:1189-95.
314. Wang Z, Etienne M, Kohring G-W, Bon Saint Côme Y, Kuhn A, Walcarius, A. . Electrochemically assisted deposition of sol–gel bio-composite with co-immobilized dehydrogenase and diaphorase. Electrochim Acta 2011;56:9032-40.
315. Qu F, Nasraoui R, Etienne M, Bon Saint Côme Y, Kuhn A, Lenz J, Gajdzik J, Hempelmann R, Walcarius A. Electrogeneration of ultra-thin silica films for the functionalization of macroporous electrodes. Electrochem Commun. 2011;13:138-42.
316. Mazurenko I, Etienne M, Ostermann R, Smarsly B, Tananaiko O, Zaitsev V, Walcarius A. Controlled electrochemically-assisted deposition of sol–gel biocomposite on electrospun platinum nanofibers. Langmuir. 2011;27:140–7147.
317. Shacham R, Mandler D, Avnir D. Pattern recognition in oxides thin-film electrodeposition: Printed circuits CR Chim. 2010;13:237-41.
318. Liu L, Toledano R, Danieli T, Zhang J-Q, Hu J-M, Mandler D. Electrochemically patterning sol–gel structures on conducting and insulating surfaces. Chem Commun 2011;47:6909-11.
319. Guillemin Y, Etienne M, Sibottier E, Walcarius A. Microscale controlled electrogeneration of patterned mesoporous silica thin films. Chem Mater. 2011;23:5313-22.
320. Etienne M, Sallard S, Schröder M, Guillemin Y, Mascotto S, Smarsly BM, Walcarius A. Electrochemical generation of thin silica films with hierarchical porosity. Chem Mater. 2010;22:3426-32.
321. Ghach W, Etienne M, Billard P, Jorand FPA, Walcarius A. Electrochemically assisted bacteria encapsulation in thin hybrid sol–gel films. J Mater Chem B. 2013;1:1052-9.
322. Kawi S. A high-surface-area silica–clay composite material. Mater Lett. 1999;38:351-5.
323. Li F, Jiang Y, Xia M, Sun M, Xue B, Ren X. A high-stability silica–clay composite: Synthesis, characterization and combination with TiO_2 as a novel photocatalyst for Azo dye. J Hazard Mater. 2009;165:1219-23.
324. Li F, Jiang Y, Xia M, Sun M, Xue B, Ren X. A novel mesoporous silica-clay composite and its thermal and hydrothermal stabilities. J Porous Mater. 2010;17:217-23.
325. Sadeh A, Sladkevich S, Gelman F, Prikhodchenko P, Baumberg I, Berezin O, Lev O. Sol-gel-derived composite antimony-doped, tin oxide-coated clay-silicate semitransparent and conductive electrodes. Anal Chem 2007;79:5188-95.
326. Deflorian F, Rossi S, Fedel M, Motte C. Electrochemical investigation of high-performance silane sol–gel films containing clay nanoparticles. Prog Org Coat 2010;69:158-66.
327. Lavrentyeva E, Vassiliev SY, Levin EE, Tsirlin AA, Polyakov SN, Leoni M, Napolskii KS, Petrii OA, Tsirlina GA. Smectite clays as the quasi-templates for platinum electrodeposition. Electrochim Acta. 2012;61:94-106.
328. Wang C-A, Chen K, Huang Y, Le H. Electrochemical synthesis and properties of layer-structured polypyrrole/montmorillonite nanocomposite films. J Mater Res 2010;25:658-64.

329. Brinker C, Gong W, Guo Y, Soyez H, Dunn B, Huang MH, Zink JI. Continuous formation of supported cubic and hexagonal mesoporous films by sol–gel dip-coating. Nature. 1997;389:364-8.
330. Wielgos T, Fitch A. A clay-modified electrode for ion-exchange voltammetry. Electroanalysis. 1990;2:449-54.
331. Caillère S, Hénin S, Rautureau M. Tome 1: Structure et propriétés physico-chimiques. Minéralogie des argiles. 2 ed. Paris, France: Masson; 1982.
332. Watanabe T, Sato T. Expansion characteristics of montmorillonite and saponite under various relative humidity conditions. Clay Sci. 1988;7:129-38.
333. Hanley H, Muzny CD, Butler BD. Surface adsorption in a surfactant/clay mineral solution. Int J Thermophys. 1998;19:1155-64.
334. Karaca S, Gürses A, Korucu ME. Investigation of the orientation of C T A^+ ions in the Interlayer of CTAB pillared montmorillonite. J Chem. 2013:ID 274838.
335. Galarneau A, Barodawalla A, Pinnavaia T. Porous clay heterostructures formed by gallery-templated synthesis. Nature. 1995;374:529-31.
336. Jieumboué Tchinda A, Ngameni E, Tonlé IK, Walcarius A. One-step preparation of thiol-functionalized porous clay heterostructures: application to Hg (II) binding and characterization of mass transport issues. Chem Mater 2009;21:4111-21.
337. Tertiş M, Florea A, Sandulescu R, Cristea C. Carbon based electrodes modified with horseradish peroxidase immobilized in conducting polymers for acetaminophen analysis. Sensors. 2013;13 4841-54.